Università degli Studi di Padova

Dipartimento di Salute della Donna e del Bambino

Scuola di Dottorato in Medicina dello Sviluppo e

Scienze della Programmazione

Indirizzo di Ematooncologia, genetica, malattie rare e medicina predittiva

Ciclo XXVII

Nanotechnologies for CNS drug delivery: therapy for the neurological compartment in the Mucopolisaccharidoses

School Director: Ch.mo Prof. Giuseppe Basso

Address Coordinator: Ch.mo Prof. Giuseppe Basso

Supervisors: Dr. Rosella Tomanin / Dr. Maurizio Scarpa

PhD Student: Dr. Laura Rigon

ABSTRACT

Lysosomal storage disorders (LSDs) are a group of neurometabolic syndromes, mostly due to the deficit of one lysosomal enzyme. Many LSDs affect most of the organ systems and about two-thirds of the patients also present neurological and cognitive impairment. Enzyme replacement therapy, the most common therapeutic strategy applied to some LSDs, although determining some clinical improvements, has revealed to be ineffective on the CNS disease, due to enzymes' inability to cross the blood-brain barrier (BBB). So alternative methods to achieve transcytosis into the CNS need to be explored.

Among LSDs, Mucopolysaccharidoses (MPS) are characterized by a totally or partially defective activity of lysosomal enzymes involved in the catabolism of the glycosaminoglycans (GAGs), which, therefore, heavily accumulate within cellular compartment and in the extracellular matrix.

In this study, in which MPS type I and type II have been in particular evaluated, polymeric nanoparticles (NPs), modified with a glycopeptide of 7 amino acids (g7), already tested for the delivery of low molecular weight molecules, were tested as possible vehicle for BBB crossing and delivering of the therapeutic recombinant enzymes to the CNS after systemic administration in mice.

Results obtained in preliminary studies in the MPS I and MPS II mouse models, clearly showed that g7-NPs are able to deliver the model drug FITC-albumin to the brain, by crossing the BBB, in all treated mice (Idua-ko, Ids-ko and wt).

The subsequent *in vivo* preliminary study in the MPS II mouse model, using g7-NPs loaded with the recombinant IDS enzyme and labelled with Rhodamine B (g7-NPs-IDS-R), confirmed that g7-NPs can transport the enzyme through the BBB and paved the way for the upcoming *in vitro* and *in vivo* efficacy studies.

In the *in vitro* study fibroblasts obtained from MPS II patients were treated with untargeted NPs (devoid of g7), loaded with the recombinant enzyme for MPS II. Data obtained suggested that nanoparticles may need more than 2 weeks to open up and release the recombinant enzyme or, otherwise, that they may need a more complex physiological system with respect to the *in vitro* one.

To evaluate transfer efficiency and the enzymatic activity induced by g7-NPs loaded with the recombinant enzyme (g7-NPs-IDS), an *in vivo* pilot study in the MPS II mouse model was conducted. Mice were treated with a single dose of enzyme and sacrificed after 7 or 14 days. No induced IDS activity or reduction in GAG storage was, however, detected in liver and brain of g7-NPs-IDS treated mice.

Although the results obtained in the *in vitro* and *in vivo* pilot studies were mostly negative, it was important to carry out a medium-term analysis to assess the possible opening of NPs in a longer time. To this aim, an *in vivo* study was conducted in the MPS II mouse model, by treating mice once a week for 6 weeks. Biochemical, histological, immunohistochemical and immunofluorescence evaluations, conducted in liver and brain of g7-NPs-IDS treated mice suggested that a period of 6 weeks is again too short to detect the opening of the NPs and the release of the encapsulated enzyme. However, results obtained from this medium-term study are encouraging as they show a slight trend towards improvement in brain and liver of g7-NPs-IDS treated mice.

Further studies, at the moment ongoing, are needed to understand the timing of release of the enzyme from the NPs; in addition, we are re-formulating the nanoparticles with the aim to maintain the same transport efficiency to the CNS, although allowing a significant reduction of the timing of drug release.

RIASSUNTO

Le malattie da accumulo lisosomiale (LSD) sono un gruppo di patologie neurometaboliche, causate principalmente dal deficit di un enzima lisosomiale. Le LSD sono malattie multisistemiche e circa due terzi dei pazienti presentano anche danno neurologico e cognitivo. La terapia enzimatica sostitutiva, la strategia terapeutica più comunemente applicata ad alcune LSD, pur determinando alcuni miglioramenti sistemici, si è rivelata inefficace nel trattamento del coinvolgimento neurologico, a causa dell'incapacità degli enzimi terapeutici di attraversare la barriera emato-encefalica (BEE). Diventa, perciò, di primaria importanza valutare metodi alternativi per il trasporto di questi farmaci al sistema nervoso centrale (SNC).

Tra le LSD, le Mucopolisaccaridosi (MPS) sono caratterizzate dalla mancanza totale o parziale di attività di enzimi lisosomiali coinvolti nel catabolismo dei glicosaminoglicani (GAG), che, pertanto, si accumulano sia nel comparto cellulare che nella matrice extracellulare.

In questo studio, nel quale sono state in particolare studiate le MPS di tipo I e di tipo II, nanoparticelle polimeriche (NPs), modificate con un glicopeptide di 7 amminoacidi (g7), già testate per il trasporto oltre barriera di molecole a basso peso molecolare, sono state valutate come possibile veicolo per l'attraversamento della BEE e il trasporto degli enzimi terapeutici ricombinanti al SNC, dopo somministrazione sistemica nei topi.

I risultati ottenuti negli studi preliminari nei modelli murini per la MPS I e la MPS II, hanno mostrato chiaramente che le g7-NPs sono in grado di trasportare al cervello l'albumina-FITC (farmaco modello), attraversando la BEE, in tutti i topi trattati (Ids-ko, Idua-ko e wt).

Il successivo studio preliminare *in vivo* nel modello murino per la MPS II, in cui sono state testate le g7-NPs caricate con l'enzima IDS ricombinante e marcate con Rodamina B (g7-NPs-IDS-R), ha confermato che le g7-NPs sono in grado di trasportare l'enzima attraverso la BEE, aprendo così la strada per i successivi studi di efficacia da effettuare *in vitro* ed *in vivo*.

Nello studio *in vitro*, fibroblasti ottenuti da pazienti affetti da MPS II sono stati trattati con NPs non targettate (prive di g7) e caricate con l'enzima ricombinante impiegato per la terapia di questa patologia. I dati ottenuti hanno suggerito che le nanoparticelle probabilmente necessitano di un tempo superiore alle 2 settimane per aprirsi e rilasciare l'enzima ricombinante o, anche, che le fasi di apertura e rilascio potrebbero necessitare di un sistema fisiologico più complesso rispetto ad un sistema *in vitro*.

Per valutare l'efficienza di trasferimento e l'attività enzimatica indotta dalle g7-NPs caricate con l'enzima ricombinante (g7-NPs-IDS), è stato di seguito condotto uno studio pilota *in vivo* nel modello murino per la MPS II. I topi sono stati trattati con una singola dose di enzima e sacrificati dopo 7 o 14 giorni. Nel fegato e nel cervello dei topi trattati con g7-NPs-IDS non è stata, tuttavia, rilevata alcuna attività IDS indotta o la riduzione dei depositi di GAG.

Sebbene i risultati ottenuti dallo studio *in vitro* e da quello pilota *in vivo* risultassero per lo più negativi, era importante effettuare un'analisi a medio termine per valutare l'eventuale apertura delle NPs in un tempo più lungo. A questo scopo, è stato condotto uno studio *in vivo* nel modello murino per la MPS II, mediante somministrazione settimanale di NPs nei topi, per un totale di 6 settimane. Le valutazioni biochimiche, istologiche, immunoistochimiche e di immunofluorescenza condotte nel fegato e nel cervello dei topi trattati con le g7-NPs-IDS hanno evidenziato che un periodo di 6 settimane di trattamento è ancora insufficiente per consentire un'efficace apertura delle NPs e il rilascio dell'enzima incapsulato. Tuttavia, i risultati ottenuti da questo ultimo studio a medio termine sono risultati incoraggianti, poiché mostrano una costante, se pur lieve, tendenza al miglioramento nel fegato e nel cervello dei topi trattati con g7-NPs-IDS.

Ulteriori studi sono necessari, e sono attualmente in corso, per capire i tempi di rilascio dell'enzima dalle NPs; inoltre, è in fase di rivalutazione la formulazione delle stesse, con l'obiettivo di mantenerne l'efficienza di trasporto al SNC, ma di ridurne i tempi di rilascio del farmaco.

TABLE OF CONTENTS

1. INTRODUCTION

1.1 LYSOSOMAL STORAGE DISEASES

Lysosomal storage diseases (LSDs) are a group of about 60 different inherited metabolic disorders caused by deficiencies in lysosomal hydrolases, lysosomal membrane proteins or lysosomal transporters, resulting in abnormal accumulation of undegraded metabolites and dysregulation of lysosomes.

Individually rare, LSDs have a prevalence ranging from 7.6 to 26.9 per 100,000 live births (*Meikle et al., 1999; Poorthuis et al., 1999; Applegarth et al., 2000; Pinto et al., 2004; Fuller et al., 2006; Spada et al., 2006; Poupetova et al., 2010; Mechtler et al., 2012; Al-Jasmi et al., 2013; Scott et al., 2013; Hult et al., 2014*).

Although many LSDs had already been recognized as clinical entities since the 19th century, their classification was born many years later with the discovery of the lysosome by Christian de Duve in 1955 (*de Duve C et al., 1955*) and with the development of the concept of lysosomal diseases by Hers in 1965 (*Hers HG, 1965*).

Typically, LSDs are classified based on the nature of the storage material or on the defective lysosomal protein: mucopolysaccharidoses, mucolipidoses, glycolipidoses and glycoproteinoses (*Alroy J et al., 2014*).

Lysosomes are membrane-bound cytoplasmic organelles containing acid hydrolases, enzymes that degrade a variety of macromolecules as part of normal cellular function. A lysosomal defect, most commonly a mutation in genes that encode catalytic enzymes, results in accumulation of undegraded material causing cell and organ dysfunction; however, the mechanisms by which the storage leads to the disease are not well understood. To explain this, in the past 25 years many investigations have been carried out, realizing that there are many factors playing a role in the pathophysiology of LSDs, including alterations of intracellular calcium homeostasis, impairment of autophagy, activation of signal transduction by non-physiological substances, inflammation, and others (*Ballabio A and Gieselmann V, 2009*).

All LSDs are monogenic disorders, inherited as autosomal recessive traits except for Fabry disease, Hunter Syndrome and Danon disease, which are X-linked conditions. Numerous mutations in the same gene in different patients have been described, including missense, nonsense and splice-site mutations, partial deletions and insertions. Some mutations lead to the complete loss of enzyme activity, whereas others lead to reduced activity. However, no obvious genotype–phenotype correlation has been found and prediction of the clinical course of the disease cannot usually be made based on mutational analysis. (*Futermann and van Meer, 2004*).

1.2 GLYCOSAMINOGLYCANS

Glycosaminoglycans (GAGs) or mucopolysaccharides are long unbranched molecules consisting of a repeating disaccharide unit. The repeating unit (except for keratan) consists of an amino sugar (N-acetylglucosamine or N-acetylgalactosamine) along with an uronic sugar (glucuronic acid or iduronic acid) or galactose. The specific monosaccharide units identify the subtype of GAG.

Four main groups of GAGs are classified based on their sugar, the type of linkage between them and the number and location of sulfate groups: hyaluronan, chondroitin sulfate (CS), dermatan sulfate (DS), heparan sulfate (HS), keratan sulfate (KS) (*Alberts et al., 2002*). With the exception of hyaluronic acid, all GAGs contain sulfate groups.

GAGs are involved in the formation of the extracellular matrix, adhesion, cell differentiation and growth, as well as apoptosis.

The degradation of GAGs is catalysed by lysosomal hydrolytic enzymes, exo- and endo-glycosidases, which act sequentially. Catabolism always proceeds from the not-reduced end by glycosidases and sulfatase. **Figure I** shows the degradative cascade of heparan, keratan, dermatan and chondroitin sulfate.

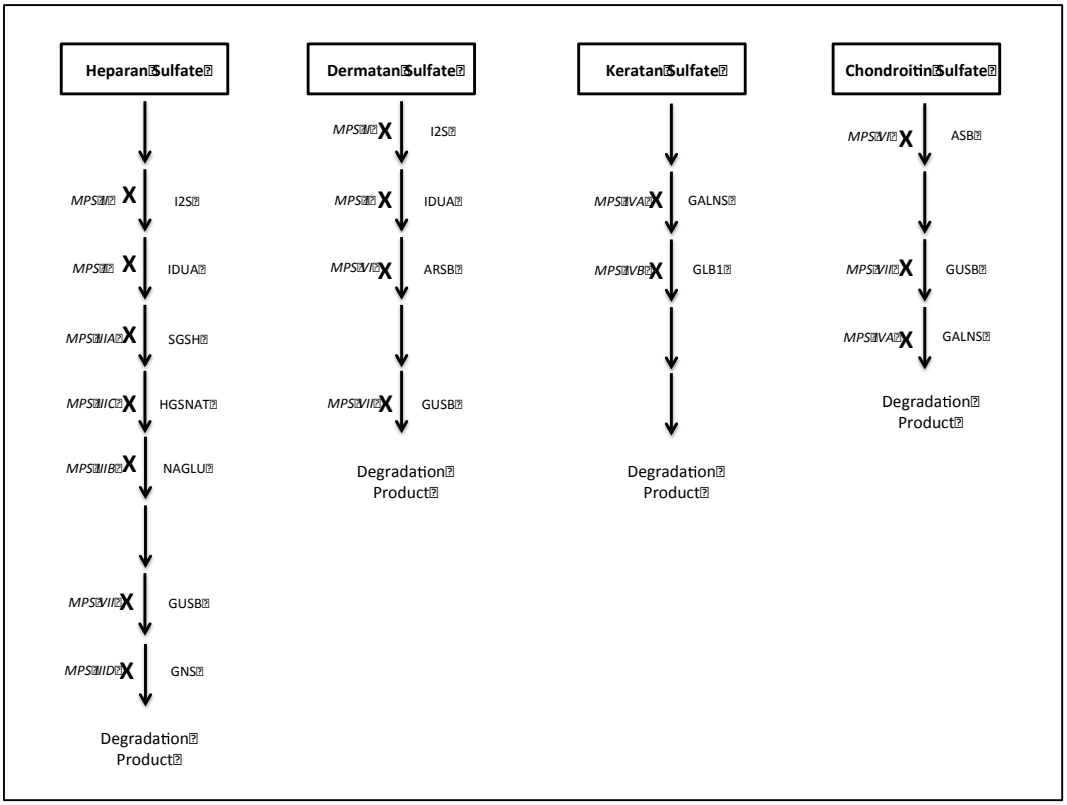

Figure I: GAG degradation pathway and the blockage of each enzyme leading to different types of mucopolysaccharidoses. Abbreviations: I2S, iduronate-2-sulphatase; IDUA, alpha-L-iduronidase; SGSH, heparan *N*-sulphatase; HGSNAT, acetyl-CoA:alpha-glucosaminide *N*-acetyltransferase; NAGLU, *N*-acetyl-alpha-glucosaminidase; GUSB, beta-glucuronidase; GNS, *N*-acetylglucosamine 6-sulphatase; ASB, *N*-acetylgalactosamine 4-sulphatase; GALNS, *N*-acetylgalactosamine-6-sulphate sulphatase; GLB1, beta-galactosidase (adapted from *Noh and Lee, 2014*).

1.3 MUCOPOLYSACCHARIDOSES

Mucopolysaccharidoses (MPSs) are a group of lysosomal storage disorders caused by deficiency of enzymes catalysing the degradation of glycosaminoglycans (or mucopolysaccharides). Depending on the enzyme deficiency, the catabolism of dermatan sulfate, heparan sulfate, keratan sulfate, chondroitin sulfate or hyaluronan may be blocked, singly or in combination (*Neufeld and Muenzer, 2001*).

Deficiency of one of these enzymes leads to development of one of eleven types and subtypes of MPSs (**Table I**).

Pathology	*OMIM*	*Gene*	*Localization*	*Enzyme deficiency*	*GAG storage material*	*ERT*
MPS I (Hurler, Hurler-Scheie, Scheie)	607014 607015 607016	*IDUA*	4p16.3	α-L-Iduronidase	Dermatan sulphate, heparan sulphate	Aldurazyme®
MPS II (Hunter)	309900	*IDS*	Xq28	Iduronate 2-sulfatase	Dermatan sulphate, heparan sulphate	Elaprase®
MPS IIIA (Sanfilippo A)	252900	*SGSH*	17q25.3	Heparan-*N*-sulfatase	Heparan sulphate	
MPS IIIB (Sanfilippo B)	252920	*NAGLU*	17q21.2	α-*N*-acetylglucosaminidase	Heparan sulphate	
MPS IIIC (Sanfilippo C)	252930	*HGSNAT*	8p11.21	Heparan acetyl-CoA: α-glucosaminide *N*-acetyltransferase	Heparan sulphate	
MPS IIID (Sanfilippo D)	252940	*GNS*	12q14.3	*N*-acetylglucosamine 6-sulfatase	Heparan sulphate	
MPS IVA (Morquio A)	253000	*GALNS*	16q24.3	Galactose 6-sulfatase	Keratan sulphate, chondroitin sulphate	Vimizim®
MPS IVB (Morquio B)	253010	*GLB1*	3p22.3	β-Galactosidase	Keratan sulphate	
MPS VI (Maroteaux-Lamy)	253200	*ARSB*	5q14.1	Arylsulfatase B (*N*-acetylglucosamine 4-sulfatase)	Dermatan sulphate, chondroitin sulphate	Naglazyme®
MPS VII (Sly)	253220	*GUSB*	7q11.21	β-Glucuronidase	Dermatan sulphate, heparan sulphate, chondroitin sulphate	
MPS IX (Natowicz)	610492	*HYAL*	3p21.31	Hyaluronidase	Hyaluronan	

Table I: MPSs classification with related OMIM code, gene symbol, localization on chromosome, enzyme deficiency, GAG storage material and, where available, the enzyme replacement therapy (ERT).

1.3.1 History

The first clinical characterization of a mucopolysaccharide disorder dates back to 1917 when Charles Hunter defined the clinical profile of a patient now identifiable as affected by MPS II (*Hunter, 1917*) and subsequently, in 1929, Luis

Morquio described four children affected by a condition now recognized as MPS IV (*Morquio, 1976*).

The very big thrust to MPS survey was, doubtless, the discovery of the lysosome during the '50s by Christian de Duve (*de Duve et al., 1955*), which allowed the settlement of the other MPS profiles and, above all, enabled a better understanding of the pathophysiology and of the basic biochemical processes involved in the disease onset.

However, the term MPS was suggested in 1952, after the identification of excessive amounts of GAGs in samples from patients with Hurler syndrome (*Brante, 1952; Dorfman and Lorincz, 1957*). Only in 1964 appeared the concept of MPSs as enzymatic deficiencies, when van Hoof and Hers proposed that these disorders were analogous to Pompe disease and therefore, due to specific lysosomal hydrolase deficiencies. Supporting this idea were the results from these two authors, who observed dramatically enlarged lysosomes in Hurler hepatocytes (*Van Hoof and Hers, 1964*) and, four years later, the studies conducted by Fratantoni and co-workers.; together, these experiments have demonstrated impaired GAG degradation (*Fratantoni et al., 1968*).

In 1966 McKusick first categorized MPS disorders in six defined groups based on clinical traits and genetic and biochemical findings (*McKusick, 1966*).

1.3.2 Genotype and Phenotype

With the exception of MPS II, which is X-linked, the MPS disorders are inherited in an autosomal recessive manner and affect both males and females equally.

Mutations underlying these diseases are extremely heterogeneous, often private, but one or a few mutated alleles may predominate in specific populations ("hot spots"). Most are point mutations or small changes in the gene, although large rearrangements and deletions can occur in MPS II. Genotype-phenotype correlation is sometimes possible, but the effect of missense mutations is generally difficult to predict (*Neufeld and Muenzer, 2001*).

MPSs are chronic and progressive syndromes that produce a spectrum of signs and symptoms in multiple organ systems. Patients typically appear normal at

birth, but during early childhood they experience the onset of clinical signs and symptoms including organomegaly, skeletal, joint, airway and cardiac involvement, hearing and vision impairment, and progressive cognitive delay in the severe forms of MPS I, MPS II and MPSVII and all subtypes of MPS III (*Muenzer, 2011*).

The overall prevalence of MPSs is difficult to assess because of the lack of epidemiological studies; the known values are shown in **Table II**.

Disease	***Prevalence per 100,000 live births***								
	Poland	*The Netherlands*	*Germany*	*Australia*	*Norway*	*Denmark*	*Sweden*	*Czech Republic*	*Italy*
MPS I	0.22	1.19	0.69	-	1.85	0.54	0.67	0.72	-
MPS II	0.46	0.67	0.64	0.31	0.13	0.27	0.27	0.43	1.21
MPS III (all type)	0.86	1.89	1.57	1.71	0.27	0.43	0.67	0.91	-
MPS IV (A+B)	0.14	0.36	0.38	0.15 (A)	0.76	0.48	0.07	0.73	-
MPSVI	0.0132	0.15	0.23	0.31	0.07	0.05	0.07	0.05	-
MPSVII	0	0.24	0	-	-	-	-	0.02	-
MPS IX	0	-	0	-	-	-	-	-	-
MPS all types	1.81	4.5	3.53	3.34	3.08	1.77	1.75	3.72	2.45

Table II: Prevalence of mucopolysaccharidoses per 100,000 live births: comparison of data in different populations (adapted from *Jurecka et al., 2014; Dionisi-Vici et al., 2002*).

1.3.3 Diagnosis

Early diagnosis of MPSs is of extreme importance to optimize treatment and outcomes, particularly for those disorders that are amenable to treatment with HSCT or ERT.

Not rarely the diagnosis of MPSs takes several months or years from the onset of the first symptoms, thus reducing the benefits of the available therapies (*Marsden and Levy, 2010*). This delay is caused by the difficult differential diagnosis and by the fact that MPSs, being rare, are not clinically well known. To confirm an MPS clinical suspect, the first laboratory step is the urinary GAG quantification and qualitative analysis. If GAG level is high and/or the qualitative spectrum is strongly suggestive, an enzymatic analysis is carried out in plasma or

peripheral leukocytes or cultured cells. Finally, the enzymatic deficit identification is confirmed by the molecular analysis of the corresponding gene.

At the beginning of the last decade Chamoles and coworkers introduced the Dried Blood Spots (DBSs) analysis for the enzymatic diagnosis of several lysosomal storage disorders including some MPSs (*Chamoles et al., 2001a, 2001b*). The use of DBSs to perform enzyme assays offers several advantages, among others little invasiveness and the requirements of extremely small amounts of blood, rendering the analysis possible even in the case of newborns, thus allowing pre-symptomatic diagnosis (*Gasparotto et al., 2009*). Since 2004 a new method combining the advantage of using DBSs for samples collection, and the high sensitivity and selectivity of tandem mass spectrometry (MS/MS) for the analysis, has been developed (*Li et al., 2004*). The procedure is having a great success, as it is suitable for high throughput and multiplex analysis of several enzymes simultaneously in hundreds of samples; however, ethical reasons suggest their application only to screen diseases for which a therapy is available.

1.3.4 Therapies

1.3.4.1 Enzyme replacement therapy

Enzyme Replacement Therapy (ERT) is based on the intravenous infusion of a recombinant human enzyme. The drug is internalized via mannose 6-phosphate (M6P) receptors, reaches its target site in the lysosomes and replaces the defective lysosomal enzyme (*Noh and Lee, 2014*).

To date, the FDA and the EMEA have approved 4 recombinant human enzymes for MPSs: laronidase (Aldurazyme®, Genzyme Corporation) for MPS I, idursulfase (Elaprase®, Shire Human Genetics Therapies Inc.) for MPS II, galsulfase (Naglazyme®, BioMarin Pharmaceutical Inc.) for MPSVI and, recently, elosulfase alpha (Vimizim®, BioMarin Pharmaceutical Inc.) for MPS IVA.

Although systemic manifestations partly ameliorate with ERT, the treatment has no effect on bone, heart valves and CNS disease (*Noh and Lee, 2014*). In fact, the low level of the BBB transport system for acid hydrolases and the high molecular

weight of these enzymes make any paracellular or transcellular diffusion of these proteins across the BBB almost non-existent. Therefore, efficient methods to achieve a safe transcytosis into the CNS need to be explored.

1.3.4.2 Hematopoietic stem cell transplantation

Hematopoietic stem cell transplantation (HSCT) with bone marrow or umbilical cord stem cells has been revealed to prevent many clinical features of the severe phenotypes of MPS I, VI and VII. Furthermore, in very young MPS I patients (earlier than 2.5 years), HSCT can significantly preserve intellectual development, differently to what happens for MPS II and MPS III. Of great importance, HSCT success depends on the age of the child, the degree of clinical involvement and the ability to achieve stable engraftment. Moreover, the procedure still maintains a significant risk of morbidity and mortality (*Cimaz and La Torre, 2014*).

1.3.4.3 Substrate reduction therapy

The principle of substrate reduction therapy (SRT) is to reduce the amount of storage material into the compromised lysosome by partially inhibiting the biosynthetic cycle instead of enhancing the activity of the degrading enzymes. Since these strategies generally propose the use of low molecular weight molecules able to cross the BBB, their administration in MPSs are expected to obtain a treatment of the brain compartment.

The first SRT protocol for MPSs was proposed in 2006 by Roberts and colleagues (*Roberts et al., 2006*); the use of rhodamine B reduced the lysosomal storage in MPS cells and demonstrated *in vivo* in MPS IIIA mice the ability of the molecule to reverse clinical parameters of disease progression. However, rhodamine B could not be used in clinical treatments due to its possible toxic effects (*Jakobkiewicz-Banecka et al., 2009*).

Since 2006 another molecule has been proposed to inhibit GAG synthesis, genistein (4',5,7- trihydroxyisoflavone or 5,7-dihydroxy-3-(4-hydroxyphenyl)-4H-1-benzopyran-4-one), an isoflavone more commonly used for menopause

(*D'Anna et al., 2009*), cardiovascular disease (*Vera et al., 2007*) and osteoporosis (*Wang et al., 2006*). It was shown to inhibit GAG synthesis in cultured fibroblasts obtained from different MPS patients (*Piotrowska et al., 2006*). Moreover, in a 1 year open-label pilot study performed in MPS III patients, improvements in urinary GAG excretion, hair morphology and cognitive function was reported (*Piotrowska et al., 2008*); however these results were not confirmed by a subsequent study by Delgadillo and colleagues (*Delgadillo et al., 2011*). *In vivo* preclinical studies have shown efficacy of genistein in MPS IIIB (*Malinowska et al., 2009, 2010*) and MPS II mice (*Friso et al., 2010*). However, an improvement in CNS correction and mice behaviour was only obtained following administration of very high dosages of genistein (*Malinowska et al., 2010*), about 30-fold higher than the dosage commonly suggested for patients.

1.3.4.4 Gene therapy

Human gene therapy consists in the insertion of normal DNA directly into cells to provide a stable source of the defective enzyme. It has the advantage to reach both the brain and the skeletal structures. The main problem is to find a safe vector that results in therapeutic levels of gene expression.

Many approaches have been tested for MPSs, both viral and non viral, *in vivo* and *ex vivo* (*Tomanin et al., 2012*). The *in vivo* approach is the most studied. In particular, intracerebral gene therapy represents a promising approach, as it could be a permanent source of the functional form of the enzyme directly on the CNS. To underline that, in LSDs enzyme activity just equal to 5-10% of the normal level was described as sufficient to obtain an effect in the deficient cells (*Sands et al., 2006; Calias et al., 2012*).

However, although the data obtained so far are encouraging, there are still limitations that must be overcome to ensure the success of these new therapeutic approaches. Among these, we need a greater understanding of the biology and pathophysiology of MPSs and the possible toxicity and immune response related to gene transfer (*Seregin et al., 2011*). Interesting will be the

results generated by the trials ongoing for MPS IIIA and IIIB involving the intrathecal injection of an adeno-associated virus.

1.3.4.5 Intrathecal injection

The direct transfer of the recombinant enzyme in CSF effectively reduces the accumulation of non-degraded metabolites in the brain parenchyma (*Valayannopoulos et al., 2011*). Experiments in animal models of mucopolysaccharidosis type I, II and IIIA have demonstrated that intrathecal ERT injection is able to distribute the recombinant enzyme throughout the central nervous system, to penetrate the brain tissue and to promote the clearance of accumulated material within the lysosomes (*Dickson, 2009).*

To date, the challenge is to translate to the patient the success so far obtained on large and small animals. Therefore, protocols for the intrathecal injection of enzyme for MPSs and other LSDs are currently the subject of clinical trials (*Dickson et al., 2011*).

Intrathecal lumbar enzyme replacement is presently under clinical trial in patients with MPS I (NCT#00852358), MPS II (NCT#00920647; #01506141) and MPS IIIA (NCT#01155778; #01299727). At the moment, only the results obtained from the administration of a very small sample of patients with MPS I and MPS VI are available (*Dickson et al., 2009, 2011; Giugliani et al., 2011*). Despite being at present the only promising approach to the treatment of the neurological manifestations of LSD, intrathecal enzyme therapy should be modified in the procedure of its administration. Indeed, the administration throughout life of the enzyme by an intrathecal catheter is unfeasible. The catheter is an artificial opening of the BBB and a possible source of infection. Moreover, agitation, aggression and hyperexcitability of MPS children with neurological involvement have already prompted changes to catheters currently used in clinical trials. For these reasons, modified enzymes able to cross the BBB are currently under preclinical studies (*Scarpa et al., 2012*).

1.4 MUCOPOLYSACCHARIDOSIS TYPE I

Mucopolysaccharidosis type I (MPS I) is a metabolic inherited disorder due to the deficit of the lysosomal enzyme α-L-iduronidase (IDUA), involved in the degradation of the glycosaminoglycans heparan- and dermatan-sulfate (**Figure I**). Clinical symptoms and pathological features of the disorder, including heart disease, corneal clouding, organomegaly, skeletal malformations and joint stiffness, are due to the progressive accumulation of undegraded GAG in the cell lysosomes (*Neufeld and Muenzer, 2001*).

Historically MPS I has been divided into three different pathologies on the basis of clinical manifestations: Hurler syndrome (severe form, OMIM #607014), also characterized by a heavy neurological involvement; Hurler-Scheie syndrome (intermediate, OMIM #607015); Scheie syndrome (mild, OMIM #607016, previously called MPS V).

Occurrences of the three different phenotypes from the global MPS I registry are shown in **Table III**.

Geographic region	*Hurler (%)*	*Hurler-Scheie (%)*	*Scheie (%)*	*Undetermined (%)*
All regions	60.9	23.0	12.9	3.2
Asia Pacific	29.2	20.8	50.0	0
Europe	61.5	22.7	14.0	1.8
Latin America	42.7	33.3	12.9	11.1
North America	71.4	18.4	8.7	1.5

Table III: Distribution of MPS I phenotypes by geographic region (adapted from *Beck et al., 2014*)

1.4.1 Genetics

The gene coding for the enzyme alpha-L-iduronidase (IDUA, EC 3.2.1.76) maps on 4p16.3. It has a length of 19492 bp and consists of 14 exons; repeated Alu sequences and highly polymorphic VNTR sequences were found in exon 2 (*Scott et al., 1992, 1995*). The cDNA consists of an open reading frame (ORF) of 2138 bp encoding the protein IDUA, formed by 653 amino acids and with 6 sites of N-glycosylation (*Zhao et al., 1997*).

MPS I is inherited in an autosomal recessive manner. Until now, 212 different mutations have been identified in this gene, including nonsense, missense and spilicing mutations, deletions and insertions. Up to 70% of mutations are recurrent and thus may be helpful in phenotype prediction; however, a 2003 comprehensive review of genotype-phenotype correlations illustrates the limitations related to the frequency of private mutations at this locus (*Terlato & Cox, 2003, Bertola et al., 2011; Wang et al., 2012*). Moreover, a 2011 study has underlined the existence of dramatic differences in mutational heterogeneity and mutation prevalence highlights the importance of multi-national screening studies in helping to elucidate the genotype-phenotype relationship (*Bertola et al., 2011*).

The most common mutations in Caucasians are W402X and Q70X; they encode for prematurely stop codons, giving rise to particularly severe forms of MPS I, and in some countries are responsible for over 70% of cases of MPS I (*Gort et al., 1998; Beesley et al., 2001*).

Most of the mutations leading to the intermediate and attenuated form of MPS I are missense and allow the synthesis of minimum levels of IDUA (*Tieu et al. 1995*).

1.4.2 Clinical features

Hurler syndrome (MPS I/H): The most severe MPS I phenotype is characterized by impaired cognitive development, hepatosplenomegaly, cardiac valvulopathy, corneal clouding, progressive coarsening of facial features, respiratory failure, recurrent otitis media, musculoskeletal manifestations such as joint stiffness and contractures, dysostosis multiplex (**Figure II**). The symptoms arise after birth and progress rapidly. Most of the patients die before 10 years of age if untreated, due to complications related to brain damage or cardiorespiratory problems (*Pastores et al., 2007; Soliman et al., 2007*).

Hurler-Scheie syndrome (MPS I H/S): This phenotype manifests in infancy with intermediate severity compared with Hurler phenotype. Generally, there is no cognitive impairment, but some patients may exhibit mild learning difficulties.

Life expectancy is reduce to the second or third decade of life (*Pastores et al., 2007; Soliman et al., 2007*).

Scheie syndrome (MPS I/S): This is the most attenuated form (*Soliman et al., 2007*), symptoms occur later and progress slowly, rarely is diagnosed in childhood. Generally, patients exhibit normal intelligence and survive until adulthood (*Pastores et al., 2007*).

Figure II: Aspect of a child with MPS I (from "MPS I, a disease with many faces" - Genzyme Corporation, 2004)

1.4.3 Therapies

1.4.3.1 Hematopoietic Stem Cell Transplantation

The hematopoietic stem cell transplantation (HSCT) is still the treatment of choice for the severe form of MPS I, especially if performed before the onset of damage to the different organs (*Guffon et al., 1998*). It may include bone marrow transplantation (BMT), peripheral blood or umbilical cord transplantation.

To date the best results have been obtained with BMT, since it generates a renewed source of enzyme, able to correct the accumulation of GAGs in the different districts of the organism (*Guffon et al., 1998*). Therefore, BMT slows down the progress of the disease and in patients with the attenuated forms also allows the preservation of cognitive development.

The first allogeneic BMT for MPS I has been successfully performed in 1981 by Hobbs and co-workers on a one year-old baby, suffering from the severe form of

the disease. Thirteen months later, the patient showed an activity of α-L-iduronidase similar to that of heterozygotes, with regression of hepatosplenomegaly and corneal opacification and with arrest in the progression of the other degenerations (*Hobbs et al., 1981*).

Since then, more than 1000 patients with the severe form of MPS I have been transplanted and, where the graft was successful, restoration of enzymatic function and subsequent amelioration of disease complications has been obtained. If HSCT is performed before the age of 2.5 years and before the onset of serious mental involvement, joint mobility, vision, hearing and cardiopulmonary functions have been shown to improve, cognition preserved and survival increased. However, benefit in bone and cornea is limited and, above all, the risks of morbidity and mortality associated with HSCT remain significant (*Noh and Lee, 2014*). Therefore, HSCT should be considered only after careful consideration and only in very young patients before the onset of symptoms.

1.4.3.2 Enzyme Replacement Therapy – Aldurazyme ®

Laronidase (recombinant human α-L-iduronidase, Aldurazyme®; Genzyme Corporation, Cambridge, MA and BioMarin Pharmaceutical, Inc., Novato, CA, USA) was the first ERT drug approved for treatment of an MPS disorder and has been available in the USA and Europe since 2003. It is a polymorphic variant of the human enzyme alpha-L-iduronidase, with a molecular weight of 83 kDa. It is produced by recombinant DNA technology in a Chinese hamster ovary cell line. The recommended dose is 0.58 mg/kg (100 U/kg) administered by intravenous infusion over 4 hours once a week, but a double dose every 2 weeks could be an acceptable alternative regimen for patients who have difficulty receiving weekly infusions (*Giugliani et al., 2009*).

ERT for MPS I became possible only after the cloning of the IDUA gene (*Scott et al., 1992*) and its high-level expression in a stable clone of CHO cells (*Kakkis et al., 1994*). After many preclinical studies, several clinical trials have demonstrated that ERT with laronidase is safe and effective in patients with MPS I, across a

wide range of ages (young children to adults) and disease severity(*Kakkis et al., 2001; Wraith et al., 2004, 2007; Clarke et al., 2009; Giugliani et al., 2009; Beck et al., 2014*). Results of clinical trials have demonstrated the efficacy of ERT in reducing hepatosplenomegaly and urinary GAG levels, increasing distance walked in the 6-min walk test, stabilizing or improving joint range motion, stabilizing or decreasing sleep apnoea, decreasing left ventricular hypertrophy and improving the quality of life. However, the results of the clinical trials, have revealed that some symptoms of the disease are not reversible, particularly heart, bone and joint disease and corneal opacification. Moreover, laronidase cannot cross BBB and correct the neurological involvement in subjects with severe forms. These studies have also shown an immune response against the recombinant protein, with a peak in the production of IgG after 12 weeks of treatment. A recent study has demonstrated that antibodies significantly reduce enzyme uptake with negative consequences on its efficacy (*Langereis et al., 2014*).

1.4.3.3 Other therapies

At present, studies are focused on the development of new forms of therapy directed to areas and organs that do not respond to ERT. Alternative routes of administration and modifications of the enzyme to reach the central nervous system are the main focus, as IDUA cannot cross the blood brain barrier.

Intrathecal ERT, tested in animals and already reported in a few patients, may become a tool to treat or prevent the CNS manifestations in the severe forms of MPS I, but, as noted earlier in section 1.3.4.5, it presents several limitations (*Vera et al., 2013*).

Another therapeutic strategy is represented by the stop-codon read-through (SCRT), which has been tried in preclinical studies for MPS I and could be a potential tool for a large subgroup of patients with nonsense mutations. The capability of chloramphenicol to suppress the stop-codon has been analysed in human MPS I fibroblasts carrying different nonsense mutations, obtaining increased IDUA activity in all tested fibroblasts (*Mayer et al., 2013*).

Recent *in vivo* studies have also evaluated the possibility of encapsulating the enzyme in microcapsules (*Piller Puicher et al., 2012*) or modifying it with appropriate molecules such as ApoE (*El-Amouri et al., 2014*)

Many preclinical studies with various type of vector and in different animal models (mouse, cat, dog, monkey) were conducted to investigate gene therapy, but, even if presented with quite encouraging results, this treatment modality took a long time to move forward into clinical studies (*Giugliani et al., 2012*).

1.5 MUCOPOLYSACCHARIDOSIS TYPE II

Mucopolysaccharidosis type II or Hunter Syndrome (MPS II; OMIM #309900) is caused by a deficit of iduronate 2-sulfatase (IDS), a key enzyme in the lysosomal catabolism of the mucopolysaccharides heparan- and dermatan-sulfate (**Figure I**). The clinical features of MPS II are similar to those of MPS I, ranging from the attenuated to the severe forms.

Table II shows the prevalence of MPS II.

1.5.1 Genetics

The human gene coding for iduronate 2-sulfatase (IDS, EC 3.1.6.13) maps on the long arm of X chromosome, at location Xq28, with minus orientation. According to Ensembl database, it spans almost 56 kilobases and has 11 transcripts.

A pseudogene (IDSP1, I2S2) located on the telomeric side of the IDS gene within 20 kb has also been identified (*Bondeson et al., 1995*); it contains sequences homologous to exons 2 and 3 and to introns 2, 3, and 7 of the longest IDS transcript, in reverse orientation.

To date, 534 mutations have been reported for the IDS gene [www.hgmd.cf.ac.uk], many of which are private (*Burton and Giugliani, 2012; Froissart et al., 2007*). They include single nucleotide substitutions, small deletions, insertions and indels, gross deletions, insertions and duplications, complex rearrangements and splicing mutations. According to a study conducted on 155 unrelated patients in 2007 (*Froissart et al., 2007*), most of them (~80%) present with small IDS gene alterations, the others present with large gene

alterations. These data have been confirmed by a recent study in 103 unrelated South-American patients (*Brusius-Facchin et al., 2014*).

MPS II is inherited as an X-linked recessive disorder; nevertheless, it has been well documented in a small number of females (*Tuschl et al., 2005; Pina-Aguilar et al., 2013*) in whom the most common mechanism of expression is skewed X-chromosome inactivation of the non-mutant allele. Additional rare causes may include the disruption of the IDS gene through an X chromosome/autosome translocation or homozygosity for an IDS gene mutation (*Cudry et al, 2000; Tuschl et al., 2005*). Females carrying a mutation in one IDS allele (carriers) are usually asymptomatic.

1.5.2 Genotype-phenotype correlation

The high phenotypic and genotypic heterogeneity, the rarity and the presence of almost exclusively private mutations render genotype-phenotype correlation in MPS II difficult to assess. However, total or partial gene deletion and gene/pseudogene rearrangement seem to result in the severe phenotype (*Froissart et al., 2002*). Deletions extending beyond the IDS locus have been associated with a severe phenotype in combination with symptoms atypical of Hunter syndrome (*Timms et al., 1997*). Conversely, small gene alterations, such as single nucleotide substitutions, have been reported to be associated with a wide range of phenotypes, spanning the entire spectrum from severe to attenuate. Even the same mutation may be associated with different phenotypes: at least two families have been described with brothers exhibiting severe and attenuated forms (*Martin et al., 2008*).

Neither the amount of IDS nor its activity correlates with phenotype severity in Hunter patients. Current methods used for measuring IDS enzymatic activity are insufficiently sensitive to differentiate between complete absence and presence of residual activity (*Froissart et al., 2002*). However, *in vitro* functional studies of IDS mutations reported a residual activity equal to 0.2–2.4% of the wild-type IDS activity for attenuated phenotypes and no detectable activity for those associated with severe phenotypes (*Sukegawa-Hayasaka et al., 2006*). Lee and

colleagues (*Lee et al., 2012*) observed a low residual IDS activity also in plasma of attenuated patients.

1.5.3 Clinical features

MPS II is a multiorgan and multisystem disease with variable age of onset and rate of progression. Phenotypic expression spans a wide spectrum of clinical severity. Patients with the most severe forms exhibit a chronic and progressive disease involving multiple organs and tissues, with increasing cognitive deterioration; they appear normal at birth, although they tend to be heavy. Clinical features manifest between 2 and 4 years of age; death from a combination of neurological deterioration and cardiorespiratory failure usually occurs in the mid-teenage years (*Wraith et al., 2008; Martin et al., 2008*). In attenuated patients, clinical signs have a later onset; they are most often diagnosed between the ages of 4 and 8 years. Neurologic dysfunctions are absent or minimal; survival to adulthood is common, but death often occurs between 20 and 30 years from cardiac or respiratory failure. A few patients are less severely affected; in these, life expectancy can be close to normal, and such affected males may have children. However, this traditional classification of patients into 'mild' (sometimes reported as 'attenuated') or 'severe' forms, on the basis of length of survival and the presence of CNS disease, is a gross simplification. The disorder should rather be regarded as a continuum between two extremes (severe and attenuated) (*Wraith et al., 2008*).

Patients with MPS II exhibit hepatomegaly, associated or not with splenomegaly, upper respiratory tract dysfunctions with recurrent respiratory infections, frequent sleep apnoea and musculoskeletal disorders, such as dysostosis multiplex, joint stiffness, pelvic dysplasia, a typical "facies" (**Figure III**) and vertebral and rib abnormalities (*Sanjurjo-Crespo, 2007; Martin et al., 2008; Wraith et al., 2008*). Cardiologic manifestations are common and are usually observed around 5 years of age, generally constituting the primary cause of death (*Martin et al., 2008*). Umbilical and inguinal hernias are also frequent findings, as well as recurrent otitis and dental abnormalities, gingival

hypertrophy and hyperplasia (*Sanjurjo-Crespo, 2007; Martin et al., 2008*). Patients with MPS II also exhibit skin disorders, Mongolian spot and papular lesions (*Martin et al., 2008; Wraith et al., 2008*).

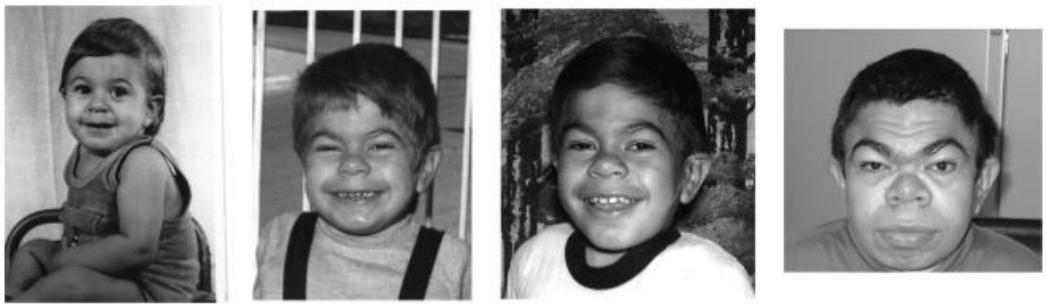

Figure III: Photographs of an MPS II patient at the age of 6 months, 5, 9 and 30 years (from left to right), showing the progression of the characteristic "facies" of Hunter syndrome.

From a neurological point of view, about two thirds of MPS II patients present with manifestations such as developmental delay and/or neurological regression (*Schwartz et al., 2007*). Patients with severe phenotype manifest an important neurological involvement with impaired cognitive abilities resulting in delayed mental developmental. In early childhood, in such patients behavioural problems, including hyperactivity, aggressiveness, obstinacy and stubbornness are common (*Young et al., 1982*). The attenuated form is characterized by little or no central nervous system involvement, with preserved intelligence and an extended life expectancy. In a study of magnetic resonance imaging (MRI) of 19 patients, the prevalence of brain atrophy, hydrocephalus and white matter lesions are significantly higher in patients with severe cognitive involvement (*Vedolin et al., 2007*). Nevertheless, the presence of these brain lesions is not diagnostic of damage of cognitive skills, as white matter lesions, enlargement of the ventricles and obvious brain atrophy sometimes are also present in patients without neurological involvement (*Muenzer et al., 2009*). Communicating hydrocephalus and spinal cord compression syndrome, as well as carpal tunnel syndrome, may also occur (*Martin et al., 2008*).

1.5.4 Therapies

1.5.4.1 Hematopoietic Stem Cells Transplantation

Hematopoietic stem cell transplantation (HSTC) via umbilical cord blood or bone marrow has been proposed as a way of providing sufficient enzyme to delay or stop the progression of the disease (*Martin et al., 2008*). In MPS II the use of HSCT has been controversial because of the associated high risk of morbidity and mortality, the lack of sufficient data on long-term follow up and some negative results obtained in a few case reports (*Vellodi, 2005; Araya et al., 2009*). However, the results of a long-term retrospective study performed in Japan in a cohort of 21 HSCT-treated patients have been recently published (*Tanaka et al., 2012*). HSCT showed effectiveness when performed before signs of brain atrophy or valvular regurgitation appear. Improvements of brain MRI, cardiac valve regurgitation and urinary GAG levels were observed in these patients together with a stabilization of brain atrophy, speech capability and activities of daily living.

1.5.4.2 Enzyme Replacement Therapy – Elaprase®

Idursulfase (Elaprase®, Shire Human Genetic Therapies, Inc, Cambridge, MA, USA) is a recombinant human IDS, produced in a human cell line, that was licensed for treatment of MPS II patients in the USA and the European Union, gaining marketing approval by the Food and Drug Administration (FDA) in 2006 and by the European Medicines Agency (EMA) in 2007. In Italy it was approved by the Italian Medicines Agency (AIFA) in 2006.

Clinical benefits of idursulfase were demonstrated in a randomized, placebo-controlled, double-blind clinical trial (*Muenzer et al. 2006*), in which 96 patients were randomly assigned to placebo or to a 0.5 mg/kg idursulfase dosage that was infused either weekly or every other week (EOW). After 1 year of treatment, a statistically significant improvement rate of the primary end point, compared with placebo, resulted both in patients in which the idursulfase was infused weekly and in the EOW group, even if in the weekly group it was more

significant. A significant reduction of GAG excretion and liver and spleen volumes was observed. On the basis of the larger clinical response in the weekly group compared with the EOW group, idursulfase was approved for the treatment of MPS II in both the USA and European Union at a dose of 0.5 mg/kg weekly.

Other clinical trials of idursulfase have been conducted in patients with MPS II. A recent study in 27 Italian paediatric patients revealed a statistically significant reduction only of urinary GAG and hepatomegaly. The evaluation of ERT efficacy in relation to the severity of the disease evidenced slightly higher improvements as for hepatomegaly, splenomegaly, otological disorders and adenotonsillar hypertrophy in severe vs attenuated patients (*Tomanin et al., 2014*).

1.5.4.3 Other therapies

Several new approaches for the treatment of MPS disorders are under investigation; some of these could be stand-alone therapies, others would likely be used as adjuvant therapy. Among these, both viral and non-viral approaches have been tested for the treatment of Hunter syndrome. Even if only in preclinical animal experiments, the obtained results have been encouraging. Gene therapy mediated by adeno-associated vectors (*Cardone et al., 2006; Jung et al., 2010*) obtained good results as well as cell therapy approaches employing intraperitoneally implanted microcapsules (*Friso et al., 2005*). Also muscle electro gene transfer has been tested, obtaining an elevated production of therapeutic protein but little curative effects in organs far from the injection site (*Friso et al., 2008*).

A therapeutic approach of substrate reduction therapy for Hunter syndrome uses genistein. It could be useful in combined therapeutic protocols and has shown efficacy in MPS II mice (*Friso et al., 2010*). Being a diet supplement, genistein can be assumed with no prescription, therefore in the last few years numerous MPS patients have regularly taken it, despite no important clinical trials evaluating both efficacy and safety have been so far carried on.

In 2012, Calias and colleagues demonstrated that IT-lumbar administration of IDS results in the delivery of a significant fraction of the administered protein to the

brain with widespread deposition in monkeys, dogs and mice, thus suggesting a clinically feasible route for the delivery of IDS to the brain (*Calias et al., 2012*). Recently it was also demonstrated that repeated intraventricular infusion (*Higuchi et al., 2012*) and continuous intrathecal infusion (*Sohn et al., 2013*) of IDS was effective in improving CNS defects in the MPS II mice and could be a valuable therapeutic method for treating patients.

1.6 MPS I AND MPS II MOUSE MODELS

1.6.1 MPS I mouse model

The first mouse model for MPS I was created in 1997 by Clarke and collaborators by homologous recombination in embryonic stem cells (ES cells).

The clinical and pathological characterization of the knock-out mouse is similar to the severe form of human MPS I, with evident dysmorphism of the muzzle, thickening of the cheek bones and long bones, enlargement of the fingers and increased urinary GAG excretion. Brain analysis also revealed an altered concentration of secondary factors such as ganglioside GM3, GM2 and GD3 (*Clarke et al., 1997*).

About 10 years ago Elizabeth Neufeld described the generation of a second knock-out mouse for MPS I, obtained with the same mechanism of specific site-recombination of the Neo cassette within exon 6 described by Clarke. This mouse model is similar, but not identical to the previous one (*Ohmi et al., 2003*).

Besides the dimorphism of the muzzle and the thickening of the fingers, it also displays cardiac hypertrophy with significant interventricular septal thickening due to infiltration of cells filled with GAG and defects to the valves and the aortic arches, reflecting the cardiomyopathy aspects observed in patients with MPS I (*Jordan et al., 2005*).

Knockout mice of the latter model were kindly provided us by Jean Michel Heard (Pasteur Institute, Paris) and have been used in the experiments described in this thesis.

1.6.2 MPS II mouse model

The Ids knock-out (Ids-ko) mouse was generated by gene disruption: a portion of exon 4 and all of exon 5 (a 1.5 kb deletion) were replaced by a neomycin-resistance gene expression cassette, in a C57BL/6 strain background (*Muenzer et al., 2002*). The Ids-ko mouse was characterized by several groups (*Muenzer et al., 2002; Friso et al., 2005; Cardone et al., 2006; Garcia et al., 2007*). The animal shows many of the metabolic and skeletal abnormalities characterizing the human disease, therefore representing a good model for MPS II. Our analysis detected hepatosplenomegaly, sometimes accompanied by cardiomegaly, and extremely high tissue GAG deposits. Significantly elevated urinary GAG levels can be measured in the model starting at 6-8 weeks of age, increasing with time, thus rendering the evaluation of urinary GAG level a useful indicator of pathology as well as of treatment efficacy. No plasmatic and tissue enzymatic activity is detected. The neurological involvement was first assessed by Cardone and colleagues (*Cardone et al., 2006*); brain GAG accumulation is mainly detected within the choroids plexus of the ventricular region (*Cardone et al., 2006; Friso et al., 2010*).

1.7 BLOOD-BRAIN BARRIER AND DRUG TRANSPORT

1.7.1 The blood-brain barrier

Each neuron is perfused by its blood vessel; it is estimated that in the human brain there are about 100 billion capillaries for a total of 600 km in length. This dense vascular network covers an area of about 20 square meters and is therefore the most important interface between the blood and the brain in terms of trade of gas and metabolites essential to support brain function (*Nag et al., 2005*).

The blood-brain barrier (BBB) is a real barrier between the bloodstream and the central nervous system (CNS), acting as a "selective biological filter", allowing or preventing the passage of substances (ions, glucose, protein, etc.) from the blood into the brain parenchyma and into the cerebrospinal fluid (CSF). Thanks

to this regulatory and selective function, BBB preserves the delicate chemical-physical homeostasis of the cerebral fluid environment. Therefore, BBB plays a protective role towards the CSF and the nervous tissue. Indeed, the BBB maintains the stable ionic environment and preserves the low aminoacidic gradient of the excitatory neurotransmitter (glutamic acid, aspartic acid and glycine), characteristic of the cerebral extracellular fluid. This is essential for a reliable synaptic transmission and an efficient neuroregulation activity. It also prevents the entry of toxic substances for cells, such metabolites and neurotoxins both endogenous and xenobiotic, potentially even fatal. In so doing, it promotes CNS longevity and prevents premature cell death and neurodegeneration (*Begley, 2004*).

The BBB consists of endothelium of brain capillaries, perivascular astrocyte processes surrounding the endothelial cells and pericytes, contractile connective cells that partially surround endothelial cells. The characteristic anatomical constitution of BBB is responsible for its functional peculiarities, such as limited permeability to most of the substances and the limited paracellular and trans-cellular transport. The brain capillaries are anatomically different from systemic peripheral capillaries, as the cells that compose them form a continuous endothelium, not fenestrated, and with a reduced number of pinocytotic cells. Moreover, there are tight junctions that prevent the free diffusion of solutes from the blood compartment (peripheral or systemic) to the CSF and brain (intrathecal), both at the level of the brain capillaries and choroid epithelium (*Abbott et al., 2010*).

Astrocytes and pericytes, located around endothelial cells, being in turn separated from the basal membrane by an extracellular matrix of collagen, help to ensure further compactness to this anatomical and functional unit (*Abbott et al., 2010*).

Therefore, to convey a drug to the brain is necessary to consider the structural and functional characteristics of the BBB and evaluate the chemical and physical properties (pKa, molecular weight, lipophilicity, etc.) of the drug. We must also consider its intrinsic ability to form bonds with the plasma proteins that prevent

the passage to the CNS; the degree of ionization (pH) (ionized drugs do not penetrate into the CNS) and the lipid/water partition coefficient. Drugs with a high partition coefficient, ie fat-soluble and with a molecular weight below 400-500 Da, are able to cross the membranes and penetrate into the CNS by simple passive diffusion; those with low partition coefficient can penetrate the CNS only by carrier-mediated transport (*Scarpa et al., 2012*).

It has been estimated that about 98% of the drugs for the treatment of cerebral pathologies cannot effectively overcome the BBB due to the lack of a specific mechanism of passage, or because of their high molecular weight or polarity (*Pardridge, 2005*).

1.7.2 Transport across the BBB

Oxygen, carbon dioxide, glucose, nucleosides, vitamins, and part of the fat-soluble drugs are able to cross the BBB due to mechanisms of passive diffusion (lipophilic substances) or through specific transport mechanisms (*Abbott et al., 1996; Begley et al., 2008*).The endogenous transport systems may be present on the luminal or abluminal side of the BBB and can be classified into three categories: 1) CMT Carrier-Mediated Transport (CMT); 2) Active Efflux Transport (AET); 3) Receptor-Mediated Transport (RMT). CMT and AET systems are responsible for the transport of small molecules between blood and brain, while the RMT systems allow the transport of larger molecules across the BBB. Among these the ATP Binding Cassette, the Organic Anion Transporting-Polypeptide and the Organic Anion Transporter play an important role.

In addition to the possibility to exploit or inhibit these and other transport mechanisms physiologically present on the BBB (*Pardridge, 2003*), other approaches, that can ensure a more effective channelling of drugs to the CNS, are being investigated. The approaches to achieve effective concentrations of drugs into the CNS may be invasive (temporary rupture of tight junctions, intracerebral injection or use of intracerebral implants such as catheters, microchip or erodible polymer systems). These approaches are still difficult to apply, expensive and potentially dangerous for patients, since the direct delivery

of the drug exposes patients to the risk of developing serious brain infections, resulting in significant decrease in their compliance. Therefore, the research is primarily aimed at developing non invasive approaches (chemical, biological or technological) (*Scherrmann, 2002*).

1.7.3 Nanotechnologies and BBB

Today knowledge in pharmaceutical nanotechnology combined with expertise in biomedical sciences represents an important promise for the distribution of drugs across the BBB (*Kreuter, 2013*). Nanomedicine, which involves the use of nanoparticles or nanostructures, is a rapidly evolving field with great expectations, given the ability of multifunctional nanoparticles to cross the BBB. Maybe the most difficult task will be to design and develop nanoparticles that can specifically target a subset of neurons without affecting other neuronal populations. Underlying this approach is the design and testing of micro/nano particles, micro/nano capsules, lipoproteins, liposomes and micelles for the transport and release of the drug into the CNS.

Various types of vesicular structures or matrix have been defined, in which the drug is localized into the cavity enclosed by the polymeric membrane or is physically and uniformly dispersed in a polymer matrix. In addition to these traditional systems other more innovative ways, such as the use of dendrimers, nanogels, nanoemulsions and nanosuspensions (*Begley et al., 2008; Wong et al., 2012; Wagner et al., 2012*) are also being tested. All these materials are carefully formulated, so as to be biodegradable, biocompatible, non-toxic and non-immunogenic. They allow a release of the drug according to predetermined kinetics. Polymeric nanoparticles, whose size generally vary between 100-400 nm, constitute one of the most promising approaches, since their polymeric structure makes them more stable in biological fluids, ensuring protection of the drug from degradation of the biological environment compared to phospholipid bilayer of vesicles or liposomes. They are generally constituted by biocompatible and biodegradable materials, such as butyl cyanoacrylate (PBCA), human serum albumin (HSA), and lactic-co-glycolic acid (PLGA). Thanks to their small size they

can transport drugs across the BBB by endocytosis, by the endothelial cells lining the blood vessels of the brain and probably also by transcytosis of the nanoparticles themselves. Given the promising perspectives, new types of nanoparticles have been developed, obtained from polymers modified with appropriate peptidic ligands, which improve the biocompatibility and increase the selectivity. This solution is able to ensure high specificity in terms of BBB crossing for efficient drug delivery to the CNS, useful in the treatment of neurodegenerative brain diseases, tumours, ischemia and cerebral infections difficult to treat (*Costantino et al., 2005*). Not only, it also results in a beneficial reduction of the therapeutic dose, resulting in a decrease of the collateral damage of the drugs; the addition of these peptidic ligands promotes direct interaction with the transport systems to the CNS (*Grabrucker et al., 2011; Tosi et al., 2011a*).

This approach probably represents the future for treatment of LSDs and not only. The ability to assemble molecules with high and low molecular weight, siRNA, etc. inside molecules that are conveyed through the BBB, without altering it, surely will have an applicative development also for more common neurodegenerative, such as Parkinson's disease, Alzheimer's disease, etc. Currently, preclinical studies have not shown particular adverse events following intravenous or repeated localized administrations; moreover, the use of peptides binding receptors on different organs enable the correction of other districts, as well as the neurological compartment (*Scarpa et al., 2012*).

Since nanoparticles are now proposed in oncology (Jabir et al., 2012), with significant results in the control of some forms of cancer, further studies are needed to verify the absence of possible side effects resulting from chronic administration, given that substances used in production may induce immunological reactions (*Syed et al., 2013*).

1.8 PLGA-NANOPARTICLES FOR CNS THERAPY

Polymeric nanoparticles (NPs) showed to be promising carriers for CNS drug delivery, due to their potential both in encapsulating drugs, hence protecting them from the body excretion and metabolism, and in delivering active agents across the BBB without inflicting any damages to the barrier itself (*Kabanov et al., 2007; Tosi et al., 2008*). Different polymers have been tested and different strategies have been applied; among these, mainly the use of poly-lactide-co-glycolide (PLGA), an FDA-approved polymer, and of specific ligands, able to render the delivery of drugs to CNS more targeted, has been recently considered (*Costantino et al., 2009; Ruozi et al., 2014a; Tosi et al., 2014a; Vilella et al., 2014; Tosi et al., 2013a; Tosi et al., 2013b; Tosi et al., 2013c*). In particular, it was shown that the PLGA-NPs derivatized with the peptide H2N-Gly-L-Phe-D-Thr-Gly-L-Phe-L-Leu-L-Ser(O-β-D-Glucose)-CONH2 [g7] are able to cross the BBB (*Tosi et al., 2007*).

Several experiments were performed, starting with an electron microscopy study and the recognition of g7-NPs at the BBB level after intravenous administration in rats and computational analysis on glycopeptides covering NPs. The results highlighted an interaction between g7-NPs and the BBB and endocytosis/macropinocytosis pathways for BBB crossing (*Tosi et al., 2011b; Sahay et al., 2010*).

The same results were also highlighted *in vitro* on neurons/glial cell cultures (*Grabrucker et al., 2011*), evidencing the endocytotic pathways as g7-NPs cell entrance as well as assessing the safety of g7-NPs since they do not create any damage to cells, even at high doses. Other previous *in vivo* biodistribution and pharmacological proof-of-evidence studies of brain delivery of model drugs (not able to reach the brain alone, such as rhodamine-123 and loperamide) demonstrated the ability of g7-NPs to create BBB interaction and trigger an efficacious BBB crossing (*Tosi et al., 2007, 2008, 2010, 2011b*), up to 10–15% of the injected dose (*Vergoni et al., 2009*).

The fate of g7-NPs inside the CNS, once crossed the BBB, was investigated in neuronal cells and in mice, elucidating the uptake pathways in neurons both *in*

vitro and *in vivo*. In particular, clathrin and Rab-5 pathways were identified as responsible for NPs uptake and trafficking into neuronal cells. Interestingly, following intracellular passage, g7-NPs were found to be transferred, in different percentages, from cell to cell by tunneling nanotubes, released outside the cells or accumulate in lysosome vesicles. This last finding, considered a drawback for drug delivery to neurons cytoplasm, as recently reported (*Chhabra et al., 2014*), in the case of LSDs can, on the opposite, be considered an advantage since lysosomes, site of NPs accumulation, are themselves targets for LSDs therapy.

At present, some clinical trials have proposed the use of PLGA-NPs as drug carriers, but none has so far evaluated their use for the treatment of CNS diseases. In the context of LSDs, the set-up of a therapeutic protocol addressing the neurological deficit would dramatically improve patients' conditions.

2. AIMS

Lysosomal Storage Disorders (LSDs) are a group of neurometabolic syndromes, mostly due to the deficit of one lysosomal enzyme. Many LSDs affect most of the organ systems and about two-thirds of the patients present neurological and cognitive impairment.

Enzyme replacement therapy (ERT), the most common therapeutic strategy applied to some LSDs, although determining some clinical improvements, has revealed to be ineffective on the CNS disease, due to enzymes' inability to cross the blood-brain barrier (BBB).

Among LSDs, Mucopolysaccharidosis type I (MPS I, Hurler syndrome) and Type II (MPS II, Hunter syndrome) are both characterized by a lack of activity of lysosomal enzymes involved in the catabolism of the glycosaminoglycans eparan- and dermatan-sulfate, therefore accumulated in the cell compartment and in the extracellular matrix. While presenting different forms of clinical severity and different degrees of progression, both diseases affect most organs and systems and about 2/3 of the patients have an important cognitive and neurological involvement.

ERT, applied to both diseases in recent years, has shown some clinical improvement, but also some limitations: among these the inability to transport acid hydrolases across the BBB, due to the high molecular weight, which makes any paracellular or transcellular diffusion of these proteins practically not-existent. Therefore, it is necessary to evaluate alternative methods to reach the CNS.

With this aim, we evaluated the ability of polymeric nanoparticles (PLGA-NPs), modified with a glycopeptide of 7 amino acids (g7), already tested for molecules of low molecular weight, to bypass the BBB and deliver the therapeutic recombinant enzymes to the CNS after systemic administration in the mouse models for the two diseases, ensuring a prolonged drug release and protection from inactivation.

Before conducting a functional and efficacy study, we performed several preliminary experiments to explore the ability of the g7-PLGA-NPs (g7-NPs) to transfer through the BBB of the MPS I and MPS II mouse models a model drug (FITC-albumin) with a high molecular weight, comparable to that of the recombinant enzymes used for ERT.

Thereafter, we evaluated *in vitro* the ability of untargeted PLGA-NPs (devoid of g7), loaded with the recombinant enzyme for MPS II (u-NPs-IDS), to maintain the therapeutic activity of the drug.

Finally, we tested *in vivo*, in the MPS II mouse model, efficiency and efficacy of the g7-NPs loaded with the recombinant enzyme (g7-NPs-IDS).

Evaluation of safe delivery systems able to transport therapeutic drugs across the blood-brain barrier, in addition to allow efficacy studies for neuronal LSDs, may also provide new hope for the treatment of other neurometabolic disorders as well as chronic neurodegenerative diseases.

3. MATERIALS AND METHODS

3.1 MOUSE MODELS

The C57BL/6 Idua knockout (Idua-ko) mouse, providing the model for MPS I, generated in the laboratory of Dr. Neufeld (David Geffen School of Medicine, UCLA, USA), was kindly provided by Dr. Heard (Pasteur Institute, Paris, France); the mouse was generated by targeted gene disruption of the murine Idua gene and previously characterized (*Ohmi et al., 2003*).

The C57BL/6 Ids knockout (Ids-ko) mouse, providing the model for MPS II, was a kind gift of Dr. Muenzer (University of North Carolina, NC, USA) and was generated by gene disruption of the murine Ids gene and previously characterized (*Muenzer et al., 2002; Friso et al., 2005; Cardone et al., 2006; Garcia et al., 2007*).

Both colonies were expanded in our animal facility and mice were genotyped by multiplex PCR. In the experiments here described Idua-ko, Ids-ko and wild-type (wt) mice were housed in light and temperature controlled conditions, with food and water provided ad libitum. All animal care and experimental procedures were conducted according to the current national and international animal ethics guidelines.

3.2 NANOPARTICLES

All different batches of nanoparticles were prepared and analysed by the Te.Far.TI group (Department of Life Sciences, University of Modena and Reggio Emilia) in the figure of Dr. Giovanni Tosi and his laboratory.

All the nanoparticles (NPs) used in this study were prepared by the technique of water/oil/water (W/O/W) double emulsion, which, as reported in literature, is the most suitable for the encapsulation of hydrophilic molecules (*Jain RA, 2000*).

3.2.1 Chemicals

Poly(D,L-lactide-co-glycolide) (PLGA, RG503H, MW near 11,000) was used as received from the manufacturer (Boehringer-Ingelheim, Ingelheim am Rhein, Germany). Polyvinyl alcohol (PVA, MW 15,000) was purchased from Sigma-Aldrich (Milan, Italy). Gly-L-Phe-D-Thr-Gly-L-Phe-L-Leu-L-Ser(O-β-D-Glucose)-$CONH_2$ (g7) linked to biotin was synthetized as previously reported (*Tosi et al., 2014*) and purchased from Mimotopes (Clayton, Victoria, Australia). PLGA conjugated with Rhodamine B piperazine amide (Sigma-Aldrich) (R-PLGA) was prepared as previously described (*Bondioli et al., 2010; Tosi et al., 2011a*). Trehalose dihydrate (MW 378.33) was purchased by Sigma-Aldrich and used as cryoprotectant. Maleimide activated Neutravidin (NA-Maleido) was obtained by Thermo Scientific. A MilliQ water system (Millipore, Bedford, MA, USA), supplied with distilled water, provided high-purity water (18 MΩ). All the other chemicals were of analytical grade.

3.2.2 NPs/Alb preparation

Nanoparticles (NPs) were prepared by a double emulsion technique (*Rosca et al., 2004; Ruozi et al., 2014b*). Briefly, 1 ml of FITC-albumin water solution (20mg/ml) was emulsified in 5 ml CH_2Cl_2 solution of polymer (95 mg of PLGA and 5 mg of R-PLGA) under cooling (5°C) by using a probe sonicator (Microson Ultrasonic cell disruptor, Misonix Inc. Farmingdale, NY, USA) at 80W for 45 sec to obtain a w/o emulsion (first inner emulsion). The first inner emulsion was rapidly added to 12 ml of 1% (w:v) PVA aqueous solution and the w/o/w emulsion was formed under sonication (80W for 45 sec) at 5°C. Formulation was mechanically stirred (1,500 rpm) for at least 1h (RW20DZM, Janke&Kunkel, IKA-Labortechnik, Staufen, Germany) at RT until the complete solvent evaporation and finally purified by Hi-Speed Refrigerated Centrifugation (Beckman J21) at 17000 rpm for 10 min at 5°C, washed several times with water and re-suspended in water. This technique allowed to obtain labelled Alb-loaded un-modified NPs (u-NPs/Alb), used as controls. As control samples, un-loaded NPs were obtained by substituting the

FITC-albumin solution with saline solution, leading to un-targeted un-loaded NPs (u-NPs).

In order to obtain brain targeted NPs (un-loaded g7-NPs or loaded g7-NPs/Alb) g7 was conjugated on the surface of NPs using a post-modification approach (*Nobs et al., 2004*).

Briefly, 50 mg of each preparation was suspended in 2-(N-morpholino) ethanesulfonic acid (MES, Sigma Aldrich) buffer and reacted with 50 mg of N-Hydroxy-succinimide (NHS, Sigma Aldrich) and 150 mg of 1-Ethyl-3-(3-dimethylaminopropyl)-carbodiimide (EDC; Sigma Aldrich, Saint Luis, MO) to activate carboxylic group of the polymer. After 1 hour, activated NPs were collected by ultracentrifugation at 17000 rpm for 10 min at 4°C and the excess of reagents was removed. NPs were re-suspended in PBS pH 7.4 and reacted with 2 mg NA-Maleido, previously activated by adding 20 µl of cysteamine (2mg/ml). Mixture was mechanically stirred for 2 hours at RT and the neutravidin modified NPs (NA-NPs) were purified by Hi-Speed Refrigerated Centrifugation (Beckman J21) at 17000 rpm for 10 min at 5°C. Finally, biotinylated g7 peptide (2.6 mg) was solubilized in 1 ml of water and reacted with NA-NPs for 1 hour at room temperature. G7 modified nanoparticles were than purified by centrifugation as previously described for un-targeted NPs.

All the NP formulations were frozen using trehalose as cryoprotectant (1:1 w:w polymer/trehalose ratio) and stored at -20°C.

Other control samples included a mixture of un-loaded targeted NPs (g7-NPs) suspended in FITC-albumin solution (MIX1), un-loaded un-targeted NPs (u-NPs) suspended in FITC-albumin solution (MIX2).

3.2.3 NPs-IDS preparation

2.5 ml of Elaprase® (corresponding to 5 mg of IDS enzyme) were lyophilized and then resuspended in 500 µl of deionized water to obtain an enzyme solution with a concentration of about 10 mg/ml. This solution was emulsified in 2.5 ml CH_2Cl_2 solution of polymer (45 mg PLGA + 5 mg g7-PLGA for g7-NPs-IDS, or 42.5 mg PLGA + 5 mg g7-PLGA + 2.5mg R-PLGA) under cooling (5°C) by using a probe

sonicator (Microson Ultrasonic cell disruptor, Misonix Inc. Farmingdale, NY, USA) at 80W for 45 sec to obtain a w/o emulsion (first inner emulsion). The first inner emulsion was rapidly added to 8 ml of 1% (w:v) PVA aqueous solution and the w/o/w emulsion was formed under sonication (80W for 45 sec) at 5°C. Formulation was mechanically stirred (1,500 rpm) for at least 1h (RW20DZM, Janke&Kunkel, IKA-Labortechnik, Staufen, Germany) at RT until the complete solvent evaporation and finally purified by Hi-Speed Refrigerated Centrifugation (Beckman J21) at 17000 rpm for 10 min at 5°C, washed several times with water and re-suspended in water.

All the NP formulations were frozen using trehalose as cryoprotectant (1:1 w:w polymer/trehalose ratio) and stored at -20°C.

3.2.4 NPs characterization

3.2.4.1 Chemico-physical characterization

All the batches of NPs were characterized regarding their surface, chemico-physical and morphological properties. In particular, for surface properties (size and charge), NPs in distilled water were analyzed by photon correlation spectroscopy (PCS) and laser Doppler anemometry using a Zetasizer Nano ZS (Malvern, UK; Laser 4 mW He–Ne, 633 nm, Laser attenuator Automatic, transmission 100% to 0.0003%, Detector Avalanche photodiode, Q.E. > 50% at 633 nm, T = 25°C). The results were normalized with respect to a polystyrene standard solution.

To evaluate shape and morphology of NPs, a scanning electron microscope (SEM) (XL-40; Philips, Eindhoven, The Netherlands) operating at 8 kV was used. NPs were re-suspended in distilled water after at least 3 washings with water, and a drop of the suspension was placed onto a SEM sample holder and dried under vacuum (10–2 mmHg). The dried samples were coated under argon atmosphere with a 10 nm gold palladium thickness (Emitech K550 Super Coated; Emitech Ltd, Ashford, Kent, UK) to increase electrical conductivity. The NPs were then

processed for the evaluation of their morphology and shape by analyzing images at different magnifications (13,000× to 16,000×).

Moreover, Atomic Force Microscopy (AFM) was used for morphological assessments. In particular, AFM was used (Park Instruments, Sunnyvale, CA, USA) at RT (about 20°C), at atmospheric pressure (760 mmHg) operating in air and in non-contact mode, using a commercial silicon tip-cantilever (tip diameter ≈5-10 nm) with stiffness about 40 Nm-1 and a resonance frequency around 150 kHz. A little amount of each NP sample was dispersed in deionised water (about 40 µL) on a small freshly cleaved mica disk (1 cm x 1 cm). After 2 min from the deposition, the excess of deionised water was removed by a blotting paper and the sample observed. Two kinds of images were obtained: the first one is a topographical image and the second one is the 3D elaboration. The AFM images were obtained with a scan rate of 1 Hz and processed using a ProScan Data Acquisition software developed under Windows 95.

3.2.4.2 Albumin and IDS content

Freeze-dried NPs (5 mg) were dissolved in 1 ml of DCM. Then, 3 ml of PBS, pH 7.4 were added to extract the FITC-albumin or IDS and the organic solvent was evaporated at RT under stirring (1,500 rpm for at least 1h; RW20DZM, Janke&Kunkel, IKA-Labortechnik, Staufen, Germany). The aqueous solution was filtered (cellulose acetate filter, porosity 0.2 µm, Sartorius) to remove the polymer residues and spectrophotometrically analysed at 492 nm to evaluate the FITC-albumin or IDS concentration. The drug loading was expressed as mg of FITC-albumin or IDS encapsulated/100 mg of NPs and as encapsulation efficiency (EE%), i.e. the percentage of encapsulated drug related to the initial amount of drug used in the preparation.

3.2.4.3 ESCA analysis

The presence of g7 on NPs surface was demonstrated by electron spectroscopy for chemical analysis (ESCA), showing the presence of nitrogen atoms on the surface of antibody-engineered NPs, as previously described (*Liu et al., 2010*).

ESCA was performed on a XRC 1000 X-ray source analysis system (Specs Surface Nano Analysis, Germany) and a Phoibos 150 hemispherical electron analyzer (Specs Surface Nano Analysis, Germany), using MgKα1,2 radiations. Spectra were recorded in fixed retardation ratio (FAT) mode with 40 eV pass energy. The pressure in the sample analysis chamber was around 10–9 mbar. Data were acquired and processed using the SpecsLab2 software.

3.3 IN VIVO PRELMINARY STUDY OF g7-NPs IN MPS I AND MPS II MOUSE MODELS

The preliminary study was conducted to evaluate the ability of the g7-PLGA-NPs (g7-NPs) to transport high molecular weight molecules to the CNS. Albumin was used as a model drug.

Idua-ko, Ids-ko and matched wt mice (5-8 months old) were intravenously (iv) injected as indicated in **Table IV**. For each batch of PLGA-NPs, 2 mg were intravenously injected in each mouse; as for albumin, 0.2 mg/animal were injected, both free and NPs-loaded.

3-5 animals were sacrificed 2h post-injection by cervical dislocation for all type of treatment. Mice tissues (brain and liver) were collected and fixed in 4% paraformaldehyde and 0.2% picric acid in 1X PBS for 48h. Then, tissues were subjected to a sucrose gradient: 15% sucrose in PBS for 24h and then 30% sucrose in PBS for additional 24h. Finally, tissues were embedded in Tissue-Tek® O.C.T™ Compound (Sakura) and snap-frozen using dry ice. Before freezing, brains were cut at bregma level. Serial 5 µm thick cryosections, from the bregma to the cerebellum, were obtained, washed 3 times in cold PBS, mounted with Fluoromount™ (Sigma-Aldrich) with DAPI (BioChemica, AppliChem) and stored at +4°C until confocal analysis.

MOUSE MODEL	*TYPE OF INJECTION*
Idua-ko/wt	g7-NPs
	u-NPs
	Alb
	g7-NPs/Alb
	u-NPs/Alb
	MIX1 (g7-NPs+Alb)
	MIX2 (u-NPs+Alb)
	EB
Ids-ko/wt	Alb
	g7-NPs/Alb
	EB

Table IV: g7-NPs = un-loaded and targeted NPs; u-NPs = un-loaded and un-targeted NPs; Alb = Albumin; g7-NPs/Alb = targeted NPs loaded with albumin; u-NPs/Alb = un-targeted NPs loaded with albumin; MIX1 (g7-NPs+Alb) = un-loaded targeted NPs suspended in FITC-albumin solution; MIX2 (u-NPs+Alb) = un-loaded and un-targeted NPs suspended in FITC-albumin solution; EB = 2% Evans blue solution. *n=3-5* for all type of injection and for both mouse model (Idua-ko and syngeneic wt; Ids-ko and syngeneic wt).

3.4 CHECKING BBB INTEGRITY

To check BBB integrity and exclude possible damages, we used Evans blue (EB) fluorescent dye (MW: 960.8, Sigma-Aldrich), as a tracer. Since serum albumin cannot cross the barrier, and virtually all EB is bound to albumin, if BBB is intact, the neural tissue remains unstained (*Kozler and Pokorný, 2003*); instead, when BBB is compromised, the albumin-bound EB enters the CNS. In this study 50 µl of a 2% solution EB in 0.9% NaCl was iv-injected in Idua-ko, Ids-ko and respective wt mice. Four hours later mice were sacrificed by cervical dislocation and the brains collected and processed as described in *section 3.3*.

3.5 IN VIVO PRELMINARY STUDY OF g7-NPs-IDS-R IN THE MPS II MOUSE MODELS

To confirm that g7-NPs can transport IDS through the BBB, a preliminary study was conducted using g7-NPs loaded with recombinant IDS (Elaprase®, Shire Human Genetic Therapies, Inc, Cambridge, MA, USA) and marked with Rhodamine (g7-NPs-IDS-R).

6 Ids-ko and 6 wt mice were iv-injected with g7-NPs-IDS-R (corresponding to 0.5 mg/kg of IDS) and sacrificed after 2h. Livers and brains of 3 Ids-ko and 3 wt mice were fixed in 4% paraformaldehyde and 0.2% picric acid in 1X PBS for 48h; then they were processed as described in section 3.3.

Brains of 3 Ids-ko and 3 wt mice were separated in the capillary and parenchymal fractions and the last one analyzed for IDS activity (see *section 3.9* for both protocol details).

3.6 IN VITRO ANALYSIS OF u-NPs-IDS EFFICACY

To verify NPs capability to encapsulate the recombinant enzyme and transport it to the cells maintaining its therapeutic efficacy, an *in vitro* study was conducted on primary fibroblasts obtained from MPS II and healthy control patients.

Human fibroblasts from skin biopsy of 3 MPS II pediatric patients, carrying different mutation in IDS gene, were obtained from “Cell Line and DNA Bank from Patients Affected by Genetic Diseases”, Gaslini Institute (Genoa, Italy). As healthy controls, human fibroblasts from 3 children circumcisions were used; they were obtained from the Histology Unit of the Department of Histology, Microbiology and Medical Biotechnology (University of Padua, Padua, Italy). Written informed consents were obtained from patients at the time of biopsy. All cells were anonymously obtained.

Primary fibroblasts were cultured at 37°C in 5% CO_2 atmosphere in RPMI medium supplemented with 15% fetal bovine serum (FBS), 100 U/ml penicillin and 100 ng/ml streptomycin (all Life Technologies, Milan, Italy).

Cells were either treated with 15 mM free IDS or with IDS encapsulated in NPs (u-NPs-IDS) or untreated. Fibroblasts were treated for 7 days, then the treatment

was removed and cells sacrificed after 0, 7 and 14 days. Cell pellet was washed with 0.9% NaCl and then re-suspended in the same solution, sonicated and analyzed for induced IDS activity and GAG content (see *section 3.9* for protocol details).

3.7 IN VIVO PILOT STUDY IN THE MPS II MOUSE MODEL

To evaluate transfer efficiency and the enzymatic activity induced by g7-NPs loaded with the recombinant enzyme (g7-NPs-IDS), we conducted an *in vivo* pilot study in the MPS II mouse model.

Mice were treated with a single dose of free IDS, g7-NPs-IDS, u-NPS-IDS (all corresponding to 1mg/kg of IDS) or untreated. Plasma was collected by submandibular sampling after 4h, 24h, 7 and 14 days; then, it was analyzed for induced IDS activity (see *section 3.9* for protocol details).

After 7 or 14 days, 3 animals per treatment were sacrificed by cervical dislocation; organs (liver, kidney, spleen, heart) were collected and livers analyzed for induced IDS activity; brains were separated in the capillary and parenchymal fractions and the last one analyzed for IDS activity (see *section 3.9* for protocol details).

3.8 IN VIVO MEDIUM-TERM EFFICACY STUDY IN THE MPS II MOUSE MODEL

To assess the efficacy of g7-NPs-IDS, an *in vivo* study was conducted in the MPS II mouse model. 8 mice were treated once a week with g7-NPs-IDS (corresponding to 1 mg/kg of IDS) for 6 weeks. As control, 8 Ids-ko mice treated with free IDS, 8 untreated Ids-ko mice and 8 wt were also analyzed.

Before starting treatment (pre), after 3 weeks and after 6 weeks of treatment plasma was collected by submandibular sampling; urine was also collected using metabolic cages for 24 hours. Plasma was analyzed for induced IDS activity and urine for GAG content (see *section 3.9* for protocol details).

Mice were sacrificed by cervical dislocation after 6 weeks of treatment. Organs (liver, kidney, spleen, heart) of 5 mice per treatment (Ids-ko with g7-NPs-IDS, Ids-

ko with free IDS, untreated Ids-ko and wt) were collected and livers analyzed for induced enzyme activity and GAG content. Brains were separated in the capillary and parenchymal fractions and the second one subjected to the same analysis of livers.

The organs (brain, liver, kidneys, spleen, heart) of 3 mice per treatment were collected, and fixed in Bouin's solution. Brains and livers were analyzed by histological staining with Alcian Blue/Nuclear Fast Red for GAG content. Brains were also analyzed by staining with Toluidine (neurons), immunohistochemistry for GFAP (neuroinflammation) and MOMA-2 (monocyte/macrophage infiltration) (see *section 3.9* for protocol details).

3.9 PROTOCOLS

3.9.1 Brain capillary depletion

Brains were separated in the parenchyma and capillary fractions using a dextran density centrifugation as previously described by Triguero (*Triguero et al., 1990*). The brain was homogenised at 4° C (about 10 strokes) in 2 times the volume of a physiological buffer at pH 7.4, containing: 10 mM HEPES, 141 mM NaCl, 4 nM KCl, 2.8 mM $CaCl_2$, 1 mM $MgSO_4$, 1 mM NaH_2PO_4, and 10 mM D-glucose. Dextran solution was then added to a final concentration of 19% and homogenised for a further 10 stokes. Homogenate was centrifuged at 5000 g for 15 minutes at 4°C and supernatant (parenchyma) and pellet (capillary) were carefully separated.

3.9.2 IDS enzyme assay

Cell pellet was sonicated in 0.9% NaCl and tissue samples were homogenized in 0.9% NaCl using a Polytron® PT1200E Disperser (Kinematica AG, Luzern, Switzerland); after centrifugation, supernatants were recovered and protein concentration determined by the Bradford assay, using the Bio-Rad Protein Assay (Bio-Rad Laboratories, Milan, Italy).

Blood was collected in heparinized tubes and plasma obtained through microcentrifugation at 1000 rcf for 20 minutes; a volume of 10 µl of 5X diluted plasma was used to perform the enzyme assay, processed as described below.

IDS activity was evaluated by performing a fluorometric assay (*Vozny et al., 2001*) employing the substrate 4-methylumbelliferyl-α-iduronide-2-sulfate (MU-αIdu-2S; Moscerdam Substrates, Erasmus University, Rotterdam, The Netherlands). Briefly, 10 µg of protein were assayed by adding 20 µl of 1.25 mM substrate and incubating at 37°C for 4h. Afterwards, 20 µl of double concentrated McIlvains phosphate/citrate buffer and 10 µl of LEBT (lysosomal enzymes purified from bovine testis) were added to each sample and incubated at 37°C for a further 20h. The reaction was stopped by adding 1440 µl/sample of stop buffer (0.5 M $NaHCO_3$/0.5 M Na_2CO_3, pH 10.7, 0.025% Triton X-100); 4-methylumbelliferone (Sigma-Aldrich) was used as standard. Fluorescence was measured in 24-well plates on a multi-well reader Victor2 1420 (PerkinElmer, Milano, Italy). Positive and negative controls were used in each assay. IDS activity is given in nanomoles of substrate hydrolyzed in 4 h per milligram of protein or milliliter of plasma [1 nmol/4 h/mg (ml) = 1 Unit/mg (ml)].

3.9.3 Cell/tissue GAG content

Cell pellet was sonicated in 0.9% NaCl before using it for the assay. Tissue were lyophilized, homogenized in 0.9% NaCl + 0.2% Triton X-100 (PanReac AppliChem GmbH, Darmstadt, Germany) by a Polytron® PT1200E Disperser (Kinematica AG, Luzern, Switzerland), left under stirring overnight at 4°C, centrifuged at 1000 rcf for 5 min and the supernatant recovered.

GAG content was measured by using Bjornsson's protocol (*Bjornsson, 1993*), with modifications previously described by Friso and colleagues (*Friso et al., 2008*). The assay was performed by diluting 50 µl of blank (water), calibrators (chondroitin sulphate C) or samples with an equal volume of 8 M guanidine HCl, and then 0.3% H_2SO_4/0.75% Triton X-100. Samples were incubated o/n at 4°C in the presence of Alcian Blue solution. Following centrifugation, pellets were washed with 40% DMSO/0.05% $MgCl_2$ and re-suspended in 4 M guanidine

HCl/33% isopropanol/0.25% Triton X-100. All reagents were purchased from Sigma-Aldrich (Milan, Italy). Absorbance was measured at 620 nm in a multi-well reader Victor2 1420 (PerkinElmer, Milano, Italy). GAG content was calculated as mg GAG/mg protein, and protein content was determined using the Bio-Rad Protein Assay (Bio-Rad Laboratories, Milan, Italy).

3.9.4 Urinary GAG content

Urinary GAG content (calculated as mg GAG per mg creatinine) was determined using the protocol described by de Jong and colleagues (*de Jong et al., 1992*) with modifications. GAG content was determined in 24h urine samples, diluted 1:16, 1:32, 1:64 and mixed with 8 M 1,9-dimethylmethylene blue chloride (Sigma-Aldrich, Milano, Italy), 0.05 M Na-formate (Sigma-Aldrich) and 0.18 M Tris-HCl (Merck, Milano, Italy) to pH 8.8. A standard curve was prepared using chondroitin sulphate type C (Sigma-Aldrich). Absorbance was measured at 520 nm in a multi-well reader Victor2 1420 (PerkinElmer, Milano, Italy). Urinary creatinine was measured by mixing diluted 1:5 and 1:10 urine with picric acid (Sigma-Aldrich) diluted 1:5 and 7.5 g/l sodium hydroxide. Absorbance was measured at 535 nm and compared with creatinine standard solutions (Sigma-Aldrich).

3.9.5 Alcian blue and toluidine staining

Mice were killed and tissues rapidly dissected and fixed for 48h in Bouin's solution. Thereafter, tissues were extensively washed in 70% ethyl alcohol, dehydrated through a 70–100% ethanol gradient and paraffin embedded. Sections (4 µm) were cut, deparaffinized and stained with: 1% Alcian Blue (Sigma-Aldrich) solution pH 1.0 and 0.1% Nuclear Fast Red (Sigma-Aldrich) as counterstain; 0.1% Toluidine Blue O (Sigma-Aldrich) solution pH 4.2. All sections for the same organ obtained from wild-type, untreated Ids-ko and treated Ids-ko mice were stained at the same time. Sections were analyzed without knowing the treatments (blind analysis).

3.9.6 Immunohistochemistry and immunofluorescence

Mice were killed and tissues rapidly dissected and fixed for 48h in Bouin's solution. Thereafter, tissues were extensively washed in 70% ethyl alcohol, dehydrated through a 70–100% ethanol gradient and paraffin embedded.

4 µm thick serial sections were treated for antigen retriever with a 10mM sodium citrate buffer pH 6.0 for 15 min at 100°C in a moist environment. The specimens were incubated for 1 h with blocking buffer (10% FBS in PBS1X) (Gibco, Life technologies) before incubation overnight with the primary antibodies.

For immunohistochemistry a polyclonal rabbit antibody against GFAP (diluted 1:1000, Novus Biological, Cambridge, UK) was used. Then, a secondary AP(alkalin-phosfatse)-conjugated antibody (Life Technologies) was incubated for 1h. The color was developed for about 15 min using the NBT/BCIP (nitro-blue tetrazolium chloride/5-bromo-4-chloro-3'-indolyphosphate p-toluidine salt) method (Roche, Milan, Italy). In the end, a counterstain with a 0.5% eosin solution was performed and sections mounted with Eukitt® (Sigma-Aldrich).

For immunofluorescence a rat monoclonal antibody against mouse LAMP2 (diluted 1:100, ABCAM, Cambridge, UK) was used. Then, a secondary Alexa594-conjugated antibody (Life Technologies) was incubated for 1h. Stained sections were mounted with Fluoromount™ (Sigma-Aldrich) with DAPI (Applichem).

All sections for the same organ obtained from wild-type, untreated Ids-ko and treated Ids-ko mice were stained at the same time. Sections were analyzed without knowing the treatments (blind analysis).

3.9.7 Statistical analysis

Statistically significant differences between groups were determined using Student's t test. Data are presented as mean ± standard deviation. Null hypothesis probabilities < 0.05 were considered statistically significant.

3.10 MICROSCOPY ANALYSIS

Confocal analysis (Confocal Microscope Leica DM IRE 2, Bannockburn, IL, USA) was performed following the same procedure already reported (*Bondioli et al., 2011*). Visible analysis was performed using a Microscope Leica DM 4000B.

All samples were analysed in multiple procedures and in triplicate for each analysis using ImageJ software (http://imagej.nih.gov/ij). In particular, the analysis on confocal microscopy was performed by evaluating at least 6-8 optical fields (with 20 as average number of nuclei each field) for each sample analysed. For each brain, at least 5 slices were analysed.

Statistical evaluation was performed by using Student's t-test. Differences were considered statistically significant for $p < 0.05$.

4. RESULTS AND DISCUSSION

Drug delivery to the brain represents one of the most stimulating challenges in neuro-research, giving the limited number of therapeutics capable to reach the CNS. In fact, 98% of the drugs are unable to cross the BBB owing to their high molecular weight or chemico-physical properties (*Pardridge, 2005*). To improve drug delivery to the brain, non-invasive techniques have been investigated and, among them, the nanotechnology-based approach surely represents one of the most promising.

In this study, we evaluated the ability of polymeric nanoparticles (PLGA-NPs), modified with a glycopeptide of 7 amino acids (g7), already tested for molecules of low molecular weight, to bypass the BBB and deliver the therapeutic recombinant enzymes to the CNS, after systemic administration in the mouse models for two diseases, ensuring a prolonged drug release and protection from inactivation.

4.1 NPs FEATURES

All different batches of nanoparticles were prepared and analysed by the Te.Far.TI group (Department of Life Sciences, University of Modena and Reggio Emilia) in the figure of Dr. Giovanni Tosi and his laboratory, under a project partly funded by the CaRiPaRo Foundation (Padova, Italy).

All the nanoparticles (NPs) used in this study were prepared by the technique of water/oil/water (W/O/W) double emulsion, which, as reported in literature, is the most suitable for the encapsulation of hydrophilic molecules (*Jain, 2000*).

4.1.1 NPs for preliminary in vivo experiment with Albumin

All NPs were characterized in terms of size, surface charge, drug loading and surface composition (**Table 1**). In particular, all NPs, independently from surface modification or loading, were featured by dimension under 300 nm, thus compatible with a systemic administration, good homogeneity (as PDI values are ranging between 0.08 and 0.1 indicating an homogeneous population of NPs)

and negative surface charges, as usual when considering PLGA NPs (*Tosi et al., 2007; Vergoni et al., 2009*).

Some differences in chemico-physical parameters could be recognized by comparing un-loaded and loaded NPs; in particular, loaded samples, formulated at 1:5 drug to polymer molar ratio, were characterized by a significant increase in Z-Average diameter (form 230 to 260), probably due to the encapsulation of a high MW molecule, but resulting however in an homogeneous size distribution (PDI=0.01). In these samples, ζ-pot slightly decreased (about -22 mV) probably for the different reorganization of polymer chains in the presence of loaded albumin.

Samples	*Z-Average[a] nm (±S.D)*	*PDI[a] (±S.D)*	*Di50[a] nm (±S.D)*	*Di90[a] nm (±S.D)*	*ζ-pot[a] mV (±S.D)*	*mg of FITC Alb/100 mg NPs (±S.D)*	*EE%[b] (±S.D)*	*N/C ratio*
u-NPs	221 (7)	0.08 (0.02)	230 (9)	330 (4)	-16 (4)	/	/	0.010
g7-NPs	234 (8)	0.11 (0.03)	231 (5)	335 (9)	-14 (3)	/	/	0.024
u-NPs/Alb	260 (7)	0.11 (0.03)	275 (5)	480 (8)	-21 (5)	10.4 (1.1)	50 (5)	0.012
g7-NPs/Alb	261 (8)	0.08 (0.02)	268 (4)	375 (9)	-24 (4)	7.3 (0.1)	36 (4)	0.025

Table 1: chemico-physical characterization of nanoparticles.

PDI means Poly dispersity index, ζ-pot represents zeta potential indicating surface charge, EE is encapsulation efficiency. N/C is reported for each sample where C represents the percentage of Carbon signals onto NPs surface and N represents Nitrogen signals. As commonly accepted, when the molecule (i.e. g7 peptide) modifying the surface of NPs is rich of N, the presence of N signals onto NPs surface is considered as the proof of the surface engineering. The lower is the N/C value the lower is the presence of the molecule modifying the NPs surface.Di50 and Di90 are referring to dimensional distribution values (50 and 90).

[a]Values are given as mean±S.D. (n=9)

[b]The percentage of encapsulation efficiency was determined as the ratio of the encapsulated out of the total (encapsulated + free) drug per cent (%). Values are intended as mean±S.D. (n = 9).

Percent of loading efficiency (EE%) of u-NPs and g7-NPs is quite different, with a decrease in Alb content of about 30% in g7-NPs/Alb with respect to u-NPs/Alb. This data is not surprising, since the loading process with Alb represents the first step in the formulation of NPs, followed by activation of NPs and conjugation with peptides, suspended and stirred in aqueous medium, thus leading to a possible lost in drug content (*Bondioli et al., 2011*).

Interestingly, the surface analysis of NPs by ESCA described the presence of g7 onto NPs surface, as confirmed by an increased nitrogen/oxygen ratio in g7-NPs (both unloaded and loaded with Alb). As expected, the same data were not recovered for un-modified NPs, and this nicely correlates with previous reports on the surface engineering of PLGA NPs (*Nobs et al., 2006; Hao Yan et al., 2012; Nobs et al., 2004; Nobs et al., 2003*). The analysis conducted on the activated NPs (intermediate step of formulation obtained by neutravidin activation) did not show a significant increase in N/C ratio with respect to un-modified NPs (i.e. N/C ratio=0.12) (data not shown) as previously reported (*Nobs et al., 2006; Hao Yan et al., 2012; Nobs et al., 2004; Nobs et al., 2003*). This confirmed that the amount of nitrogen onto activated NPs is negligible with respect to that derived from g7 surface modification.

From a morphological point of view, AFM (Atomic Force Microscopy) and SEM (Scanning Electron Microscopy) (**Figure 1a and 1b**) analyses confirmed that unloaded samples were formed by spherical structures with diameter in agreement with photon correlation spectroscopy (PCS) data and regular surface.

Considering loaded NPs, microscopic examination, and particularly AFM outputs, displayed more complicated structures. Although still spherical, u-NPs/Alb showed a discontinuous and rough surface (**Figure 1c**). On the opposite, g7-NPs/Alb appeared with a more regular and homogeneous surface; this fact is likely to be attributed to the surface modification process, when the adsorbed FITC-albumin is partially removed and washed from the NPs surface. This finding is also evident by the content analysis previously exposed, evidencing a decrease of Alb content in g7-NPs versus u-NPs. Moreover, a slight tendency to

aggregation, once on mica surface, could be highlighted in the case of g7-NPs, probably due to the presence of neutravidin and g7 on the surface (**Figure 1e**).

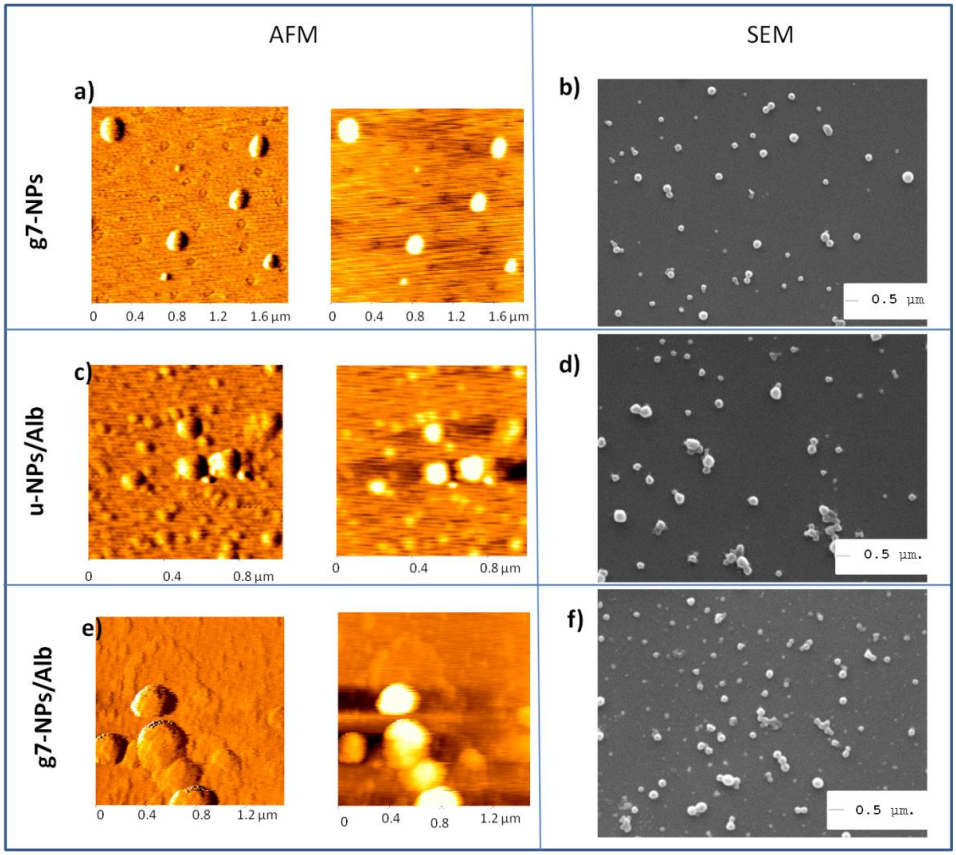

Figure 1: Morphologic characterization of nanoparticles. Left columns (panels a,c,e) AFM and right column (panel b, d, f) SEM images of unloaded g7-NPs as control and loaded u-NPs/Alb and g7-NPs/Alb.

4.1.2 NPs for in vitro and in vivo experiment with IDS

All NPs were characterized in terms of size, surface charge and drug loading (**Table 2**). In particular, all NPs, independently from surface modification or loading, were featured by dimension under 250 nm, thus compatible with a systemic administration, good homogeneity and negative surface charges, as usual when considering PLGA NPs (*Tosi et al., 2007; Vergoni et al., 2009*). Percent of loading efficiency (EE%) of u-NPs-IDS and g7-NPs-IDS is quite different, with a decrease in IDS content of about 50% in g7-NPs-IDS with respect to u-NPs-IDS. As underlined in the previous paragraph, this data is not surprising, since the loading process with IDS happens as first step in the formulation of NPs, thus

leading to a possible lost in drug content in the subsequent steps (*Bondioli et al., 2011*).

Samples	*Z-Average[a] nm*	*PDI[a]*	*ζ-pot[a] mV*	*mg of IDS/100 mg NPs*	*EE%[b]*
u-NPs-IDS	207	0.19	-36	3.1	31%
g7-NPs-IDS	207	0.214	-34	1.5	15%
g7-NPs-IDS-R	227	0.162	-36	1.65	16.5%

Table 2: chemico-physical characterization of nanoparticles loaded with recombinant IDS. PDI means Poly dispersity index, ζ-pot represents zeta potential indicating surface charge, EE is encapsulation efficiency.

4.2 IN VIVO PRELIMINARY STUDIES OF g7-NPs IN MPS I AND MPS II MOUSE MODELS

4.2.1 In vivo preliminary study in the MPS I mouse model

Baseline experiments, aimed to confirm in the MPS I animal model results previously obtained in the wt mouse (*Tosi et al., 2007; Tosi et al., 2014; Vilella et al., 2014; Tosi et al., 2013a; Tosi et al., 2013b; Tosi et al., 2013c*), included injection of 2 mg/animal of g7-NPs in the tail vein of Idua-ko and wt mice (n=3), as well as 2 mg/animal of u-NPs in the same mice (n=3). As shown in **Figure 2 and 3**, results confirmed for the Idua-ko mouse model and for the syngeneic wt control, an efficient g7-NPs crossing of the BBB, with a higher efficiency, of about 5.5 fold, for the Idua-ko (mean value: 1641 g7-NPs per optical field) vs the wt mouse (mean value: 288 g7-NPs per optical field).

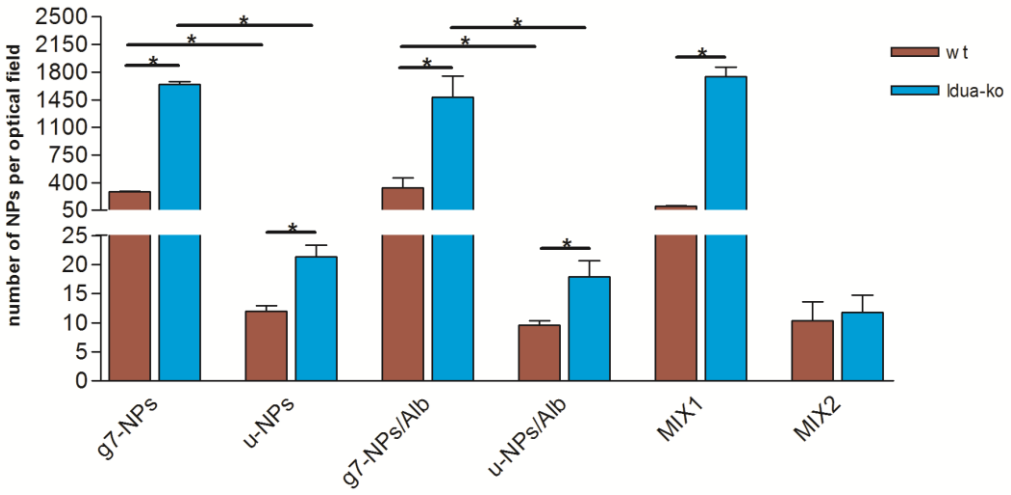

Figure 2: number of NPs per optical field in the brain of the Idua-ko mouse model and in the syngeneic wt control.Type of treatments: g7-NPs = un-loaded and targeted NPs; u-NPs = un-loaded and un-targeted NPs; Alb = Albumin; g7-NPs/Alb = targeted NPs loaded with albumin; u-NPs/Alb = un-targeted NPs loaded with albumin; MIX1 (g7-NPs+Alb) = un-loaded targeted NPs suspended in FITC-albumin solution; MIX2 (u-NPs+Alb) = un-loaded and un-targeted NPs suspended in FITC-albumin solution. *n=3-5* for all type of injection.

On the opposite, u-NPs BBB crossing looks extremely poor or totally absent in our wt mouse (mean value: 12 u-NPs per optical field), as previously shown in other mouse strains, and slightly higher in the Idua-ko mouse, although still very low (mean value: 21 u-NPs per optical field).

BBB status in LSDs was previously investigated especially in the MPS III condition (*Garbuzova-Davis et al., 2013; Garbuzova-Davis et al., 2011; Begley et al., 2008*): endothelial cells damage with possible compromise of the BBB was described indicated, among others, by Evans Blue and albumin microvascular leakage in various brain structures. On the opposite, a similar analysis conducted in this work for both wt and Idua-ko mice, by using Evans Blue (see *Section 4.3*) and FITC-albumin, detected no altered permeability, thus suggesting possible altered uptake pathways. This hypothesis is supported by the fact that also in the liver a higher efficiency of uptake in the Idua-ko vs wt mouse was found (**Figure 4)**. Therefore, similarly to what previously reported with the brain-targeted (with receptor binding peptide for ApoE3) pro-drug of the therapeutic enzyme (α-L-iduronidase) (*Wang et al., 2013*), NPs, although with remarkable differences in

terms of success (g7-NPs>>u-NPs), could take advantage of the improved transcytotic pathways to reach Idua-ko brains.

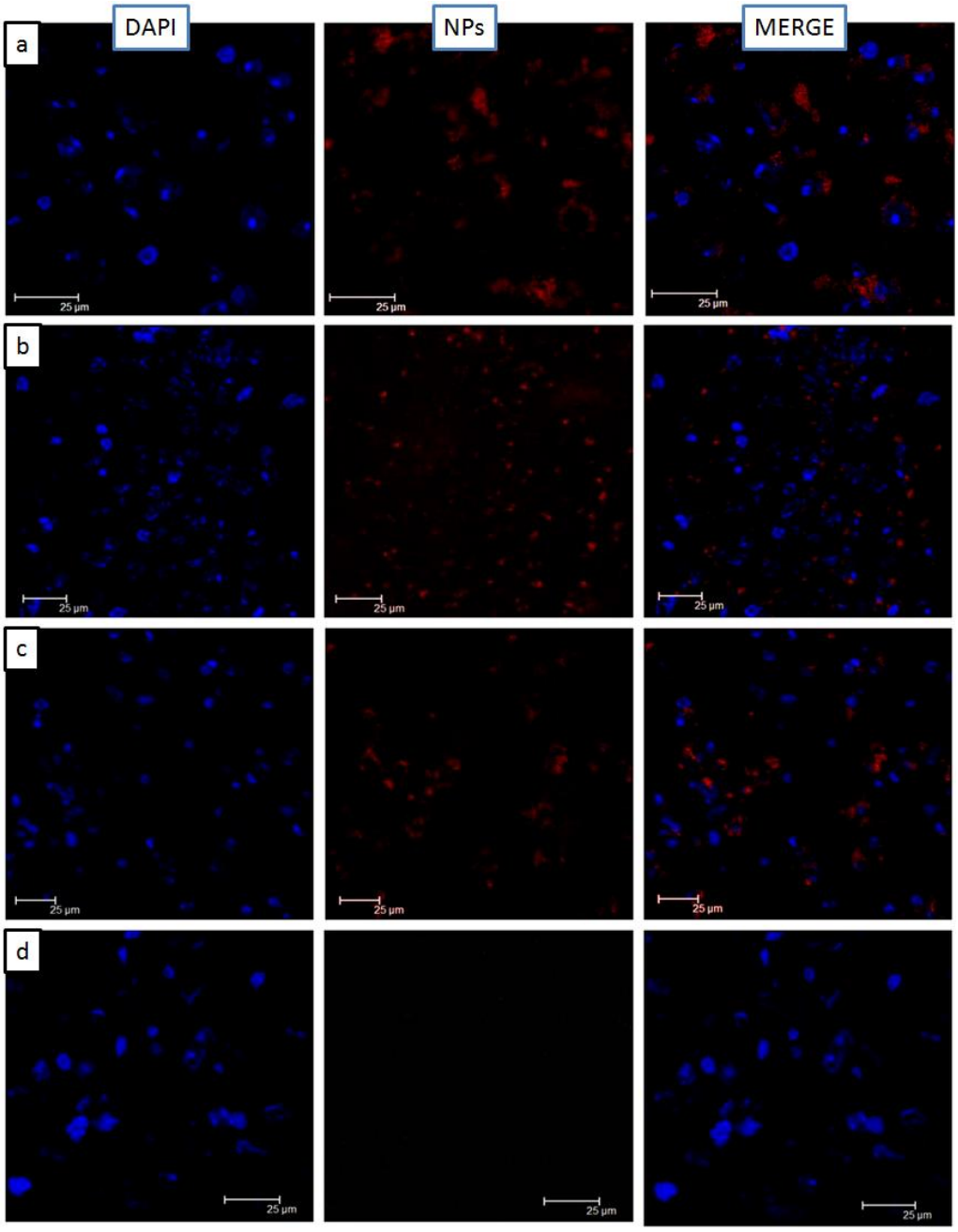

Figure 3: Brains of the Idua-ko and wt mice injected with targeted and untargeted unloaded PLGA-NPs. **a)** Idua-ko injected with g7-NPs; **b**) wt injected with g7-NPs; **c**) Idua-ko injected with u-NPs; **d**) wt injected with u-NPs.

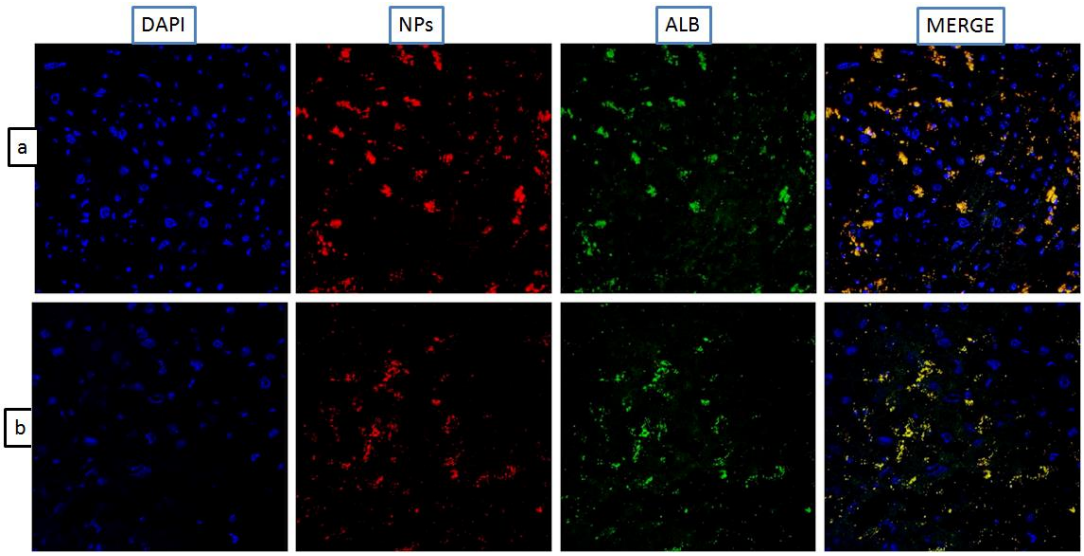

Figure 4: Livers of **a**) Idua-ko and **b**) wt mice injected with g7-NPs/Alb. Magnification: 40-60 x. From the left: blue DAPI staining (nuclei), red NPs, due to rhodamine labeling, green FITC labeling of Alb and the last one is the merge image.

We next administered targeted nanoparticles loaded with albumin (g7-NPs/Alb) in both animal types (Idua-ko n=3, wt n=4) to evaluate efficiency of g7-NPs BBB crossing as well as ability to carry over the albumin. As shown in **Figure 5**, there is a co-localization of g7-NPs and albumin in both animal types, thus demonstrating for the first time that g7-NPs can carry high MW molecules, as albumin, through the BBB. Moreover, **Figure 2** shows how the number of g7-NPs/Alb per optical field is much higher in Idua-ko than in wt mice, about 4.4 fold. As control, the administration of free albumin solution (0.2 mg/mouse) in Idua-ko and wt mice (both n=3) did not lead to any significant signals of albumin, thus excluding the possibility of FITC-albumin BBB crossing and also confirming, indirectly, the maintenance of BBB integrity and impermeability to high MW molecules in Idua-ko mice (not shown).

As further control, we also injected un-targeted NPs loaded with albumin (u-NPs/Alb) in Idua-ko and wt mice (both n=3). As expected, the extent of BBB crossing is almost non-existent in both animal types (17 and 9 u-NPs/Alb per optical field in Idua-ko and ko mice, respectively) (**Figure 2 and 5**), confirming that the g7-targetor moiety is needed to allow brain targeting of PLGA-NPs, as well as brain delivery of the loaded Alb.

To consider whether Alb adsorbed onto NPs (targeted or not) can be driven across the BBB, we additionally injected Idua-ko (n=4) and wt (n=3) mice with un-loaded g7-NPs suspended in free FITC-albumin (MIX1). Unexpectedly, as shown in **Figure 2 and 6a**, we observed that albumin could cross the BBB also if administered as MIX1; as supposed, the perfect co-localization of Alb and NPs suggests that Alb likely binds externally to the surface of the NPs and is carried into the CNS together with the NPs. This result is not surprising as it was hypothesized for other types of NPs able to transfer into the CNS high MW molecules, which were both adsorbed onto NPs surface and loaded into NPs (*Wohlfart et al., 2012*).

As supposed, the injection of un-loaded u-NPs suspended in free FITC-albumin (MIX2), did not lead to any Alb signal in the CNS, confirming the inability of un-targeted NPs to cross the BBB thus delivering any adsorbed material (as Alb) (**Figure 6b)**.

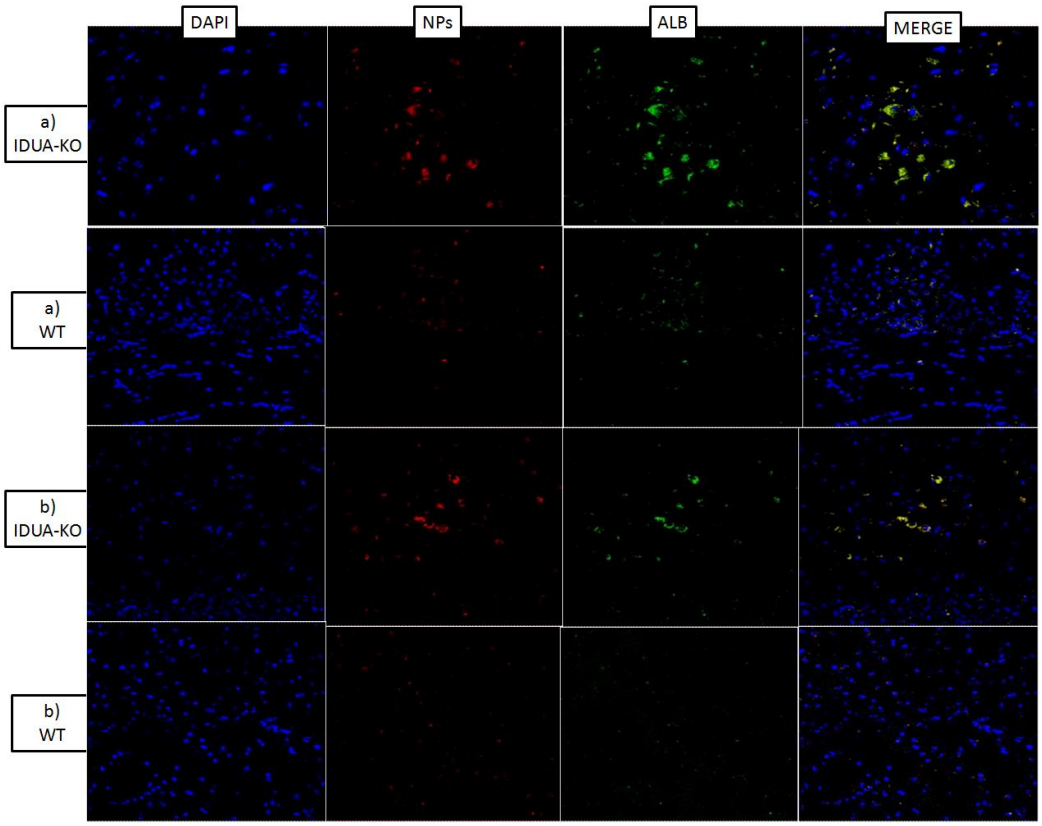

Figure 5: Brains of the Idua-ko and wt mice injected with **a)** g7-NPs/Alb and **b)**u-NPs/Alb. Magnification 40-60x.

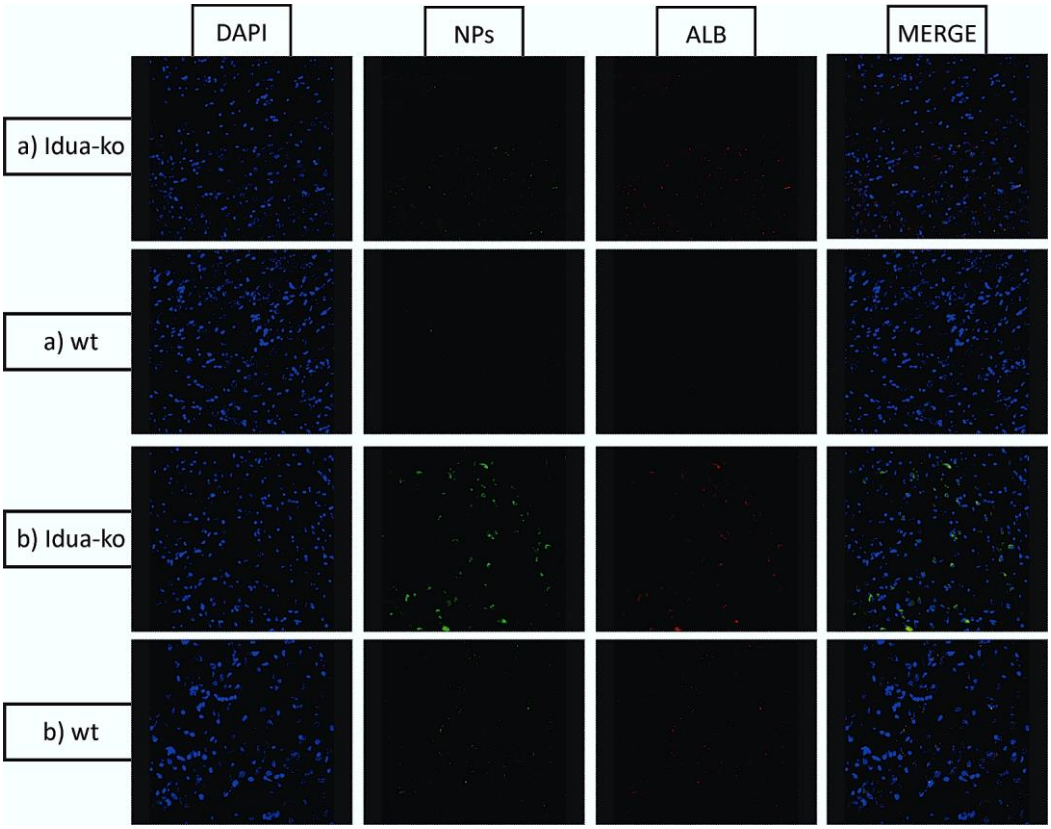

Figure 6: Brains of the Idua-ko and wt mice injected with: **a)** MIX1 (g7-NPs+Alb), **b**) MIX2 (u-NPs+Alb).

In conclusion, there is a higher, statistically significant, amount of g7-NPs (p-value=0.0002) and g7-NPs/Alb (p-value=0.0007) that can cross the BBB with respect to u-NPs and u-NPs/Alb respectively. This provides excellent prerequisites for the use of these g7-NPs with the recombinant enzymes, as well as with other high molecular weight molecules, to treat neurological diseases.

4.2.2 In vivo preliminary study in the MPS II mouse model

Efficiency of g7-NPs/Alb BBB crossing was afterwards evaluated in the MPS II mouse model (Ids-ko). These experiments aimed to extend the potential use of this kind of carriers to transport high molecular weight therapeutic molecules to the brain district in other LSDs and hopefully many other neurological disorders.

As show in **Figure 7,** g7-NPs/Alb can cross BBB also in the Ids-ko mouse model and, as already seen in the Idua-ko mice, and shown in **Figure 8**, we found a

significantly higher (p-value = 1.52E-07) number of NPs per optical field in the Ids-ko than in the wt mice (both n=5), about 3.6 fold.

In this case, the extent of g7-NPs/Alb reaching the brain is significantly lower (1.5 fold, p=0.006) with respect to Idua-ko mice and this might be due to a different BBB permeability or modified processes in BBB crossing pathways in the two different animal models or pathologies. This finding represents an open question regarding the different status of the BBB in very similar pathologies (MPS I, MPS II and MPS III), but with different outputs in terms of BBB crossing and endothelial dynamic damage. Moreover, it is important to note that in these experiments we did not monitor crossing efficiency with the progression of the pathology and further experiments will be targeted to check whether g7-NPs BBB crossing in LSDs-ko mice may be function of the disease progression (from early to late stage).

As a control, we also injected free albumin in Ids-ko and wt mice (n=3) and the results confirmed that albumin cannot cross BBB in both mice (not shown).

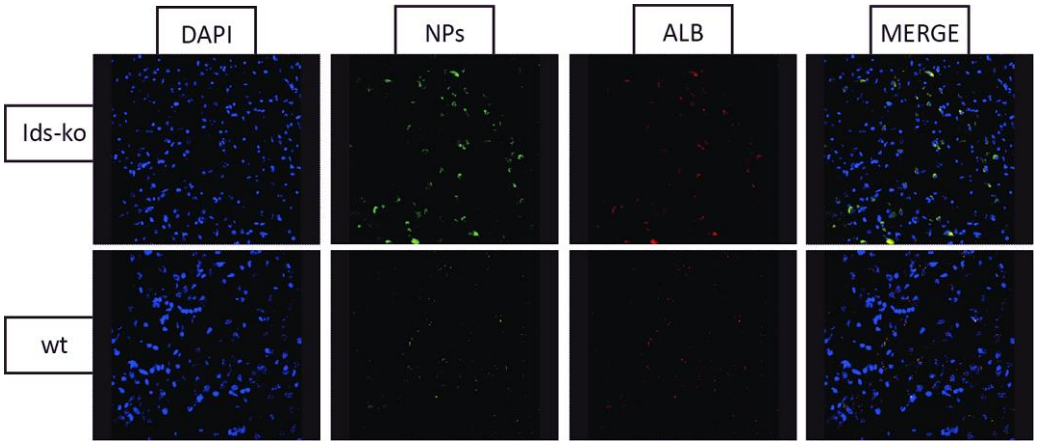

Figure 7: Ids-ko mouse model and syngeneic wt injected with g7-NPs/Alb. Magnification 20X.

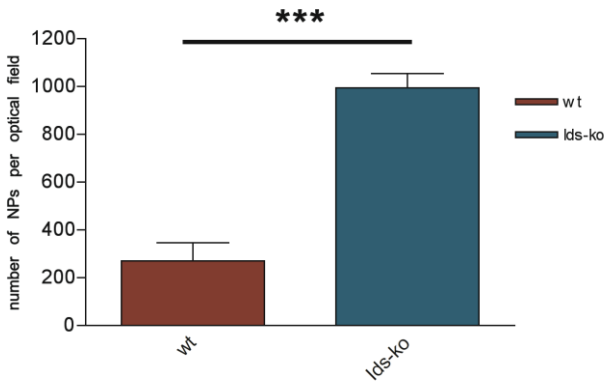

Figure 8: number of NPs per optical field in the brain of the Ids-ko mouse and syngeneic wt, injected with g7-NPs/Alb.

4.3 CHECKING OF BBB INTEGRITY

To exclude that the higher g7-NPs/Alb uptake in the ko mouse models may be due to possible damages in their BBB, we performed experiments aimed to check BBB integrity. To this aim we injected Idua-ko, Ids-ko and the respective wt mice with Evans Blue solution (*Deng et al., 1998*); none of the animals showed a BBB crossing of the dye, this indicating an undamaged BBB. Therefore, the difference in the NPs uptake may hypothetically reside in other factors, as a different expression of transporters on the endothelium as well as a modification in the endocytosis process in both ko mice vs wt controls. As previously reported in *section 4.2.1*, also the results obtained in the liver support this hypothesis.

Therefore, more studies will be necessary to understand what leads to the difference in the uptake of NPs and, most of all, to understand the basic differences in the BBB composition/structure of both ko animals vs the related wt mice.

4.4 IN VIVO PRELIMINARY STUDY OF g7-NPs-IDS-R IN MPS II MOUSE MODEL

To confirm that g7-NPs can transport IDS through the BBB, a preliminary study was conducted using g7-NPs loaded with recombinant IDS (Elaprase®, Shire Human Genetic Therapies, Inc, Cambridge, MA, USA) and marked with Rhodamine B (g7-NPs-IDS-R).

As shown in **Figure 9**, g7-NPs-IDS-R can cross BBB both in the wt and Ids-ko mice and, as already seen for g7-NPs/Alb, we found a significantly higher (p-value = 0.03) number of NPs per optical field in the Ids-ko than in the wt mice (both n=3), about 3.4 fold.

However, IDS enzyme assay carried out in 3 Ids-ko and 3 wt mice showed an induced activity equal to zero in all tested animals (data not shown). Consequently, we can hypothesize that nanoparticles may take longer than 2 hours to open up and release the encapsulated enzyme. To assess this hypothesis, *in vitro* and *in vivo* studies were necessary to evaluate possible times of enzyme release.

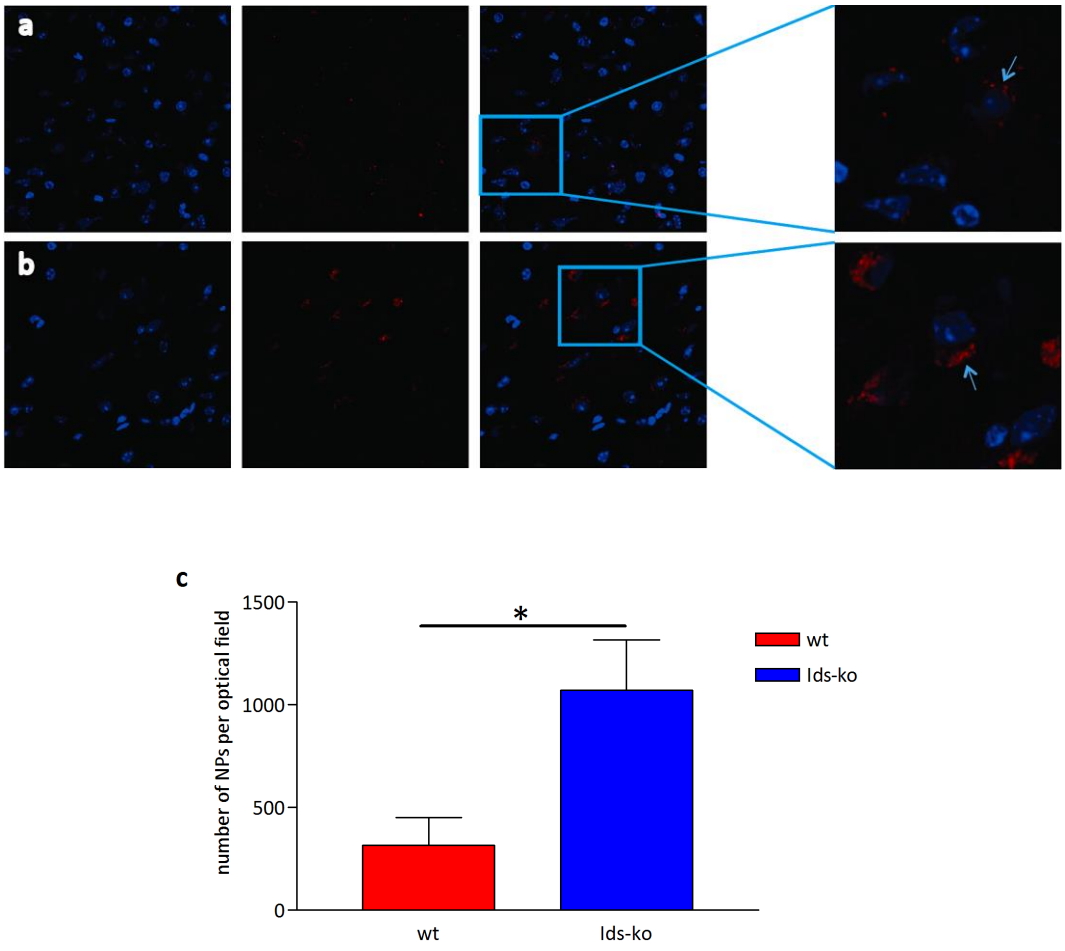

Figure 9: wt (**a**) and syngeneic Ids-ko mouse model (**b**) injected with targeted NPs loaded with IDS enzyme and labeled with Rhodamine B (g7-NPs-IDS-R). Arrows indicate g7-NPs-IDS-R. Magnification 40X with respective 3X digital zoom. **c)** number of NPs per optical field in the brain of the Ids-ko mouse and syngeneic wt, injected with g7-NPs-IDS-R.

4.5 IN VITRO ANALYSIS OF u-NPs-IDS EFFICACY

To verify NPs capability to encapsulate the recombinant enzyme and transport it to the cells, maintaining its therapeutic efficacy, an *in vitro* study was conducted on primary fibroblasts obtained from MPS II patients and healthy human controls.

Cells were treated with free recombinant IDS, IDS encapsulated in NPs (u-NPS-IDS) or remained untreated. Fibroblasts were treated for 7 days, then the treatment was removed and cells sacrificed after 0, 7 and 14 days.

The *in vitro* analysis confirmed the ability of NPs to load the IDS recombinant enzyme and transport it into the cells, maintaining its activity.

Although cells treated with the u-NPs-IDS showed a lower activity with respect to the ones treated with free enzyme (**Figure 10**), this was similar to that measured in healthy control cells and sufficient to reduce the content of GAG to non-pathological levels (**Figure 11**).

These data suggest that nanoparticles may need more time to open up and release the recombinant enzyme or, otherwise, that they may need a more complex physiological system with respect to the *in vitro* one.

Since data were promising, but it was impossible to prolong the time of the *in vitro* test for technical reasons, evaluation on the nanoparticles efficacy was turned to the mouse model.

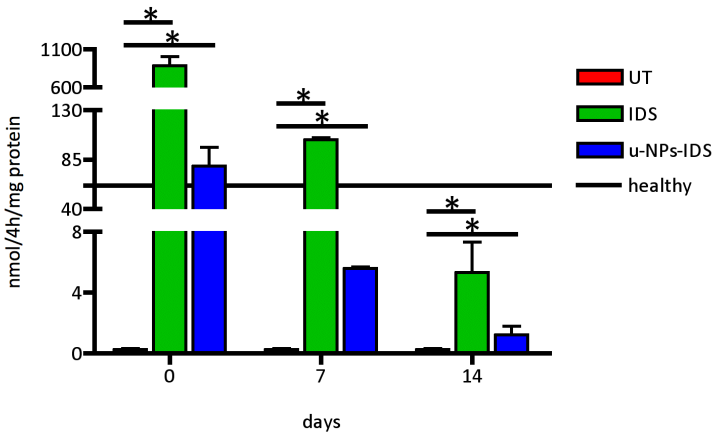

Figure 10: IDS activity (nmol/4h/mg protein) induced after 7days of treatment in cells from MPS II patients. Type of treatment: free recombinant IDS (IDS), unmodified NPs loaded with recombinant IDS (u-NPs-IDS), untreated MPS II fibroblast (UT). The solid line is the reference value of cells from healthy patients (healthy). Evaluation was carried out0, 7 and 14 days after the end of the treatment. Activities expressed in nmoles of 4MU (4-Methylumbelliferil-α-L-iduronide-2-sulphate.Na2) produced in 4 hours per mg of protein.*$p<0.05$

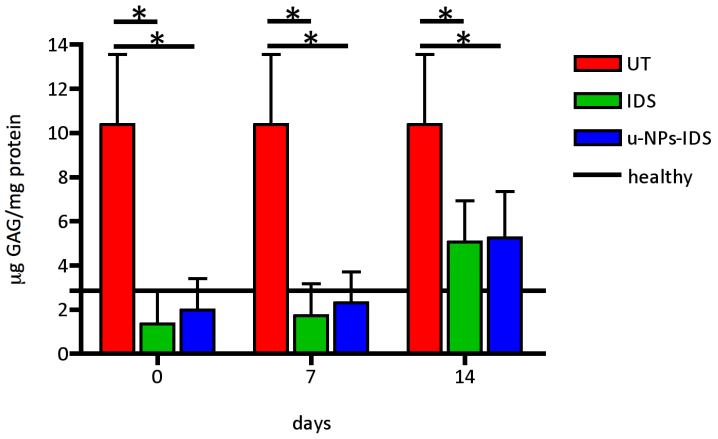

Figure 11: GAG content (µg GAG/mg protein) after 7days of treatment in cells from MPS II patients. Type of treatment: free recombinant IDS (IDS), unmodified NPs loaded with recombinant IDS (u-NPs-IDS), untreated MPS II fibroblast (UT). The solid line is the reference value of cells from healthy patients (healthy). Evaluation was carried out 0, 7 and 14 days after the end of the treatment.*$p<0.05$

4.6 IN VIVO PILOT STUDY IN THE MPS II MOUSE MODEL

To evaluate transfer efficiency and the enzymatic activity induced by g7-NPs loaded with the recombinant enzyme (g7-NPs-IDS), an *in vivo* pilot study in the MPS II mouse model was first conducted.

As observed in the *in vitro* experiments, NPs (targeted or not) were able to deliver the recombinant IDS enzyme, although a very low plasmatic IDS activity was induced by the treatment with respect to what induced by the free IDS 4h after injection (**Figure 12**). After 24 hours, the enzymatic activity induced by NPs was practically undetectable, while it was still substantial for free IDS treated mice.

A similar situation was also found in the liver after 7 days, where the induced enzymatic activity could be detected for the Ids-ko mice treated with free IDS, but it was almost non-existent for those treated with NPs (targeted or not) (**Figure 13**).This was also confirmed by the results obtained from the evaluation of the GAG content in the liver, which was found reduced after 7 and 14 days for mice treated with free IDS, but not for those treated with NPs (**Figure 14**).

Differently from what expected for g7-NPs-IDS, but in line with the results of the liver, induced IDS activity was not detected in the brain parenchyma for all types of treatment (**Figure 15**).

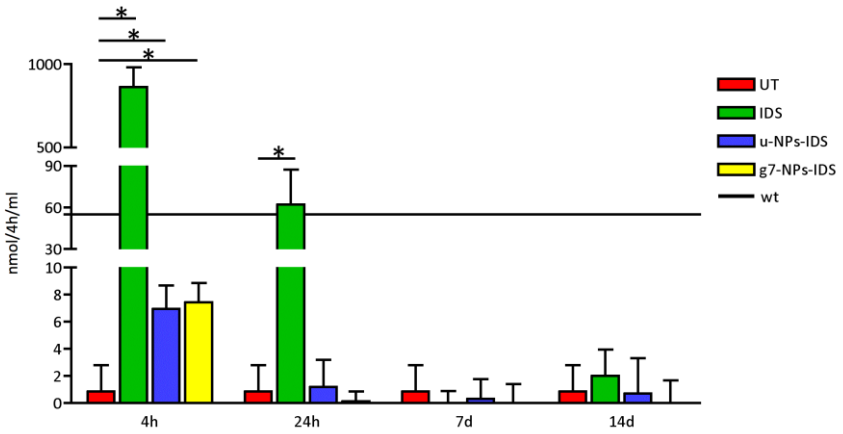

Figure 12: IDS activity (nmol/4h/ml) detected after 4 hours (4h), 24 hours (24 hours), 7 days (7d) and 14 days (14d) in the plasma of Ids-ko mice treated with free IDS, u-NPs-IDS and g7-NPs-IDS, compared with the activity detected in the plasma of untreated Ids-ko (UT)and wild-type (wt) mice. Activities expressed as nmoles of 4MU (4-Methylumbelliferil-α-L-iduronide-2-sulphate.Na2) produced in 4 hours per ml of plasma. **p<0.05*

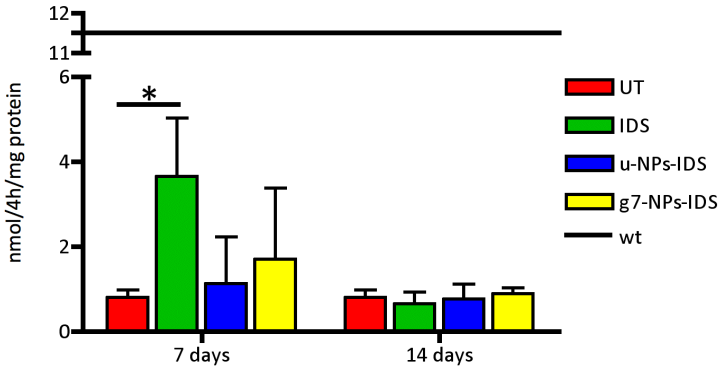

Figure 13: IDS activity (nmol/4h/mg protein) detected after 7 and 14 days in the liver of Ids-ko mice treated with free IDS, u-NPs-IDS and g7-NPs-IDS, compared with the untreated Ids-ko (UT) and wild-type (wt) mice. Activities expressed as nmoles of 4MU (4-Methylumbelliferil-α-L-iduronide-2-sulphate.Na2) produced in 4 hours per mg of protein. **p<0.05*

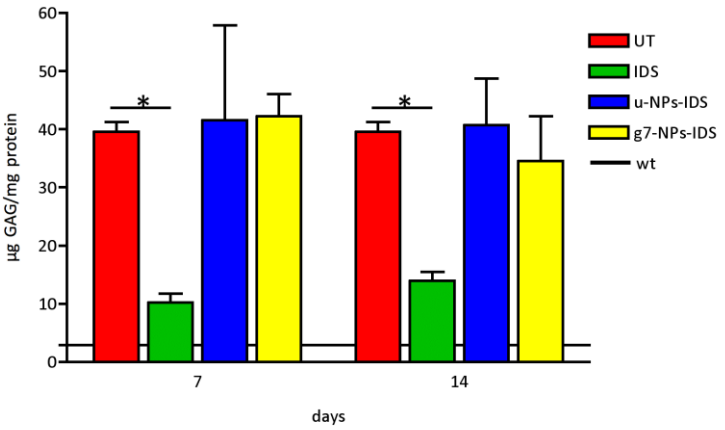

Figure 14: GAG content (µg GAG/mg protein) detected after 7 and 14 days in the liver of Ids-ko mice treated with free IDS, u-NPs-IDS and g7-NPs-IDS, compared with the untreated Ids-ko (UT) and wild-type (wt) mice. **p<0.05*

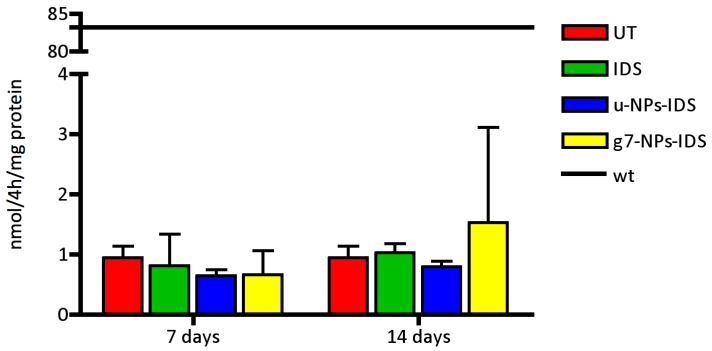

Figure 15: IDS activity (nmol/4h/mg protein) detected after 7 and 14 days in the brain parenchyma of Ids-ko mice treated with free IDS, u-NPs-IDS and g7-NPs-IDS, compared with the untreated Ids-ko (UT) and wild-type (wt) mice. Activities expressed as nmoles of 4MU (4-Methylumbelliferil-α-L-iduronide-2-sulphate.Na2) produced in 4 hours per mg of protein. **p<0.05*

All these data could be explained by the need of a longer time for nanoparticles to open up and release the encapsulated enzyme. To date there are still no conclusive studies in the medium/long term with this type of NPs and the time of release of the incorporated molecules is therefore still undefined.

The IDS activity detected in the plasma for both types of NPs can be justified by a possible external binding of the recombinant enzyme to the surface of the NPs. This is not surprising as it was hypothesized for other types of NPs able to transfer high MW molecules, which were both adsorbed onto NPs surface and loaded into NPs (*Wohlfart et al., 2012*).

4.7 IN VIVO MEDIUM-TERM EFFICACY STUDY IN THE MPS II MOUSE MODEL

Although the results obtained in the *in vitro* and *in vivo* pilot studies were mostly negative, it was important to carry out a medium-term analysis to assess the possible opening of NPs in a longer time.

With this aim, an *in vivo* study was conducted in the MPS II mouse model, by treating mice once a week for 6 weeks.

After 6 weeks treatment, mice (8 untreated Ids-ko, 8 Ids-ko treated with g7-NPs-IDS and 8 wt) were sacrificed and used for biochemical as well as histological, immunohistochemical and immunofluorescence evaluations.

4.7.1 Biochemical evaluations

Induced IDS activity was evaluated in liver (**Figure 16**) and brain parenchyma (**Figure 17**) of 5 mice/treatment. An increased enzyme activity was detected only in livers of free IDS treated mice; however, although not significant, a slight trend of increasing enzyme activity could be seen in the brain parenchyma of mice treated with g7-NPs-IDS. These data suggest that a period of 6 weeks is again too short to detect the opening of these NPs and the release of the encapsulated enzyme, although some NPs have probably opened.

Data obtained from the biochemical evaluation of tissue GAG levels partially confirm this hypothesis. **Figure 18** and **19** show, respectively, GAG content detected in liver and brain parenchyma of the same mice. In the liver a significant decrease of GAG content (about 30%) in mice treated with g7-NPs-IDS compared to untreated Ids-ko mice was detected, although this decrease is much lower than that observed in free IDS treated mice (about 95%). In the brain parenchyma no significant GAG decreases were detected; however, a slight trend in this direction could be seen in the brain parenchyma of mice treated with g7-NPs-IDS. Probably a decrease was significant detected only in the liver, though activity was not recorded, since liver is the organ usually receiving the largest amount of drug, therefore even the little amount of enzyme released by the NPs was rapidly taken up by the cells with a consequent reduction of the storage material.

Figure 20 shows the urinary GAG content before and after 6 weeks of treatment. Respect to the starting point and to UT mice, only free IDS treated mice have shown a decreased GAG content. Again, the little amount of enzyme released by NPs was likely insufficient to reduce GAG accumulated in the organs as well as to obtain a reduction of urinary GAG.

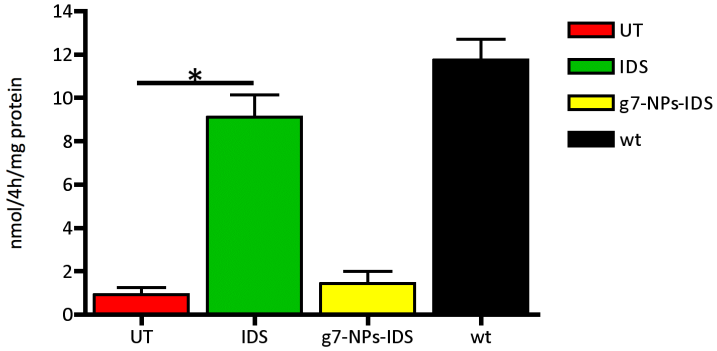

Figure 16: IDS activity (nmol/4h/mg protein) detected in the liver after 6 weeks of treatment in Ids-ko mice treated with free IDS and g7-NPs-IDS, compared with untreated (UT) Ids-ko and wild-type (wt) mice (n=5 for each treatment). **p<0.05*

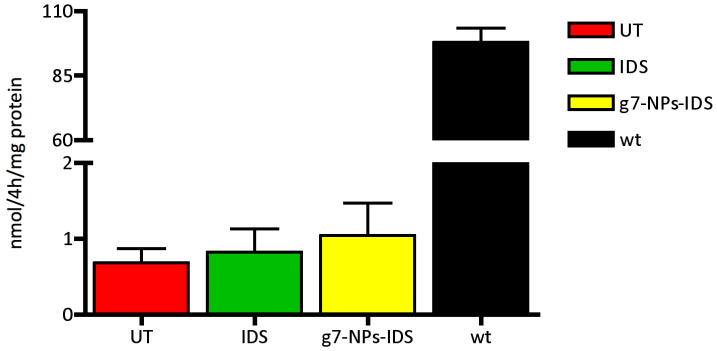

Figure 17: IDS activity (nmol/4h/mg protein) detected in the brain parenchyma after 6 weeks of treatment in Ids-ko mice treated with free IDS and g7-NPs-IDS, compared with untreated (UT) Ids-ko and wild-type (wt) mice (n=5 for each treatment). **p<0.05*

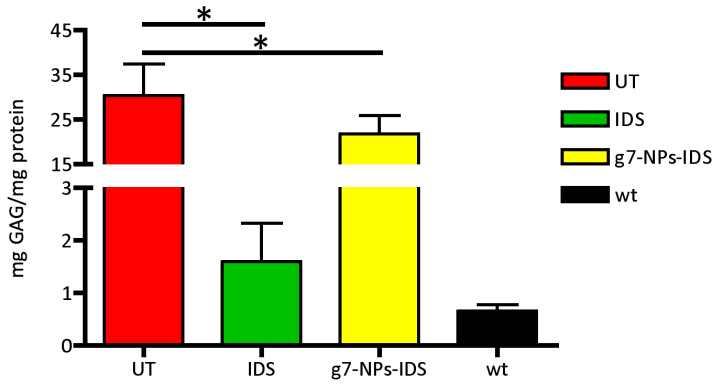

Figure 18: GAG content (µg GAG/mg protein) detected in the liver after 6 weeks of treatment in Ids-ko mice treated with free IDS and g7-NPs-IDS, compared with untreated (UT) Ids-ko and wild-type (wt) mice (n=5 for each treatment). **p<0.05*

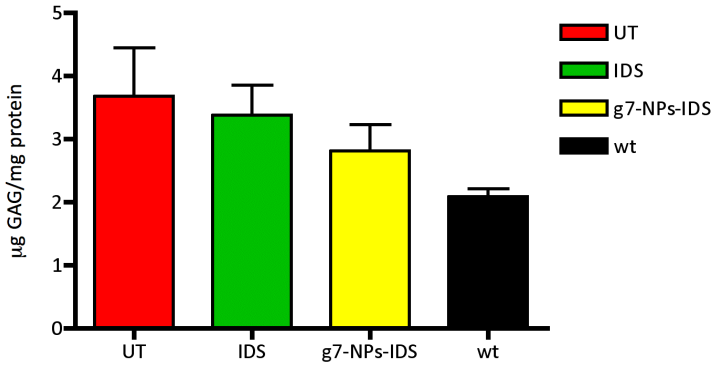

Figure 19: GAG content (µg GAG/mg protein) detected in the brain parenchyma after 6 weeks of treatment in Ids-ko mice treated with free IDS and g7-NPs-IDS, compared with untreated (UT) Ids-ko and wild-type (wt) mice (n=5 for each treatment). **p<0.05*

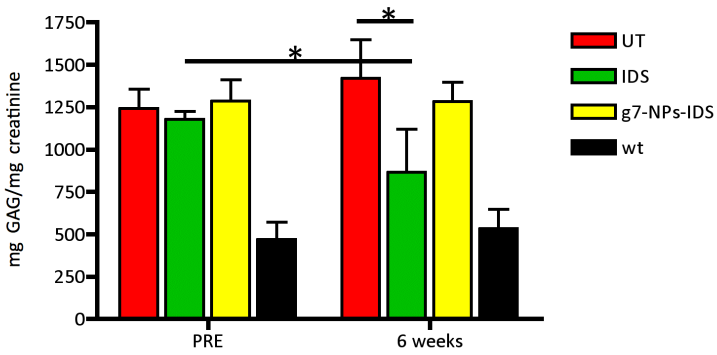

Figure 20: Urinary GAG content (mg GAG/mg creatinine) detected before starting (PRE) and at the end after 6 weeks of treatment in Ids-ko mice treated with free IDS and g7-NPs-IDS, compared with untreated (UT) Ids-ko and wild-type (wt) mice (n=8 for each treatment). **p<0.05*

4.7.2 Histological, immunohistochemical and immunofluorescence evaluations

Brains and livers were fixed for 48h in Bouin's solution and processed for paraffin embedding. The results of histochemical analysis for GAG deposits in liver and brain are shown in **Figure 21** and **22**, respectively.

As previously reported in the literature (*Friso et al., 2010*), in the liver of untreated Ids-ko animals, accumulation of undegraded GAGs was observed in the Glisson's capsule and in the layer of mesothelial cells (**Figure 21a**), as well as around the portal tract and in the extracellular matrix of hepatocytes (**Figure 21b**, blue arrow); some hepatic lobules showed a vacuolated structure (**Figure 21b**, yellow arrow). The same accumulation was found also in the liver of Ids-ko

mice treated with g7-NPs-IDS, although at a visible lower extent (**Figure 21c and 21f**). These data confirmed those obtained by the biochemical analysis of GAG content in the same organ, stressing again the ability of g7-NPs-IDS to reduce the accumulation of GAG, although not normalizing them to the level of healthy animals.

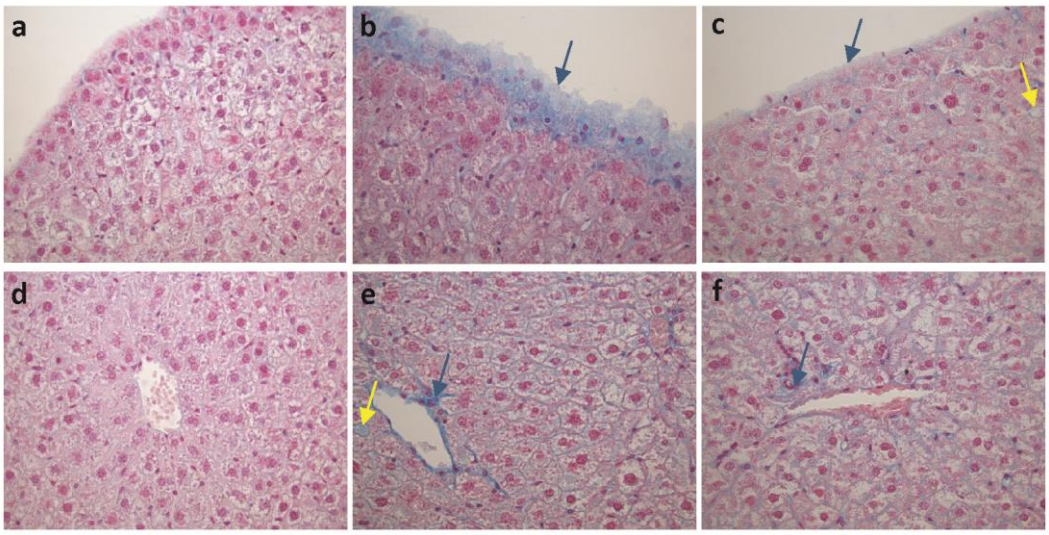

Figure 21: Histochemical analysis of glycosaminoglycan (GAG) in the liver of wt mice (**a,d**), untreated Ids-ko mice (**b,e**) and Ids-ko mice treated with g7-NPs-IDS (**c,f**) after 6 weeks of treatment. Representative sections of the external surface (**a,b,c**) and of a portal tract (**d,e,f**). Blue arrows indicate GAG deposits, yellow arrows indicate vacuolated structures. Sections (4µm) were stained with 1% Alcian Blue, counterstained with 0.1% Nuclear Fast Red. Magnification 40X.

Neuropathological defects were described for the MPS II mouse model as cellular vacuolization in different brain regions (*Cardone et al., 2006*) and as neuronal necrosis in the brainstem and spinal cord (*Garcia et al., 2007*). As previously described for the mouse model of MPS IIIB (*Fu et al., 2007*), the animal model for MPS II showed lower accumulation of GAG in the brain, compared with other tissues when a biochemical analysis was performed. Approximately, a twofold increase in GAG levels compared to wild-type mice was previously described (*Garcia et al., 2007; Friso et al., 2010*) and here confirmed (**Figure 19**).

Histochemical analysis of brain GAG content is presented in **Figure 22**. As previously reported (*Cardone et al., 2006*), the major areas of GAG accumulation

in Ids-ko brain was within the third (**Figure 22e**) and fourth (**Figure 22h**) ventricles, and at a lower extent in the cerebral cortex (**Figure 22b**). The same deposits were visible also in the brain of Ids-ko mice treated with g7-NPs-IDS, although at a slightly lower level (**Figure 22c,f,i**).These data confirmed the ones obtained by the biochemical analysis of GAG deposits in the same organ, indicating a slight downward trend of accumulation although not statistically significant.

Figure 23 shows representative sections of the cerebellum stained with 0.1% toluidine solution. As shown in the digital zoom, the Purkinje cells were vacuolated both in untreated and treated Ids-ko mice, indicating that the little amount of enzyme released by the nanoparticles was insufficient to improve or correct the damage at this level.

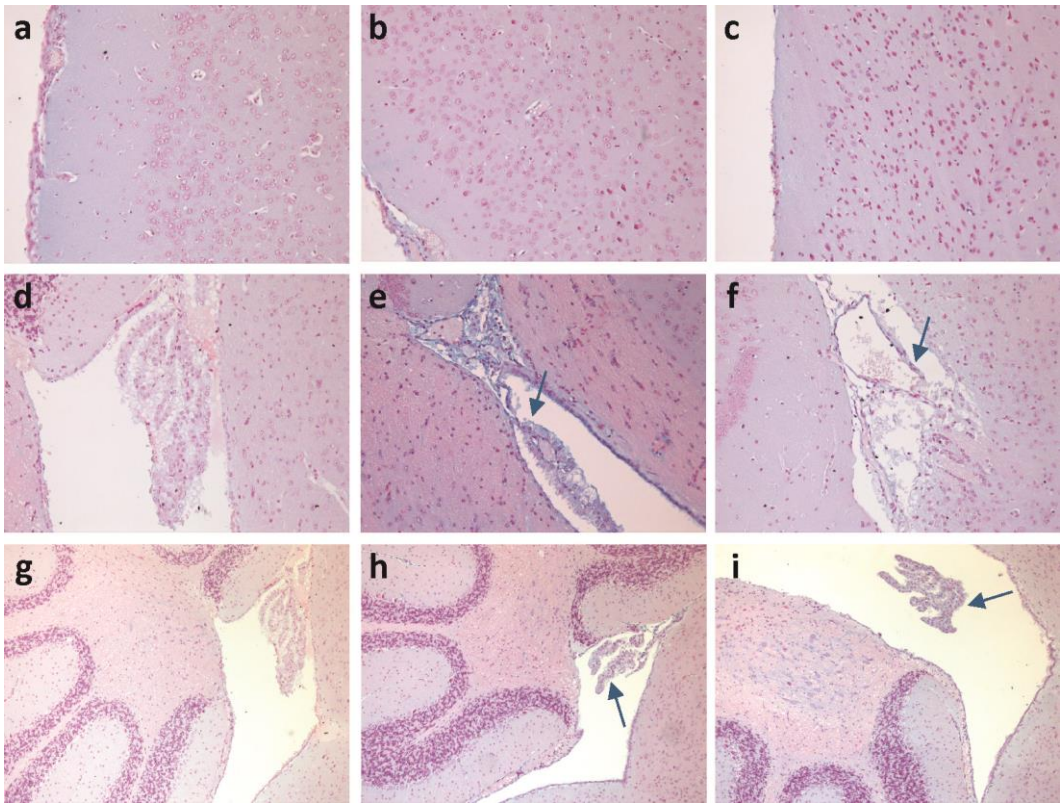

Figure 22: Histochemical analysis of glycosaminoglycan (GAG) in the brain of wt mice (**a,d,g**), untreated Ids-ko mice (**b,e,h**) and Ids-ko mice treated with g7-NPs-IDS (**c,f,i**) after 6 weeks of treatment. Representative sections of the cortex (**a,b,c**), the choroid plexus (**d,e,f**) and the cerebellum (**g,h,i**). Arrows indicate GAG deposits. Sections (4 µm) were stained with 1% Alcian Blue, counterstained with 0.1% Nuclear Fast Red. Magnification 20X (**a,b,c,d,e,f**) and 10X (**g,h,i**).

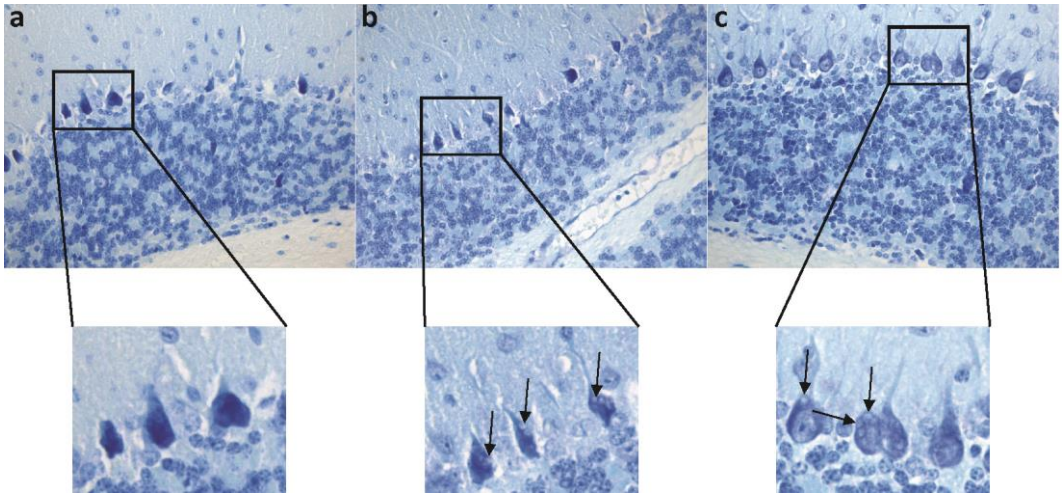

Figure 23: Histochemical analysis of the brain of wt mice (**a**), untreated Ids-ko mice (**b**) and Ids-ko mice treated with g7-NPs-IDS (**c**) after 6 weeks of treatment. Representative sections of the cerebellum stained with 0.1% toluidine solution. Arrows indicate vacuolated Purkinje cells. Magnification 40X and relative digital zoom of the Purkinje cells.

To observe the size of the late endosomal/lysosomal compartment and hence to measure the amount of lysosomal storage, sections of paraffin embedded-brain were stained with lysosomal associated membrane protein 2 (LAMP2) (**Figure 25**). As shown in the panel, positive lysosomal signals were detected in all the three areas of the brain in both untreated and treated Ids-ko mice. The number of positive cells to LAMP2 per total number of cells (**Figure 25j**) showed a slight tendency to decrease in the hippocampus and cortex of the animals treated with g7-NPs-IDS, and although not significantly, this was coherent with the other data obtained from biochemical and histological/immunohistochemical analysis.

To determine whether nanoparticles could reduce neuroinflammation in Ids-ko mice, we counted the number of positive astrocytes for GFAP (a neuromarker for astrogliosis) in the cerebral cortex, in the hippocampus and in the cerebellum (**Figure 24**). Ids-ko mice exhibit a marked increase in neuroinflammatory astrocytes compared to wt. g7-NPs-IDS seemed to slightly reduce GFAP-positive astrocytes in the cerebellum, although not significantly, but not in the cerebral cortex and in the hippocampus.

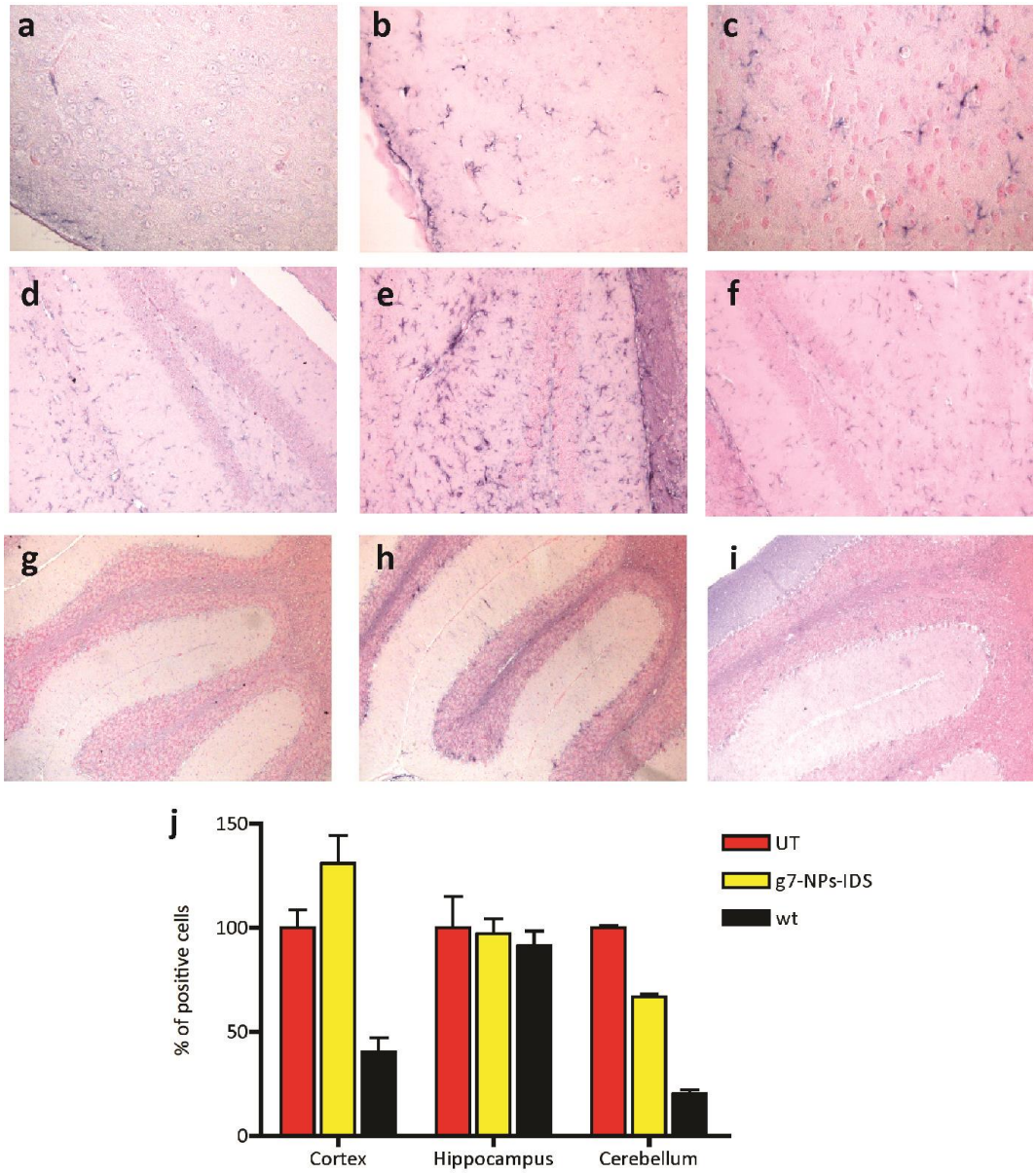

Figure 24: Immunohistochemical analysis of GFAP in the brain of wt mice (**a,d,g**), untreated Ids-ko mice (**b,e,h**) and Ids-ko mice treated with g7-NPs-IDS (**c,f,i**) after 6 weeks of treatment. Representative sections of the cortex (**a,b,c**), the hippocampus (**d,e,f**) and the cerebellum (**g,h,i**) (magnification 40X).**j** shows the % of positive cells to GFAP in wt mice and Ids-ko mice treated with g7-NPs-IDS with respect to untreated Ids-ko mice (UT=100%).

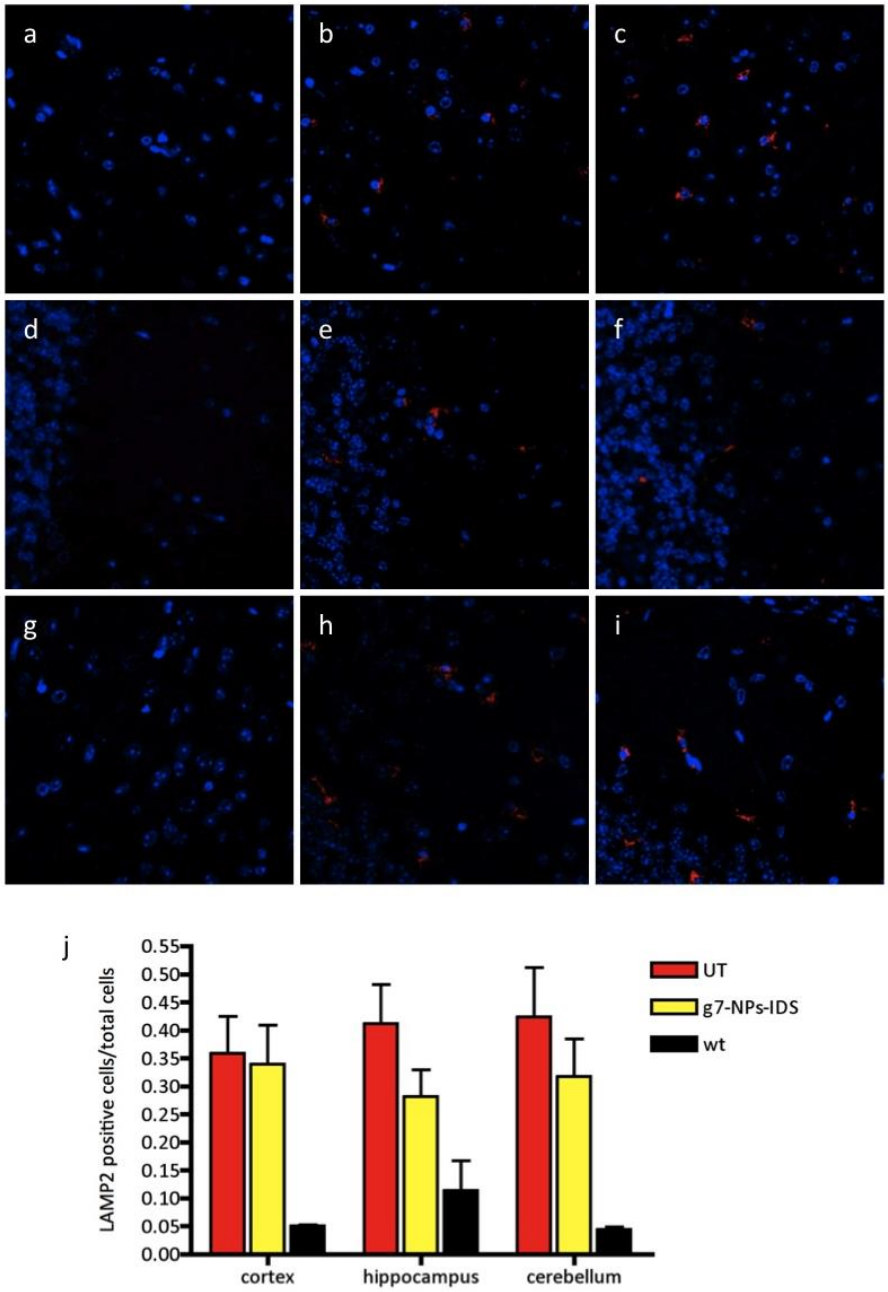

Figure 25: Immunofluorescence analysis of LAMP2 in the brain of wt mice (**a,d,g**), untreated Ids-ko mice (**b,e,h**) and Ids-ko mice treated with g7-NPs-IDS (**c,f,i**) after 6 weeks treatment. Representative sections of the cortex (**a,b,c**), the hippocampus (**d,e,f**) and the cerebellum (**g,h,i**) (magnification 40X). **j** shows the number of positive cells to LAMP2 per total number of cells.

Results obtained from this medium-term study are encouraging as they show a slight trend towards improvement in brain and liver of g7-NPs-IDS treated mice assessed with most of the techniques applied.

Based on their formulation, it is expected that nanoparticles gradually release the encapsulated enzyme, likely providing it in low doses, although more constant and prolonged in time with respect to the free IDS. Therefore, even in the phase of maximum release of the enzyme, it is expected that the activity detected in peripheral organs, as liver, will be likely lower than that induced by the administration of free enzyme.

However, this assumption is not sufficient to explain the results obtained in this medium-term study, as the efficacy results here obtained also suggest that 6 weeks of treatment are likely insufficient to observe the release of the encapsulated enzyme in a therapeutic amount.

To conclude, longer studies would be necessary to understand the timing of release of the enzyme from this kind of NPs. However, the main point will be to rethink about the formulation of nanoparticles, in order to obtain the generation of other NPs with the same transport efficiency to the CNS, but with shorter times of release.

To this purpose, the group of the University of Modena collaborating with us in this project, is already working to constitute softer nanoparticles, that will be likely more easily biodegradable, therefore characterized by shorter opening times and consequent faster release of the encapsulated therapeutic molecules.

5. CONCLUSIONS

Lysosomal Storage Disorders are a group of neurometabolic syndromes, mostly due to the deficit of one lysosomal enzyme. Many LSDs affect most of the organ systems and about two-thirds of the patients present neurological and cognitive impairment.

Among these, Mucopolysaccharidoses type I and type II are both characterized by a lack of activity of lysosomal enzymes involved in the catabolism of the glycosaminoglycans heparan- and dermatan-sulfate, therefore accumulating in the cell compartment and in the extracellular matrix. To date the available therapeutic options for these MPSs are mainly based on ERT; however, the neurological involvement is unlikely to benefit from this kind of treatment. In fact, although positive results have been reported in the animal models following ERT in neonates (*Urayama et al., 2004; 2008*) or using doses far higher those conventionally used in clinical treatment (*Vogler et al., 2005; Tomatsu et al., 2007*), with the current dosages and formulation, diffusion of the proteins involved in ERT across the BBB is almost non-existent (*Boado et al., 2008*).

This problem deserves a solution and would suggest the use of modified enzymes or vehicle able to cross the BBB.

In general, clinical efficacy of conventional therapies for neurological diseases is in most cases limited by the ability of the drugs to reach the cerebral district. In addition, the rapid removal from the bloodstream decreases the bioavailability and reduces the amount usable for the target site.

Recent studies show that carriers as the engineered nanoparticles may cross the BBB without damage (*Tosi et al, 2007; Tosi et al., 2014; Vilella et al., 2014; Tosi et al., 2013a; Tosi et al., 2013b*) and carry drugs and genetic material to the brain, thus being considered as potential strategies to implement the treatment of brain disorders. Therefore, it is hopefully that the use of nanotechnologies, able to protect their content and to carry therapeutics to the CNS, fits perfectly with the need to carry specifically to this district the recombinant enzymes, necessary to correct neurological involvement in some LSDs. Moreover, the features of g7-

NPs, as internalization and up-take by neurons by the clathrin pathway, submission to an intracellular trafficking based on Rab5 and accumulation in the lysosomes (*Tosi et al., 2014; Vilella et al., 2014; Chhabra et al., 2014*), could represent a plus, since the deficient enzyme needs to be transported to the organelle where the pathological storage is metabolized.

To this aim, in this study preliminary experiments were conducted using g7-NPs loaded with the model drug FITC-albumin or the recombinant IDS enzyme and labelled with Rhodamine B, demonstrating that g7-NPs can transport high molecular weight molecule such as enzyme through the BBB and paving the way for the upcoming *in vitro* and *in vivo* efficacy studies.

However, *in vitro* and *in vivo* pilot studies suggested that nanoparticles might need more than 2 weeks to open up and release the recombinant enzyme. Indeed, to date there are still no conclusive studies in the medium/long term with this type of NPs and the time of release of the incorporated molecules is thus still undefined.

Therefore, it was important to carry out a medium-term analysis to assess the possible opening of NPs in a longer time. Biochemical, histological, immunohistochemical and immunofluorescence evaluation in liver and brain of g7-NPs-IDS treated mice suggested that a period of 6 weeks is again too short to detect the opening of the NPs and the release of the encapsulated enzyme. However, results obtained from this medium-term study are encouraging as they show a slight trend towards improvement in brain and liver of g7-NPs-IDS treated mice.

Starting from this study, we can conclude that further studies, at the moment ongoing, are needed to understand the timing of release of the enzyme from the NPs; in addition, we are re-formulating the nanoparticles with the aim to maintain the same transport efficiency to the CNS, although allowing a significant reduction of the timing of drug release. For example, nanoparticles with cholesterol in the formulation would be likely more easily biodegradable and with shorter opening and releasing times.

In conclusion, delivery of recombinant enzymes through nanoparticles may represent a prototype of the transfer of other high molecular weight molecules that may be conveyed, thereafter, to the brain, allowing a more targeted treatment. In addition, nanoparticles could be engineered *ad hoc*, not only to cross the BBB, but also to reach other organs or other specific targets as tumours. This would also allow treating diseases for which there are currently no treatments available due to inability of the drugs to target specific sites.

In particular for LSDs, mainly due to deficits of the lysosomal enzymes, PLGA NPs probably represent the best vector, given the specific targeting of the NPs, which have been demonstrated to enter and accumulate right inside cell lysosomes.

In general, a selective transport of big/heavy drugs to the CNS could greatly improve therapy for brain diseases, which have a very negative impact on patients, their families and society.

6. REFERENCES

1. Abbott, N.J., and Romero, I.A. (1996). Transporting therapeutics across the blood-brain barrier. Mol. Med. Today *2,* 106-113.
2. Abbott, N.J., Patabendige, A.A., Dolman, D.E., Yusof, S.R., and Begley, D.J. (2010). Structure and function of the blood-brain barrier. Neurobiol. Dis. *37,* 13-25.
3. Alberts, B., Johnson, A., Lewis, J. et al. (2002). Molecular Biology of the Cell, 4th edition, (New York: Garland Science).
4. Al-Jasmi, F.A., Tawfig, N., Berniah, A., Ali, B.R., Taleb, M., Hertecant, J.L., Bastaki, F., and Souid, A.K. (2013). Prevalence and Novel Mutations of Lysosomal Storage Disorders in United Arab Emirates: LSD in UAE. JIMD Rep. *10,* 1-9.
5. Alroy, J., Garganta, C., and Wiederschain, G. (2014). Secondary biochemical and morphological consequences in lysosomal storage diseases. Biochemistry (Mosc) *79,* 619-636.
6. Applegarth, D.A., Toone, J.R., and Lowry, R.B. (2000). Incidence of inborn errors of metabolism in British Columbia, 1969-1996. Pediatrics *105,* e10.
7. Araya, K., Sakai, N., Mohri, I., Kagitani-Shimono, K., Okinaga, T., Hashii, Y., Ohta, H., Nakamichi, I., Aozasa, K., Taniike, M., and Ozono, K. (2009). Localized donor cells in brain of a Hunter disease patient after cord blood stem cell transplantation. Mol. Genet. Metab. *98,* 255-263.
8. Ballabio, A., and Gieselmann, V. (2009). Lysosomal disorders: from storage to cellular damage. Biochim. Biophys. Acta *1793,* 684-696.
9. Beck, M., Arn, P., Giugliani, R., Muenzer, J., Okuyama, T., Taylor, J., and Fallet, S. (2014). The natural history of MPS I: global perspectives from the MPS I Registry. Genet. Med. *16,* 759-765.
10. Beesley, C.E., Meaney, C.A., Greenland, G., Adams, V., Vellodi, A., Young, E.P., and Winchester, B.G. (2001). Mutational analysis of 85 mucopolysaccharidosis type I families: frequency of known mutations, identification of 17 novel mutations and in vitro expression of missense mutations. Hum. Genet. *109,* 503-511.
11. Begley, D.J. (2004). Delivery of therapeutic agents to the central nervous system: the problems and the possibilities. Pharmacol. Ther. *104,* 29-45.
12. Begley, D.J., Pontikis, C.C., and Scarpa, M. (2008). Lysosomal storage diseases and the blood-brain barrier. Curr. Pharm. Des. *14,* 1566-1580.
13. Bertola, F., Filocamo, M., Casati, G., Mort, M., Rosano, C., Tylki-Szymanska, A., Tuysuz, B., Gabrielli, O., Grossi, S., Scarpa, M*., et al.* (2011). IDUA mutational profiling of a cohort of 102 European patients with mucopolysaccharidosis type I: identification and

characterization of 35 novel alpha-L-iduronidase (IDUA) alleles. Hum. Mutat. *32,* E2189-210.

14. Bjornsson, S. (1993). Simultaneous preparation and quantitation of proteoglycans by precipitation with alcian blue. Anal. Biochem. *210,* 282-291.
15. Boado, R.J., Zhang, Y., Zhang, Y., Xia, C.F., Wang, Y., and Pardridge, W.M. (2008). Genetic engineering of a lysosomal enzyme fusion protein for targeted delivery across the human blood-brain barrier. Biotechnol. Bioeng. 99, 475-484.
16. Bondeson, M.L., Malmgren, H., Dahl, N., Carlberg, B.M., and Pettersson, U. (1995). Presence of an IDS-related locus (IDS2) in Xq28 complicates the mutational analysis of Hunter syndrome. Eur. J. Hum. Genet. *3,* 219-227.
17. Bondioli, L., Costantino, L., Ballestrazzi, A., Lucchesi, D., Boraschi, D., Pellati, F., Benvenuti, S., Tosi, G., and Vandelli, M.A. (2010). PLGA nanoparticles surface decorated with the sialic acid, N-acetylneuraminic acid. Biomaterials *31,* 3395-3403.
18. Bondioli, L., Ruozi, B., Belletti, D., Forni, F., Vandelli, M.A., and Tosi, G. (2011). Sialic acid as a potential approach for the protection and targeting of nanocarriers. Expert Opin. Drug Deliv. *8,* 921-937.
19. Brante, G. (1952). Gargoylism; a mucopolysaccharidosis. Scand. J. Clin. Lab. Invest. *4,* 43-46.
20. Brusius-Facchin, A.C., Schwartz, I.V., Zimmer, C., Ribeiro, M.G., Acosta, A.X., Horovitz, D., Monlleo, I.L., Fontes, M.I., Fett-Conte, A., Sobrinho, R.P.*, et al.* (2014). Mucopolysaccharidosis type II: identification of 30 novel mutations among Latin American patients. Mol. Genet. Metab. *111,* 133-138.
21. Burton, B.K., and Giugliani, R. (2012). Diagnosing Hunter syndrome in pediatric practice: practical considerations and common pitfalls. Eur. J. Pediatr. *171,* 631-639.
22. Calias, P., Papisov, M., Pan, J., Savioli, N., Belov, V., Huang, Y., Lotterhand, J., Alessandrini, M., Liu, N., Fischman, A.J., Powell, J.L., and Heartlein, M.W. (2012). CNS penetration of intrathecal-lumbar idursulfase in the monkey, dog and mouse: implications for neurological outcomes of lysosomal storage disorder. PLoS One *7,* e30341.
23. Cardone, M., Polito, V.A., Pepe, S., Mann, L., D'Azzo, A., Auricchio, A., Ballabio, A., and Cosma, M.P. (2006). Correction of Hunter syndrome in the MPSII mouse model by AAV2/8-mediated gene delivery. Hum. Mol. Genet. *15,* 1225-1236.
24. Chamoles, N.A., Blanco, M., and Gaggioli, D. (2001a). Diagnosis of alpha-L-iduronidase deficiency in dried blood spots on filter paper: the possibility of newborn diagnosis. Clin. Chem. *47,* 780-781.
25. Chamoles, N.A., Blanco, M.B., Gaggioli, D., and Casentini, C. (2001b). Hurler-like phenotype: enzymatic diagnosis in dried blood spots on filter paper. Clin. Chem. *47,* 2098-2102.

26. Chhabra, R., Grabrucker, A.M., Veratti, P., Belletti, D., Boeckers, T.M., Vandelli, M.A., Forni, F., Tosi, G., and Ruozi, B. (2014). Characterization of lysosome-destabilizing DOPE/PLGA nanoparticles designed for cytoplasmic drug release. Int. J. Pharm. *471,* 349-357.
27. Cimaz, R., and La Torre, F. (2014). Mucopolysaccharidoses. Curr. Rheumatol. Rep. *16,* 389-013-0389-0.
28. Clarke, L.A., Russell, C.S., Pownall, S., Warrington, C.L., Borowski, A., Dimmick, J.E., Toone, J., and Jirik, F.R. (1997). Murine mucopolysaccharidosis type I: targeted disruption of the murine alpha-L-iduronidase gene. Hum. Mol. Genet. *6,* 503-511.
29. Clarke, L.A., Wraith, J.E., Beck, M., Kolodny, E.H., Pastores, G.M., Muenzer, J., Rapoport, D.M., Berger, K.I., Sidman, M., Kakkis, E.D., and Cox, G.F. (2009). Long-term efficacy and safety of laronidase in the treatment of mucopolysaccharidosis I. Pediatrics *123,* 229-240.
30. Costantino, L., Gandolfi, F., Tosi, G., Rivasi, F., Vandelli, M.A., and Forni, F. (2005). Peptide-derivatized biodegradable nanoparticles able to cross the blood-brain barrier. J. Control. Release *108,* 84-96.
31. Costantino, L., Tosi, G., Ruozi, B., Bondioli, L., Vandelli, M.A., and Forni, F. (2009). Chapter 3 - Colloidal systems for CNS drug delivery. Prog. Brain Res. *180,* 35-69.
32. Cudry, S., Tigaud, I., Froissart, R., Bonnet, V., Maire, I., and Bozon, D. (2000). MPS II in females: molecular basis of two different cases. J. Med. Genet. *37,* E29.
33. D'Anna, R., Cannata, M.L., Marini, H., Atteritano, M., Cancellieri, F., Corrado, F., Triolo, O., Rizzo, P., Russo, S., Gaudio, A.*, et al.* (2009). Effects of the phytoestrogen genistein on hot flushes, endometrium, and vaginal epithelium in postmenopausal women: a 2-year randomized, double-blind, placebo-controlled study. Menopause *16,* 301-306.
34. de Duve, C., Pressman, B.C., Gianetto, R., Wattiaux, R., and Appelmans, F. (1955). Tissue fractionation studies. 6. Intracellular distribution patterns of enzymes in rat-liver tissue. Biochem. J. *60,* 604-617.
35. de Jong, J.G., Wevers, R.A., and Liebrand-van Sambeek, R. (1992). Measuring urinary glycosaminoglycans in the presence of protein: an improved screening procedure for mucopolysaccharidoses based on dimethylmethylene blue. Clin. Chem. *38,* 803-807.
36. Delgadillo, V., O'Callaghan Mdel, M., Artuch, R., Montero, R., and Pineda, M. (2011). Genistein supplementation in patients affected by Sanfilippo disease. J. Inherit. Metab. Dis. *34,* 1039-1044.
37. Deng, S.X., Panahian, N., James, H., Gelbard, H.A., Federoff, H.J., Dewhurst, S., and Epstein, L.G. (1998). Luciferase: a sensitive and quantitative probe for blood-brain barrier disruption. J. Neurosci. Methods *83,* 159-164.
38. Dickson, P.I. (2009). Novel treatments and future perspectives: outcomes of intrathecal drug delivery. Int. J. Clin. Pharmacol. Ther. *47 Suppl 1,* S124-7.

39. Dickson, P.I., and Chen, A.H. (2011). Intrathecal enzyme replacement therapy for mucopolysaccharidosis I: translating success in animal models to patients. Curr. Pharm. Biotechnol. *12,* 946-955.

40. Dionisi-Vici, C., Rizzo, C., Burlina, A.B., Caruso, U., Sabetta, G., Uziel, G., and Abeni, D. (2002). Inborn errors of metabolism in the Italian pediatric population: a national retrospective survey. J. Pediatr. *140,* 321-327.

41. Dorfman, A., and Lorincz, A.E. (1957). Occurrence of Urinary Acid Mucopolysaccharides in the Hurler Syndrome. Proc. Natl. Acad. Sci. U. S. A. *43,* 443-446.

42. El-Amouri, S.S., Dai, M., Han, J.F., Brady, R.O., and Pan, D. (2014). Normalization and improvement of CNS deficits in mice with hurler syndrome after long-term peripheral delivery of BBB-targeted iduronidase. Mol. Ther. *22,* 2028-2037.

43. Fratantoni, J.C., Hall, C.W., and Neufeld, E.F. (1968). The defect in Hurler's and Hunter's syndromes: faulty degradation of mucopolysaccharide. Proc. Natl. Acad. Sci. U. S. A. *60,* 699-706.

44. Friso, A., Tomanin, R., Alba, S., Gasparotto, N., Puicher, E.P., Fusco, M., Hortelano, G., Muenzer, J., Marin, O., Zacchello, F., and Scarpa, M. (2005). Reduction of GAG storage in MPS II mouse model following implantation of encapsulated recombinant myoblasts. J. Gene Med. *7,* 1482-1491.

45. Friso, A., Tomanin, R., Zanetti, A., Mennuni, C., Calvaruso, F., La Monica, N., Marin, O., Zacchello, F., and Scarpa, M. (2008). Gene therapy of Hunter syndrome: evaluation of the efficiency of muscle electro gene transfer for the production and release of recombinant iduronate-2-sulfatase (IDS). Biochim. Biophys. Acta *1782,* 574-580.

46. Friso, A., Tomanin, R., Salvalaio, M., and Scarpa, M. (2010). Genistein reduces glycosaminoglycan levels in a mouse model of mucopolysaccharidosis type II. Br. J. Pharmacol. *159,* 1082-1091.

47. Froissart, R., Moreira da Silva, I., Guffon, N., Bozon, D., and Maire, I. (2002). Mucopolysaccharidosis type II--genotype/phenotype aspects. Acta Paediatr. Suppl. *91,* 82-87.

48. Froissart, R., Da Silva, I.M., and Maire, I. (2007). Mucopolysaccharidosis type II: an update on mutation spectrum. Acta Paediatr. Suppl. *96,* 71-77.

49. Fu, H., Kang, L., Jennings, J.S., Moy, S.S., Perez, A., Dirosario, J., McCarty, D.M., and Muenzer, J. (2007). Significantly increased lifespan and improved behavioral performances by rAAV gene delivery in adult mucopolysaccharidosis IIIB mice. Gene Ther. *14,* 1065-1077.

50. Fuller, M., Meikle, P.J., and Hopwood, J.J. (2006). Epidemiology of lysosomal storage diseases: an overview. In Fabry Disease: Perspectives from 5 Years of FOS, Mehta, A., Beck, M. and Sunder-Plassmann, G. eds., (Oxford: Oxford PharmaGenesis)

51. Futerman, A.H., and van Meer, G. (2004). The cell biology of lysosomal storage disorders. Nat. Rev. Mol. Cell Biol. *5,* 554-565.

52. Garbuzova-Davis, S., Louis, M.K., Haller, E.M., Derasari, H.M., Rawls, A.E., and Sanberg, P.R. (2011). Blood-brain barrier impairment in an animal model of MPS III B. PLoS One *6,* e16601.

53. Garbuzova-Davis, S., Mirtyl, S., Sallot, S.A., Hernandez-Ontiveros, D.G., Haller, E., and Sanberg, P.R. (2013). Blood-brain barrier impairment in MPS III patients. BMC Neurol. *13,* 174-2377-13-174.

54. Garcia, A.R., Pan, J., Lamsa, J.C., and Muenzer, J. (2007). The characterization of a murine model of mucopolysaccharidosis II (Hunter syndrome). J. Inherit. Metab. Dis. *30,* 924-934.

55. Gasparotto, N., Tomanin, R., Frigo, A.C., Niizawa, G., Pasquini, E., Blanco, M., Donati, M.A., Keutzer, J., Zacchello, F., and Scarpa, M. (2009). Rapid diagnostic testing procedures for lysosomal storage disorders: alpha-glucosidase and beta-galactosidase assays on dried blood spots. Clin. Chim. Acta *402,* 38-41.

56. Giugliani, R., Rojas, V.M., Martins, A.M., Valadares, E.R., Clarke, J.T., Goes, J.E., Kakkis, E.D., Worden, M.A., Sidman, M., and Cox, G.F. (2009). A dose-optimization trial of laronidase (Aldurazyme) in patients with mucopolysaccharidosis I. Mol. Genet. Metab. *96,* 13-19.

57. Giugliani, R., Carvalho, C.G., Herber, S., and de Camargo Pinto, L.L. (2011). Recent Advances in Treatment Approaches of Mucopolysaccharidosis VI. Curr. Pharm. Biotechnol. *12,* 956-962.

58. Giugliani, R., Federhen, A., da Silva A.A., Bittar C.M., Souza C.F.M., Netto C., Quoos Mayer F, Baldo G, Matte U (2012) *Emerging treatment options for the mucopolysaccharidoses.* Research and Reports in Endocrine Disorders, *2*:53-64.

59. Gort, L., Chabas, A., and Coll, M.J. (1998). Analysis of five mutations in 20 mucopolysaccharidois type 1 patients: high prevalence of the W402X mutation. Mutations in brief no. 121. Online. Hum. Mutat. *11,* 332-333.

60. Grabrucker, A.M., Garner, C.C., Boeckers, T.M., Bondioli, L., Ruozi, B., Forni, F., Vandelli, M.A., and Tosi, G. (2011). Development of novel Zn2+ loaded nanoparticles designed for cell-type targeted drug release in CNS neurons: in vitro evidences. PLoS One *6,* e17851.

61. Guffon, N., Souillet, G., Maire, I., Straczek, J., and Guibaud, P. (1998). Follow-up of nine patients with Hurler syndrome after bone marrow transplantation. J. Pediatr. *133,* 119-125.

62. Hers, H.G. (1965). Inborn Lysosomal Diseases. Gastroenterology *48,* 625-633.

63. Higuchi, T., Shimizu, H., Fukuda, T., Kawagoe, S., Matsumoto, J., Shimada, Y., Kobayashi, H., Ida, H., Ohashi, T., Morimoto, H*., et al.* (2012). Enzyme replacement therapy (ERT)

procedure for mucopolysaccharidosis type II (MPS II) by intraventricular administration (IVA) in murine MPS II. Mol. Genet. Metab. *107,* 122-128.

64. Hobbs, J.R., Hugh-Jones, K., Barrett, A.J., Byrom, N., Chambers, D., Henry, K., James, D.C., Lucas, C.F., Rogers, T.R., Benson, P.F.*, et al.* (1981). Reversal of clinical features of Hurler's disease and biochemical improvement after treatment by bone-marrow transplantation. Lancet *2,* 709-712.
65. Hult, M., Darin, N., von Dobeln, U., and Mansson, J.E. (2014). Epidemiology of lysosomal storage diseases in Sweden. Acta Paediatr. *103,* 1258-1263.
66. Hunter, C. (1917). A Rare Disease in Two Brothers. Proc. R. Soc. Med. *10,* 104-116.
67. Jabir, N.R., Tabrez, S., Ashraf, G.M., Shakil, S., Damanhouri, G.A., and Kamal, M.A. (2012). Nanotechnology-based approaches in anticancer research. Int. J. Nanomedicine *7*, 4391-4408.
68. Jain, R.A. (2000). The manufacturing techniques of various drug loaded biodegradable poly(lactide-co-glycolide) (PLGA) devices. Biomaterials *21,* 2475-2490.
69. Jakobkiewicz-Banecka, J., Piotrowska, E., Narajczyk, M., Baranska, S., and Wegrzyn, G. (2009). Genistein-mediated inhibition of glycosaminoglycan synthesis, which corrects storage in cells of patients suffering from mucopolysaccharidoses, acts by influencing an epidermal growth factor-dependent pathway. J. Biomed. Sci. *16,* 26-0127-16-26.
70. Jordan, M.C., Zheng, Y., Ryazantsev, S., Rozengurt, N., Roos, K.P., and Neufeld, E.F. (2005). Cardiac manifestations in the mouse model of mucopolysaccharidosis I. Mol. Genet. Metab. *86,* 233-243.
71. Jung, S.C., Park, E.S., Choi, E.N., Kim, C.H., Kim, S.J., and Jin, D.K. (2010). Characterization of a novel mucopolysaccharidosis type II mouse model and recombinant AAV2/8 vector-mediated gene therapy. Mol. Cells *30,* 13-18.
72. Jurecka, A., Lugowska, A., Golda, A., Czartoryska, B., and Tylki-Szymanska, A. (2014). Prevalence rates of mucopolysaccharidoses in Poland. J. Appl. Genet.
73. Kabanov, A.V., and Gendelman, H.E. (2007). Nanomedicine in the diagnosis and therapy of neurodegenerative disorders. Prog. Polym. Sci. *32,* 1054-1082.
74. Kakkis, E.D., Matynia, A., Jonas, A.J., and Neufeld, E.F. (1994). Overexpression of the human lysosomal enzyme alpha-L-iduronidase in Chinese hamster ovary cells. Protein Expr. Purif. *5,* 225-232.
75. Kakkis, E.D., Muenzer, J., Tiller, G.E., Waber, L., Belmont, J., Passage, M., Izykowski, B., Phillips, J., Doroshow, R., Walot, I., Hoft, R., and Neufeld, E.F. (2001). Enzyme-replacement therapy in mucopolysaccharidosis I. N. Engl. J. Med. *344,* 182-188.
76. Kozler, P., and Pokorny, J. (2003). Altered blood-brain barrier permeability and its effect on the distribution of Evans blue and sodium fluorescein in the rat brain applied by intracarotid injection. Physiol. Res. *52,* 607-614.

77. Kreuter, J. (2013). Mechanism of polymeric nanoparticle-based drug transport across the blood-brain barrier (BBB). J. Microencapsul. *30,* 49-54.

78. Langereis, E.J., van Vlies, N., Church, H.J., Geskus, R.B., Hollak, C.E., Jones, S.A., Kulik, W., van Lenthe, H., Mercer, J., Schreider, L*., et al.* (2014). Biomarker responses correlate with antibody status in mucopolysaccharidosis type I patients on long-term enzyme replacement therapy. Mol. Genet. Metab. [Epub ahead of print].

79. Lee, O.J., Kim, S.J., Sohn, Y.B., Park, H.D., Lee, S.Y., Kim, C.H., Ko, A.R., Yook, Y.J., Lee, S.J., Park, S.W*., et al.* (2012). A study of the relationship between clinical phenotypes and plasma iduronate-2-sulfatase enzyme activities in Hunter syndrome patients. Korean J. Pediatr. *55,* 88-92.

80. Li, Y., Scott, C.R., Chamoles, N.A., Ghavami, A., Pinto, B.M., Turecek, F., and Gelb, M.H. (2004). Direct multiplex assay of lysosomal enzymes in dried blood spots for newborn screening. Clin. Chem. *50,* 1785-1796.

81. Liu, Y., Li, K., Pan, J., Liu, B., and Feng, S.S. (2010). Folic acid conjugated nanoparticles of mixed lipid monolayer shell and biodegradable polymer core for targeted delivery of Docetaxel. Biomaterials *31*, 330-338.

82. Malinowska, M., Wilkinson, F.L., Bennett, W., Langford-Smith, K.J., O'Leary, H.A., Jakobkiewicz-Banecka, J., Wynn, R., Wraith, J.E., Wegrzyn, G., and Bigger, B.W. (2009). Genistein reduces lysosomal storage in peripheral tissues of mucopolysaccharide IIIB mice. Mol. Genet. Metab. *98,* 235-242.

83. Malinowska, M., Wilkinson, F.L., Langford-Smith, K.J., Langford-Smith, A., Brown, J.R., Crawford, B.E., Vanier, M.T., Grynkiewicz, G., Wynn, R.F., Wraith, J.E., Wegrzyn, G., and Bigger, B.W. (2010). Genistein improves neuropathology and corrects behaviour in a mouse model of neurodegenerative metabolic disease. PLoS One *5,* e14192.

84. Marsden, D., and Levy, H. (2010). Newborn screening of lysosomal storage disorders. Clin. Chem. *56,* 1071-1079.

85. Martin, R., Beck, M., Eng, C., Giugliani, R., Harmatz, P., Munoz, V., and Muenzer, J. (2008). Recognition and diagnosis of mucopolysaccharidosis II (Hunter syndrome). Pediatrics *121,* e377-86.

86. Mayer, F.Q., Artigalás, O.A., Lagranha, V.L., Baldo, G., Schwartz, I.V., Matte, U., Giugliani, R. (2013). Chloramphenicol enhances IDUA activity on fibroblasts from mucopolysaccharidosis I patients. Curr Pharm Biotechnol., *14*(2), 194-8.

87. McKusick, V.A. (1966). Heritable Disorders of Connective Tissue (St.Louis, MO, USA: C.V. Mosby Co.).

88. Mechtler, T.P., Stary, S., Metz, T.F., De Jesus, V.R., Greber-Platzer, S., Pollak, A., Herkner, K.R., Streubel, B., and Kasper, D.C. (2012). Neonatal screening for lysosomal storage

disorders: feasibility and incidence from a nationwide study in Austria. Lancet *379,* 335-341.

89. Meikle, P.J., Hopwood, J.J., Clague, A.E., and Carey, W.F. (1999). Prevalence of lysosomal storage disorders. Jama *281,* 249-254.
90. Morquio, L. (1976). The classics: On a form of familial osseous dystrophy. Bull. Soc. Pediat. 27:145, 1929. Clin. Orthop. Relat. Res. *(114),* 10-11.
91. Muenzer, J., Lamsa, J.C., Garcia, A., Dacosta, J., Garcia, J., and Treco, D.A. (2002). Enzyme replacement therapy in mucopolysaccharidosis type II (Hunter syndrome): a preliminary report. Acta Paediatr. Suppl. *91,* 98-99.
92. Muenzer, J., Wraith, J.E., Beck, M., Giugliani, R., Harmatz, P., Eng, C.M., Vellodi, A., Martin, R., Ramaswami, U., Gucsavas-Calikoglu, M.*, et al.* (2006). A phase II/III clinical study of enzyme replacement therapy with idursulfase in mucopolysaccharidosis II (Hunter syndrome). Genet. Med. *8,* 465-473.
93. Muenzer, J., Beck, M., Eng, C.M., Escolar, M.L., Giugliani, R., Guffon, N.H., Harmatz, P., Kamin, W., Kampmann, C., Koseoglu, S.T.*, et al.* (2009). Multidisciplinary management of Hunter syndrome. Pediatrics *124,* e1228-39.
94. Muenzer, J. (2011). Overview of the mucopolysaccharidoses. Rheumatology (Oxford) *50 Suppl 5,* v4-12.
95. Nag, S., and Begley, D.J. (2005). Blood Brain Barrier, Exchange of metabolites and gases. In Pathology and Genetics: Cerebrovascular Diseases, Kalimo, Hannu ed., (Basel: ISN Neuropath Press) pp. 22-29.
96. Neufeld, E.F., and Muenzer, J. (2001). The mucopolysaccharidoses. In The Metabolic and Molecular Bases of Inherited Disease, Scriver, C. R., Beaudet, A. L., Sly, W. S., Valle, D., Childs, B., Kinzler, K. W. and Vogelstein, B. eds., (New York, NY, USA: McGraw-Hill) pp. 3421-3452.
97. Nobs, L., Buchegger, F., Gurny, R., and Allemann, E. (2003). Surface modification of poly(lactic acid) nanoparticles by covalent attachment of thiol groups by means of three methods. Int. J. Pharm. *250,* 327-337.
98. Nobs, L., Buchegger, F., Gurny, R., and Allemann, E. (2004). Poly(lactic acid) nanoparticles labeled with biologically active Neutravidin for active targeting. Eur. J. Pharm. Biopharm. *58,* 483-490.
99. Nobs, L., Buchegger, F., Gurny, R., and Allemann, E. (2006). Biodegradable nanoparticles for direct or two-step tumor immunotargeting. Bioconjug. Chem. *17,* 139-145.
100. Noh, H., and Lee, J.I. (2014). Current and potential therapeutic strategies for mucopolysaccharidoses. J. Clin. Pharm. Ther. *39,* 215-224.

101. Ohmi, K., Greenberg, D.S., Rajavel, K.S., Ryazantsev, S., Li, H.H., and Neufeld, E.F. (2003). Activated microglia in cortex of mouse models of mucopolysaccharidoses I and IIIB. Proc. Natl. Acad. Sci. U. S. A. *100,* 1902-1907.

102. Pardridge, W.M. (2003). Blood-brain barrier drug targeting: the future of brain drug development. Mol. Interv. *3,* 90-105, 51.

103. Pardridge, W.M. (2005). The blood-brain barrier: bottleneck in brain drug development. Neurorx *2,* 3-14.

104. Pastores, G.M., Arn, P., Beck, M., Clarke, J.T., Guffon, N., Kaplan, P., Muenzer, J., Norato, D.Y., Shapiro, E., Thomas, J., Viskochil, D., and Wraith, J.E. (2007). The MPS I registry: design, methodology, and early findings of a global disease registry for monitoring patients with Mucopolysaccharidosis Type I. Mol. Genet. Metab. *91,* 37-47.

105. Piller Puicher, E., Tomanin, R., Salvalaio, M., Friso, A., Hortelano, G., Marin, O., and Scarpa, M. (2012). Encapsulated engineered myoblasts can cure Hurler syndrome: preclinical experiments in the mouse model. Gene Ther. *19,* 355-364.

106. Pina-Aguilar, R.E., Zaragoza-Arevalo, G.R., Rau, I., Gal, A., Alcantara-Ortigoza, M.A., Lopez-Martinez, M.S., and Santillan-Hernandez, Y. (2013). Mucopolysaccharidosis type II in a female carrying a heterozygous stop mutation of the iduronate-2-sulfatase gene and showing a skewed X chromosome inactivation. Eur. J. Med. Genet. *56,* 159-162.

107. Pinto, R., Caseiro, C., Lemos, M., Lopes, L., Fontes, A., Ribeiro, H., Pinto, E., Silva, E., Rocha, S., Marcao, A.*, et al.* (2004). Prevalence of lysosomal storage diseases in Portugal. Eur. J. Hum. Genet. *12,* 87-92.

108. Piotrowska, E., Jakobkiewicz-Banecka, J., Baranska, S., Tylki-Szymanska, A., Czartoryska, B., Wegrzyn, A., and Wegrzyn, G. (2006). Genistein-mediated inhibition of glycosaminoglycan synthesis as a basis for gene expression-targeted isoflavone therapy for mucopolysaccharidoses. Eur. J. Hum. Genet. *14,* 846-852.

109. Piotrowska, E., Jakobkiewicz-Banecka, J., Tylki-Szymanska, A., Liberek, A., Maryniak, A., Malinowska, M., Czartoryska, B., Puk, E., Kloska, A., Liberek, T.*, et al.* (2008). Genistin-rich soy isoflavone extract in substrate reduction therapy for Sanfilippo syndrome: An open-label, pilot study in 10 pediatric patients. Curr. Ther. Res. Clin. Exp. *69,* 166-179.

110. Poorthuis, B.J., Wevers, R.A., Kleijer, W.J., Groener, J.E., de Jong, J.G., van Weely, S., Niezen-Koning, K.E., and van Diggelen, O.P. (1999). The frequency of lysosomal storage diseases in The Netherlands. Hum. Genet. *105,* 151-156.

111. Poupetova, H., Ledvinova, J., Berna, L., Dvorakova, L., Kozich, V., and Elleder, M. (2010). The birth prevalence of lysosomal storage disorders in the Czech Republic: comparison with data in different populations. J. Inherit. Metab. Dis. *33,* 387-396.

112. Roberts, A.L., Thomas, B.J., Wilkinson, A.S., Fletcher, J.M., and Byers, S. (2006). Inhibition of glycosaminoglycan synthesis using rhodamine B in a mouse model of mucopolysaccharidosis type IIIA. Pediatr. Res. *60,* 309-314.

113. Rosca, I.D., Watari, F., and Uo, M. (2004). Microparticle formation and its mechanism in single and double emulsion solvent evaporation. J. Control. Release *99,* 271-280.

114. Ruozi, B., Belletti, D., Pederzoli, F., Veratti, P., Forni, F., Vandelli, M.A., and Tosi, G. (2014a). Nanotechnology and Alzheimer's disease: what has been done and what to do. Curr. Med. Chem. *21,* 4169-4185.

115. Ruozi, B., Belletti, D., Forni, F., Sharma, A., Muresanu, D., Mossler, H., Vandelli, M.A., Tosi, G., and Sharma, H.S. (2014b). Poly (D,L-lactide-co-glycolide) nanoparticles loaded with cerebrolysin display neuroprotective activity in a rat model of concussive head injury. CNS Neurol. Disord. Drug Targets *13,* 1475-1482.

116. Sahay, G., Alakhova, D.Y., and Kabanov, A.V. (2010). Endocytosis of nanomedicines. J. Control. Release *145,* 182-195.

117. Sands, M.S., and Davidson, B.L. (2006). Gene therapy for lysosomal storage diseases. Mol. Ther. *13,* 839-849.

118. Sanjurjo-Crespo, P. (2007). Clinical aspects of mucopolysaccharidosis type II. Rev. Neurol. *44 Suppl 1,* S3-6.

119. Scarpa, M., Bellettato, C.M., Tomanin, R., and Zanetti, A. (2012). Barriera Emato-Encefalica e terapie farmacologiche. Prospettive in Pediatria *42*, 176-184.

120. Scherrmann, J.M. (2002). Drug delivery to brain via the blood-brain barrier. Vascul Pharmacol. *38,* 349-354.

121. Schwartz, I.V., Ribeiro, M.G., Mota, J.G., Toralles, M.B., Correia, P., Horovitz, D., Santos, E.S., Monlleo, I.L., Fett-Conte, A.C., Sobrinho, R.P.*, et al.* (2007). A clinical study of 77 patients with mucopolysaccharidosis type II. Acta Paediatr. Suppl. *96,* 63-70.

122. Scott, C.R., Elliott, S., Buroker, N., Thomas, L.I., Keutzer, J., Glass, M., Gelb, M.H., and Turecek, F. (2013). Identification of infants at risk for developing Fabry, Pompe, or mucopolysaccharidosis-I from newborn blood spots by tandem mass spectrometry. J. Pediatr. *163,* 498-503.

123. Scott, H.S., Guo, X.H., Hopwood, J.J., and Morris, C.P. (1992). Structure and sequence of the human alpha-L-iduronidase gene. Genomics *13,* 1311-1313.

124. Scott, H.S., Bunge, S., Gal, A., Clarke, L.A., Morris, C.P., and Hopwood, J.J. (1995). Molecular genetics of mucopolysaccharidosis type I: diagnostic, clinical, and biological implications. Hum. Mutat. *6,* 288-302.

125. Seregin, S.S., and Amalfitano, A. (2011). Gene therapy for lysosomal storage diseases: progress, challenges and future prospects. Curr. Pharm. Des. *17,* 2558-2574.

126. Sohn, Y.B., Lee, J., Cho, S.Y., Kim, S.J., Ko, A.R., Nam, M.H., and Jin, D.K. (2013). Improvement of CNS defects via continuous intrathecal enzyme replacement by osmotic pump in mucopolysaccharidosis type II mice. Am. J. Med. Genet. A. *161A,* 1036-1043.

127. Soliman, O.I., Timmermans, R.G., Nemes, A., Vletter, W.B., Wilson, J.H., ten Cate, F.J., and Geleijnse, M.L. (2007). Cardiac abnormalities in adults with the attenuated form of mucopolysaccharidosis type I. J. Inherit. Metab. Dis. *30,* 750-757.

128. Spada, M., Pagliardini, S., Yasuda, M., Tukel, T., Thiagarajan, G., Sakuraba, H., Ponzone, A., and Desnick, R.J. (2006). High incidence of later-onset fabry disease revealed by newborn screening. Am. J. Hum. Genet. *79,* 31-40.

129. Syed, S., Zubair, A., and Frieri, M. (2013). Immune response to nanomaterials: implications for medicine and literature review. Curr. Allergy Asthma Rep. *13,* 50-57.

130. Sukegawa-Hayasaka, K., Kato, Z., Nakamura, H., Tomatsu, S., Fukao, T., Kuwata, K., Orii, T., and Kondo, N. (2006). Effect of Hunter disease (mucopolysaccharidosis type II) mutations on molecular phenotypes of iduronate-2-sulfatase: enzymatic activity, protein processing and structural analysis. J. Inherit. Metab. Dis. *29*, 755-761.

131. Tanaka, A., Okuyama, T., Suzuki, Y., Sakai, N., Takakura, H., Sawada, T., Tanaka, T., Otomo, T., Ohashi, T., Ishige-Wada, M*., et al.* (2012). Long-term efficacy of hematopoietic stem cell transplantation on brain involvement in patients with mucopolysaccharidosis type II: a nationwide survey in Japan. Mol. Genet. Metab. *107,* 513-520.

132. Terlato, N.J., and Cox, G.F. (2003). Can mucopolysaccharidosis type I disease severity be predicted based on a patient's genotype? A comprehensive review of the literature. Genet. Med. *5,* 286-294.

133. Tieu, P.T., Bach, G., Matynia, A., Hwang, M., and Neufeld, E.F. (1995). Four novel mutations underlying mild or intermediate forms of alpha-L-iduronidase deficiency (MPS IS and MPS IH/S). Hum. Mutat. *6,* 55-59.

134. Timms, K.M., Bondeson, M.L., Ansari-Lari, M.A., Lagerstedt, K., Muzny, D.M., Dugan-Rocha, S.P., Nelson, D.L., Pettersson, U., and Gibbs, R.A. (1997). Molecular and phenotypic variation in patients with severe Hunter syndrome. Hum. Mol. Genet. *6,* 479-486.

135. Tomanin, R., Zanetti, A., Zaccariotto, E., D'Avanzo, F., Bellettato, C.M., Scarpa, M. (2012). Gene therapy approaches for lysosomal storage disorders, a good model for the treatment of mendelian diseases. Acta Paediatr. *101,* 692-701.

136. Tomanin, R., Zanetti, A., D Avanzo, F., Rampazzo, A., Gasparotto, N., Parini, R., Pascarella, A., Concolino, D., Procopio, E., Fiumara, A*., et al.* (2014). Clinical efficacy of Enzyme Replacement Therapy in paediatric Hunter patients, an independent study of 3.5 years. Orphanet J. Rare Dis. *9,* 129.

137. Tomatsu, S., Montano, A.M., Ohashi, A., Gutierrez, M.A., Oikawa, H., Oguma, T., Dung, V.C., Nishioka, T., Orii, T., and Sly, W.S. (2008). Enzyme replacement therapy in a murine model of Morquio A syndrome. Hum. Mol. Genet. 17, 815-824.

138. Tosi, G., Costantino, L., Rivasi, F., Ruozi, B., Leo, E., Vergoni, A.V., Tacchi, R., Bertolini, A., Vandelli, M.A., and Forni, F. (2007). Targeting the central nervous system: in vivo experiments with peptide-derivatized nanoparticles loaded with Loperamide and Rhodamine-123. J. Control. Release 122, 1-9.

139. Tosi, G., Costantino, L., Ruozi, B., Forni, F., and Vandelli, M.A. (2008). Polymeric nanoparticles for the drug delivery to the central nervous system. Expert Opin. Drug Deliv. 5, 155-174.

140. Tosi, G., Vergoni, A.V., Ruozi, B., Bondioli, L., Badiali, L., Rivasi, F., Costantino, L., Forni, F., and Vandelli, M.A. (2010). Sialic acid and glycopeptides conjugated PLGA nanoparticles for central nervous system targeting: In vivo pharmacological evidence and biodistribution. J. Control. Release 145, 49-57.

141. Tosi, G., Fano, R.A., Bondioli, L., Badiali, L., Benassi, R., Rivasi, F., Ruozi, B., Forni, F., and Vandelli, M.A. (2011a). Investigation on mechanisms of glycopeptide nanoparticles for drug delivery across the blood-brain barrier. Nanomedicine (Lond) 6, 423-436.

142. Tosi, G., Bondioli, L., Ruozi, B., Badiali, L., Severini, G.M., Biffi, S., De Vita, A., Bortot, B., Dolcetta, D., Forni, F., and Vandelli, M.A. (2011b). NIR-labeled nanoparticles engineered for brain targeting: in vivo optical imaging application and fluorescent microscopy evidences. J. Neural Transm. *118,* 145-153.

143. Tosi, G., Ruozi, B., and Vandelli, M.A. (2013a). Brain targeting with polymeric nanoparticles: which administration route should we take? Nanomedicine (Lond) *8,* 1361-1363.

144. Tosi, G., Ruozi, B., Belletti, D., Vilella, A., Zoli, M., Vandelli, M.A., and Forni, F. (2013b). Brain-targeted polymeric nanoparticles: in vivo evidence of different routes of administration in rodents. Nanomedicine (Lond) *8,* 1373-1383.

145. Tosi, G., Bortot, B., Ruozi, B., Dolcetta, D., Vandelli, M.A., Forni, F., and Severini, G.M. (2013c). Potential use of polymeric nanoparticles for drug delivery across the blood-brain barrier. Curr. Med. Chem. *20,* 2212-2225.

146. Tosi, G., Vilella, A., Chhabra, R., Schmeisser, M.J., Boeckers, T.M., Ruozi, B., Vandelli, M.A., Forni, F., Zoli, M., and Grabrucker, A.M. (2014a). Insight on the fate of CNS-targeted nanoparticles. Part II: Intercellular neuronal cell-to-cell transport. J. Control. Release *177,* 96-107.

147. Triguero, D., Buciak, J., and Pardridge, W.M. (1990). Capillary depletion method for quantification of blood-brain barrier transport of circulating peptides and plasma proteins. J. Neurochem. *54,* 1882-1888.

148. Tuschl, K., Gal, A., Paschke, E., Kircher, S., and Bodamer, O.A. (2005). Mucopolysaccharidosis type II in females: case report and review of literature. Pediatr. Neurol. 32, 270-272.

149. Urayama, A., Grubb, J.H., Sly, W.S., and Banks, W.A. (2008). Mannose 6-phosphate receptor-mediated transport of sulfamidase across the blood-brain barrier in the newborn mouse. Mol. Ther. 16, 1261-1266.

150. Urayama, A., Grubb, J.H., Sly, W.S., and Banks, W.A. (2004). Developmentally regulated mannose 6-phosphate receptor-mediated transport of a lysosomal enzyme across the blood-brain barrier. Proc. Natl. Acad. Sci. U. S. A. 101, 12658-12663.

151. Valayannopoulos, V., Brassier, A., Chabli, A., Caillaud, C., Lemoine, M., Odent, T., Arnoux, J.B., and de Lonlay, P. (2011). Enzyme replacement therapy for lysosomal storage disorders. Arch. Pediatr. *18,* 1119-1123.

152. Van Hoof, F., and Hers, H.G. (1964). Ultrastructure of the Hepatic Cells in Hurler's Disease (Gargoylism). C. R. Hebd. Seances. Acad. Sci. *259,* 1281-1283.

153. Vedolin, L., Schwartz, I.V., Komlos, M., Schuch, A., Puga, A.C., Pinto, L.L., Pires, A.P., and Giugliani, R. (2007). Correlation of MR imaging and MR spectroscopy findings with cognitive impairment in mucopolysaccharidosis II. AJNR Am. J. Neuroradiol. *28,* 1029-1033.

154. Vellodi, A. (2005). Lysosomal storage disorders. Br. J. Haematol. *128,* 413-431.

155. Vera, R., Sanchez, M., Galisteo, M., Villar, I.C., Jimenez, R., Zarzuelo, A., Perez-Vizcaino, F., and Duarte, J. (2007). Chronic administration of genistein improves endothelial dysfunction in spontaneously hypertensive rats: involvement of eNOS, caveolin and calmodulin expression and NADPH oxidase activity. Clin. Sci. (Lond) *112,* 183-191.

156. Vera, M., Le, S., Kan, S.H., Garban, H., Naylor, D., Mlikotic, A., Kaitila, I., Harmatz, P., Chen, A., and Dickson, P. (2013). Immune response to intrathecal enzyme replacement therapy in mucopolysaccharidosis I patients. Pediatr. Res. *74,* 712-720.

157. Vergoni, A.V., Tosi, G., Tacchi, R., Vandelli, M.A., Bertolini, A., and Costantino, L. (2009). Nanoparticles as drug delivery agents specific for CNS: in vivo biodistribution. Nanomedicine *5,* 369-377.

158. Vilella, A., Tosi, G., Grabrucker, A.M., Ruozi, B., Belletti, D., Vandelli, M.A., Boeckers, T.M., Forni, F., and Zoli, M. (2014). Insight on the fate of CNS-targeted nanoparticles. Part I: Rab5-dependent cell-specific uptake and distribution. J. Control. Release 174, 195-201.

159. Vogler, C., Levy, B., Grubb, J.H., Galvin, N., Tan, Y., Kakkis, E., Pavloff, N., and Sly, W.S. (2005). Overcoming the blood-brain barrier with high-dose enzyme replacement therapy in murine mucopolysaccharidosis VII. Proc. Natl. Acad. Sci. U. S. A. 102, 14777-14782.

160. Voznyi, Y.V., Keulemans, J.L., and van Diggelen, O.P. (2001). A fluorimetric enzyme assay for the diagnosis of MPS II (Hunter disease). J. Inherit. Metab. Dis. 24, 675-680.

161. Wagner, S., Zensi, A., Wien, S.L., Tschickardt, S.E., Maier, W., Vogel, T., Worek, F., Pietrzik, C.U., Kreuter, J., and von Briesen, H. (2012). Uptake mechanism of ApoE-modified nanoparticles on brain capillary endothelial cells as a blood-brain barrier model. PLoS One *7,* e32568.

162. Wang, D., El-Amouri, S.S., Dai, M., Kuan, C.Y., Hui, D.Y., Brady, R.O., and Pan, D. (2013). Engineering a lysosomal enzyme with a derivative of receptor-binding domain of apoE enables delivery across the blood-brain barrier. Proc. Natl. Acad. Sci. U. S. A. *110,* 2999-3004.

163. Wang, X., Zhang, W., Shi, H., Qiu, Z., Meng, Y., Yao, F., and Wei, M. (2012). Mucopolysaccharidosis I mutations in Chinese patients: identification of 27 novel mutations and 6 cases involving prenatal diagnosis. Clin. Genet. *81,* 443-452.

164. Wang, Z.L., Sun, J.Y., Wang, D.N., Xie, Y.H., Wang, S.W., and Zhao, W.M. (2006). Pharmacological studies of the large-scaled purified genistein from Huaijiao (Sophora japonica-Leguminosae) on anti-osteoporosis. Phytomedicine *13,* 718-723.

165. Wohlfart, S., Gelperina, S., and Kreuter, J. (2012). Transport of drugs across the blood-brain barrier by nanoparticles. J. Control. Release *161,* 264-273.

166. Wong, H.L., Wu, X.Y., and Bendayan, R. (2012). Nanotechnological advances for the delivery of CNS therapeutics. Adv. Drug Deliv. Rev. *64,* 686-700.

167. Wraith, J.E., Clarke, L.A., Beck, M., Kolodny, E.H., Pastores, G.M., Muenzer, J., Rapoport, D.M., Berger, K.I., Swiedler, S.J., Kakkis, E.D.*, et al.* (2004). Enzyme replacement therapy for mucopolysaccharidosis I: a randomized, double-blinded, placebo-controlled, multinational study of recombinant human alpha-L-iduronidase (laronidase). J. Pediatr. *144,* 581-588.

168. Wraith, J.E., Beck, M., Lane, R., van der Ploeg, A., Shapiro, E., Xue, Y., Kakkis, E.D., and Guffon, N. (2007). Enzyme replacement therapy in patients who have mucopolysaccharidosis I and are younger than 5 years: results of a multinational study of recombinant human alpha-L-iduronidase (laronidase). Pediatrics *120,* e37-46.

169. Wraith, J.E., Scarpa, M., Beck, M., Bodamer, O.A., De Meirleir, L., Guffon, N., Meldgaard Lund, A., Malm, G., Van der Ploeg, A.T., and Zeman, J. (2008). Mucopolysaccharidosis type II (Hunter syndrome): a clinical review and recommendations for treatment in the era of enzyme replacement therapy. Eur. J. Pediatr. *167,* 267-277.

170. Yan, H., Jiang, W., Zhang, Y., Liu, Y., Wang, B., Yang, L., Deng, L., Singh, G.K., and Pan, J. (2012). Novel multi-biotin grafted poly(lactic acid) and its self-assembling nanoparticles capable of binding to streptavidin. Int. J. Nanomedicine *7*, 457-465.

171. Young, I.D., Harper, P.S., Newcombe, R.G., and Archer, I.M. (1982). A clinical and genetic study of Hunter's syndrome. 2. Differences between the mild and severe forms. J. Med. Genet. *19,* 408-411.

172. Zhao, K.W., Faull, K.F., Kakkis, E.D., and Neufeld, E.F. (1997). Carbohydrate structures of recombinant human alpha-L-iduronidase secreted by Chinese hamster ovary cells. J. Biol. Chem. *272,* 22758-22765.